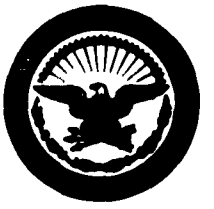

TRG

TECHNICAL RESEARCH GROUP
2 AERIAL WAY • SYOSSET, NEW YORK

THE UNSTEADY FORCES DUE TO PROPELLER-APPENDAGE INTERACTION

FINAL REPORT

CONTRACT NO. Nonr-3281(00)

TECHNICAL RESEARCH GROUP

TRG, Incorporated
2 Aerial Way
Syosset, New York

THE UNSTEADY FORCES DUE TO PROPELLER-APPENDAGE INTERACTION

Final Report Contract No. Nonr-3281(00)

Authors:

O. Pinkus

J. R. Lurye

D. Feit

Approved: J. Kotik

Submitted to:

David Taylor Model Basin
Department of the Navy
Washington 7, D.C.

March 1962

TECHNICAL RESEARCH GROUP

ACKNOWLEDGEMENT

Acknowledgements are due to Professor S. Karp of the Institute of Mathematical Sciences, New York University, for proposing the method used in Section VI for solving approximately the quasi-steady flow problem; and Dr. P. Kaplan of Oceanics, Inc. for his contributions during the initial stages of this work.

TABLE OF CONTENTS

I. SUMMARY

This report presents a study of the nature of the unsteady forces in the field of a propeller rotating in the vicinity of an appendage. The propeller is assumed to be one of a high aspect ratio while the appendage although of finite width is assumed to be infinitely long and thus the problem is reduced to a study of the two-dimensional flow field around two flat plates. An essential feature of the analysis is that the mutual interference effects of propeller blade and appendage are taken into account. Two approaches are formulated. The rigorous method leads to a set of two simultaneous integral equations which are reduced to a single integral equation involving elliptic integrals. The simplified method employs the technique of substitution vortices which yields explicit analytic expressions for the quasi-state, apparent-mass and wake forces for both the propeller and appendage. Graphs and tables give the magnitude and variation of the propeller and appendage forces as functions of tip clearance, distance and relative size of appendage and propeller.

NOMENCLATURE

a = Initial position of propeller

$a_1 = y_o - \frac{c}{2}$

$a_2 = y_o + \frac{c}{2}$

$a_{11} = \frac{y_o - i(x_o + \ell)}{\frac{c}{2}}$

$a_{12} = \frac{y_o - i(x_o - \ell)}{\frac{c}{2}}$

$a_{13} = \frac{y_o - i(x_o - x)}{\frac{c}{2}}$

$a_{14} = \frac{y_o + i(x_o - x')}{\frac{c}{2}}$

$a_{15} = \frac{y_o - i(x_o - x')}{\frac{c}{2}}$

$b = i(x_o - x)$

$b_1 = i(x_o + \ell)$

$b_2 = i(x_o - \ell)$

c = Chord of propeller blade

$\bar{c} = \frac{c}{2\ell}$

$g = i(x_o - x')$

$k^2 = \frac{(1-a_{11}\nu)(a_{12}-1)}{(a_{11}-\nu)(a_{12}-\nu)}$

$k_o = \frac{a_1 - i(x_o - x')}{a_2 - i(x_o - x')}$

$k_1 = \frac{(1-a_{11}\nu)(a_{13}-a_{12})}{(1-a_{13}\nu)(1-a_{14}\nu)}$

$k_2 = \frac{(1-\nu)(a_{11}-a_{13})(1+a_{13})}{(a_{13}-\nu)(1-\nu a_{13})}$

$k_3 = \frac{(1-\nu)(a_{11}-a_{14})(1+a_{14})}{(a_{14}-\nu)(1-a_{14}\nu)}$

$k_4 = \frac{(1-a_{11}\nu)(a_{13}-a_{15})}{(1-a_{13}\nu)(1-a_{15}\nu)}$

$k_5 = \frac{(1-\nu)(a_{11}-a_{15})(1+a_{15})}{(a_{15}-\nu)(1-\nu a_{14})}$

ℓ = Half-chord of appendage

q = Coefficient in formula for Γ

$r = \frac{V}{U}$

t, t_o = Time

u, v = Velocity components

w_o = Complex potential

x, y = Rectangular coordinates

x' = Variable along appendage

x_a = x location of appendage substitution vortex

x_o = x distance of propeller from center of appendage

x_p = x location of propeller substitution vortex

y' = Variable along propeller blade

y_a = y location of appendage substitution vortex

y_o = y distance of appendage from center of propeller

y_p = y location of propeller substitution vortex

z = Complex coordinate

$$A = \sqrt{\frac{(\bar{x}_p+1) + i\bar{y}_p}{(\bar{x}_p+1) + i\bar{y}_p}}$$

$$B = \sqrt{\frac{(\bar{y}_o-\bar{y}_a-\bar{c}) + i(\bar{x}_p-\bar{x}_a)}{(\bar{y}_o-\bar{y}_a+\bar{c}) + i(\bar{x}_p-\bar{x}_a)}}$$

C = Correction term for Appendage Wake Force

C_o = Vorticity strength for concentrated vortex

D = Correction term for Propeller Wake Force

F = Force per unit span

K(k) = Complete elliptic integral of 1st kind

P = (y_o-y_{om})

$$R = \frac{Ut}{\ell}$$

$$R_o = \frac{Ut_o}{\ell}$$

$$S = \frac{Vt}{\frac{c}{2}}$$

$$S_o = \frac{Vt_o}{\frac{c}{2}}$$

T = Unperturbed propeller thrust, $\rho\pi c U V$

U = Free Stream Velocity

V = Velocity of propeller blade

α = Angle of attack

β^2 = $\left(\frac{1 - a_{13}}{a_{13}}\right)^2$

$\gamma(x)$ = Vorticity distribution along x

λ = $\left(\frac{\quad}{a_{12}}\right)^2$

$\gamma_{oa}(x)$ = Quasi-steady vorticity on appendage

$\gamma_{oa}(x)$ = Vorticity on appendage due to $\gamma_{pi}(y)$

$\gamma_{oa}(x)$ = Vorticity on appendage due to $\gamma_{p\infty}(y)$

$\gamma_{op}(y)$ = Quasi-steady vorticity on propeller

$\gamma_{pi}(y)$ = Vorticity on propeller due to $\gamma_{oa}(x)$

$\gamma_{p\infty}(y)$ = Vorticity on propeller at infinity

γ_w = Vorticity due to wake

μ^2 = $\left(\frac{1 + a_{11}}{a_{12}}\right)^2$

ν = $\frac{1+a_{11}a_{12}}{a_{11}+a_{12}} + \sqrt{\left(\frac{1+a_{11}a_{12}}{a_{11}+a_{12}}\right)^2 - 1}$

ρ = Density

τ = Time variable

$\bar{\tau}$ = $\frac{Vt}{\ell}$

Γ = Circulation

$\bar{\Gamma}$ = $\frac{\Gamma}{\pi U c}$

Γ_{pi} = Circulation on propeller due to Γ_{oa}

$\Gamma_{p\infty}$ = Circulation on propeller at infinity

$\prod(\nu^2, k)$ = Complete elliptic integral of the 3rd kind

Subscripts

a = Appendage

i = Induced

o = Quasi-steady state

m = Maximum or Minimum

p = Propeller

1 = Apparent-mass effect

2 = Wake effect

Superscripts

- pertains to quantities normalized by ℓ

$$\bar{y}_o = \frac{y_o}{\ell} \text{ etc.}$$

(1) Unit

II INTRODUCTION

The purpose of this study is to evaluate the effects due to a propeller rotating in the vicinity of an appendage both subject to a uniform stream parallel to the appendage, as shown in Fig. 1.

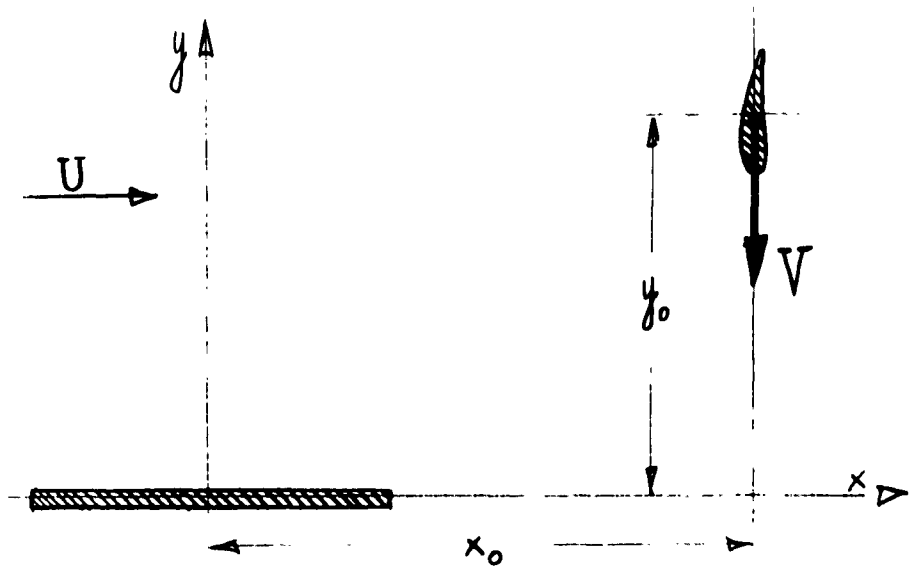

Figure 1.
Propeller Appendage System

Specifically it is desired to analyze the nature and magnitude of the forces acting on both the propeller and appendage. These forces due to the rotation of the propeller will be time dependent functions and as such will induce vibrations either by direct excitation of the appendage or by the transmission of forces via the propeller shaft The knowledge of the relation between these forces and

such design parameters as tip clearnace, relative size of appendage and propeller and the location and number of blades may provide a means for new and more effective design procedures.

Of the early work dealing with forces induced by rotating propellers are the papers by Lewis [1,2] who by use of models and electrical analogy charted the pressure field induced on a wall parallel to the propeller axis. However the results while setting down the nature of the vibratory forces do not correlate these with the various design parameters inherent in propeller-appendage assemblies. The most recent work on the subject is that of Breslin[3], who solved the problem analytically by representing the propeller blade by a single concentrated vortex sweeping by a moving plate. The present work follows Breslin's approach but differs from it and extends it in several important respects. Instead of a concentrated single vortex the blade is here represented by a chord-wise vorticity distribution which in addition to yielding a more correct value for the forces on the appendage, enables us also to calculate the forces on the propeller which was impossible to do in Breslin's case. The second important difference is that we have here included the mutual interference effects of propeller blade and appendage; for as the propeller moves through the velocity field of the appendage these velocities modify and are in turn themselves modified by the velocity potential of the travelling propeller.

Two approaches will be formulated, one rigorous and a simplified method. The rigorous analysis leads to a set of two simultaneous integral equations which by proper inversion and

integration are eventually reduced to a single non-homogeneous integral equation. This equation, given in terms of elliptic integrals with complex moduli and parameters, can be solved only by numerical methods and represents a formidable computational task. The simplified method is the Method of Substitution Vortices which leads directly to explicit analytic expressions for the vorticities and forces involved. These expressions are then evaluated for a number of pertinent parameters for both the propeller and appendage. A discussion of these results and the main conclusions are given at the end of the report.

The analysis is based on the usual assumptions of potential theory, namely that the flow is incompressible and irrotational and on the assumption that the velocity $V \gg U$ so that the flow is nearly parallel for both the appendage and the propeller. The propeller is treated as one of a very high aspect ratio so that its three-dimensional configuration can be replaced by a representative blade cross section of finite chord. The appendage too though infinitely long has a finite width in the plane of the propeller chord. The problem thus is essentially reduced to an analysis of the unsteady flow field round two flat plates.

III - GENERAL FORCE EQUATIONS

The basic relations for circulation and lift on a flat plate are well known from elementary aerodynamics. The infinite-span, infinitely-thin plate of chord 2a is represented by an unknown chordwise vorticity distribution $\gamma_0(x)$ which gives the velocity field around the plate By imposing the conditions of zero normal velocity along the plate and the Kutta condition of zero velocity at the trailing edge the velocity u(x) along the plate is obtained. Used in Bernoulli's equation these velocities will provide the pressure distribution on the plate and by integration these pressures will yield the total lift.

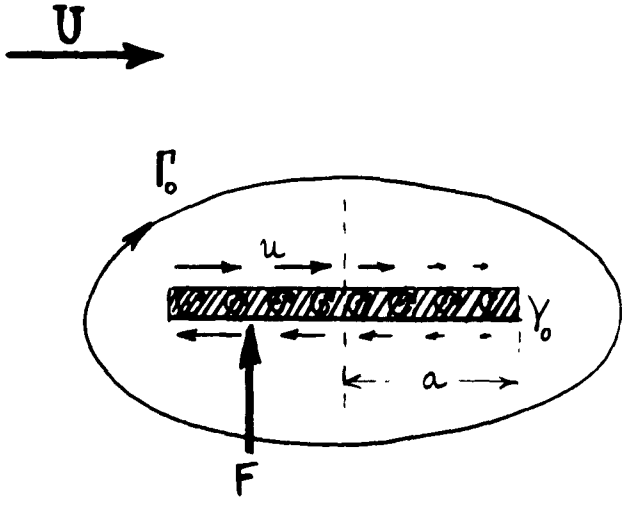

Figure 2.

Vorticity, Circulation and Lift on a Flat Plate

When the plate is subject to an unsteady free-stream velocity, a varying angle of attack, or is otherwise affected by unsteady phenomena, the vorticity γ_o, the circulation Γ_o and the resultant forces become time dependent functions. Under these conditions vonKarman and Sears [4] have shown that the total force on the plate is made up of three parts. These are:

1. F_o - Quasi-steady Force. This is the force that would have resulted from a steady state case in which all parameters are equal to the instantaneous values of the unsteady motion. The expression for this force is

$$F_o = \rho U \Gamma_o \tag{3-1}$$

2. F_1 - Apparent-Mass Force. This is the inertia force on the plate due to the acceleration of the mass of fluid around the plate. It is given by

$$F_1 = - \rho \frac{\partial}{\partial t} \int_a^a x\gamma_o(x,t)dx \tag{3-2}$$

3. F_2 - Wake Force. Due to the variation of $\gamma_o(x,t)$ with time the foil will shed vortices behind it giving rise to a vorticity distribution $\gamma(\zeta,t)$ in the wake. With respect to the coordinate axes of Figure 3 this $\gamma(\zeta,t)$ will be a function of both t and ζ although in space it would not be a function of time. This new vorticity distribution will give rise to a normal velocity component on the foil which must be supressed by an additional vorticity $\gamma_2(x,t)$ on the foil.

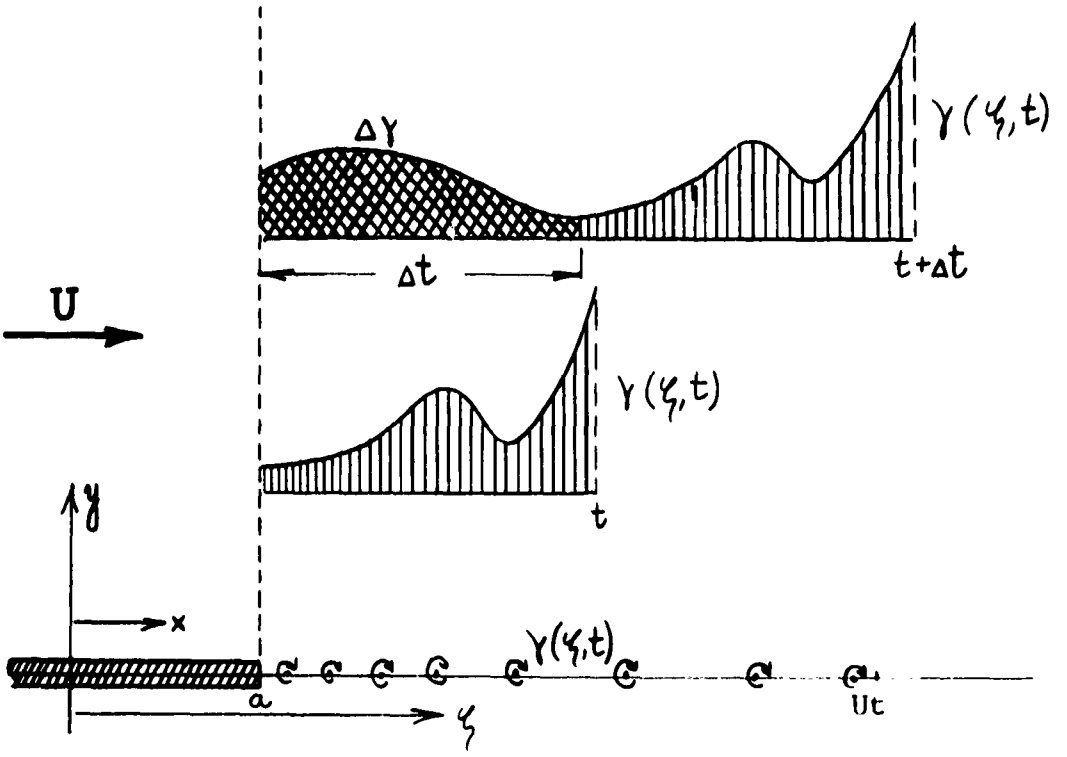

Figure 3.

Wake Vorticity Due to The Unsteady Circulation

It is shown in Section VII that the circulation induced on a plate 2a by a single vortex at z is given by

$$\Gamma' = \frac{C_o}{2\pi} \left(\mathrm{Re} \sqrt{\frac{x-a+iy}{x+a+iy}} - 1 \right)$$

For the case of a single vortex located at y=0 this becomes

$$\Gamma'(x,o) = \frac{C_o}{2\pi} \left(\mathrm{Re} \sqrt{\frac{x-a}{x+a}} - 1 \right)$$

For a vorticity distribution $\gamma(\zeta,t)$ along the wake we thus have

$$\Gamma_2 = a \int_1^{1+R} \gamma(\bar{\zeta},t) \quad \left(\sqrt{\frac{\bar{\zeta}-1}{\bar{\zeta}+1}} -1\right) d\bar{\zeta} \tag{3-3}$$

where $\zeta = \bar{\zeta}a$ $R = \frac{Ut}{a}$ and Γ_2 is the additional circulation on the plate due to the wake vorticity.

We now have three circulations to consider; two about the foil given by Γ_o and Γ_2; and one in the wake, Γ, caused by the unsteady motion of the foil. By Kelvin's theorem the sum of these three circulations must at any time be zero. We thus have

$$\Gamma_o + \Gamma_2 + \Gamma = 0$$

or

$$\Gamma_o + a \int_1^{1+R} \gamma(\bar{\zeta},t) \quad \left(\sqrt{\frac{\bar{\zeta}-1}{\bar{\zeta}+1}} -1\right) d\bar{\zeta} + a \int_1^{1+R} \gamma(\bar{\zeta},t) d\bar{\zeta} = 0$$

which yields

$$\int_1^{1+R} \gamma(\bar{\zeta},t) \sqrt{\frac{\bar{\zeta}-1}{\bar{\zeta}+1}} \, d\bar{\zeta} = -\frac{\Gamma_o(t)}{a} \tag{3-4}$$

The above is an integral equation in $\gamma(\bar{\zeta}, t)$ which must be solved for the particular function $\Gamma_o(t)$ given by (2-11).

The force on the foil due to the additional circulation Γ_2 can be shown to be given by

$$F_2 = \rho U a \int_1^{1+R} \gamma(\bar{\zeta},t) \quad \frac{d\bar{\zeta}}{\sqrt{\bar{\zeta}^2-1}} \tag{3-5}$$

The total force on the foil is then

$$F = F_o + F_1 + F_2 \tag{3-6}$$

IV. FORCES ON A SINGLE FOIL

In this section the vorticity distribution, velocity potential and the forces arising from the motion of a single foil in a perfect fluid will be set down to serve as a starting point for the treatment of the more complex propeller-appendage problem. The results derived here will also be needed later on in the text. The elementary model considered is that of a simple flat plate moving with a velocity U at some attack angle α as shown in Figure 4. In this sketch we have the coordinate axes fixed with respect to the plate and we let the stream flow past the foil with a velocity $Ue^{i\alpha}$.

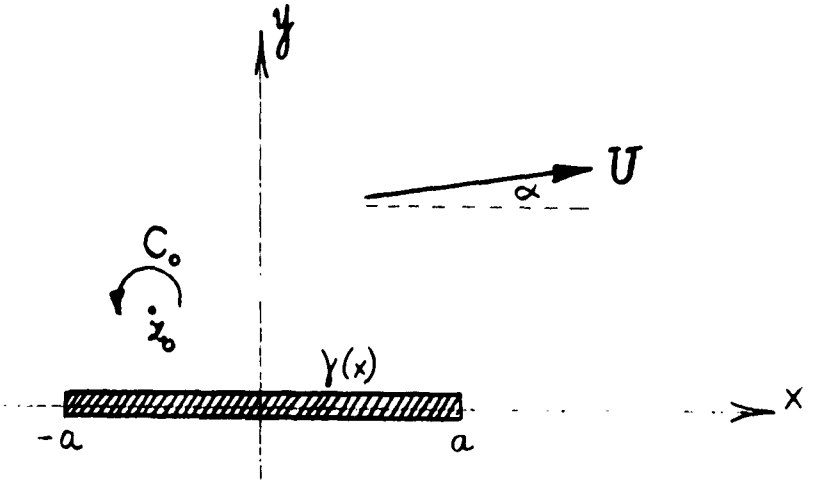

Figure 4.

Flat Plate in Uniform Stream

The complex potential for a simple concentrated vortex of strength C_o located as $z = z_o$ is

$$w = \frac{i}{2\pi} C_o \ln(z-z_o)$$

and for the uniform stream U

$$w = - Ue^{i\alpha}z \quad .$$

From the above, representing the flat plate by a distributed vorticity $\gamma_o(x)$, we have

$$w = - Ue^{i\alpha}z + \frac{i}{2\pi} \int_{-a}^{a} \gamma_o(x') \ln(z-x')dx' \qquad (4\text{-}1)$$

From (4-1) the total complex velocity is then

$$\frac{dw}{dz} = - Ue^{i\alpha} + \frac{i}{2\pi} \int_{-a}^{a} \frac{\gamma_o(x')dx'}{z-x'}$$

Since $\frac{dw}{dz} = - u + iv$ we obtain for the velocity components parallel and normal to the foil

$$u = U\cos\alpha - \frac{y}{2\pi} \int_{-a}^{a} \frac{\gamma_o(x')dx'}{(x-x')^2+y^2} \qquad (4\text{-}2)$$

$$v = U\sin\alpha + \frac{1}{2\pi} \int_{-a}^{a} \frac{\gamma_o(x')(x-x')}{(x-x')^2+y^2} dx' \qquad (4\text{-}3)$$

The condition of zero normal flow along the plate requires that

$$v = 0 \quad \text{at} \quad y = 0 \quad -a \leq x \leq a$$

and thus

$$\frac{1}{\pi}\int_{-a}^{a}\frac{\gamma_o(x')dx'}{x-x'} = 2U\sin\alpha \qquad (4\text{-}4)$$

This represents an integral equation in $\gamma_o(x)$ and its solution can be obtained[5] from the following general inversion formula. If

$$\frac{1}{\pi}\int_{a_1}^{a_2}\frac{\gamma(s)ds}{s-z} = v(z) \qquad (4\text{-}6)$$

then together with the Kutta condition $v(a_2) = 0$, we have

$$\gamma(z) = -\frac{1}{\pi}\sqrt{\frac{a_2-z}{z-a_1}}\int_{a_1}^{a_2}\sqrt{\frac{s-a_1}{a_2-s}}\,\frac{v(s)}{s-z}\,ds \qquad (4\text{-}7)$$

For the case of equ (4-4) we thus have

$$\gamma_o(x) = \frac{2U\sin\alpha}{\pi}\sqrt{\frac{a-x}{a+x}}\int_{-a}^{a}\sqrt{\frac{a+x'}{a-x'}}\,\frac{dx'}{x'-x}$$

Since

$$\int_{-a}^{a}\sqrt{\frac{a+x'}{a-x'}}\,\frac{dx'}{x'-x} = \pi \qquad (4\text{-}8)$$

we have

$$\gamma_o(x) = 2U\sin\alpha\sqrt{\frac{a-x}{a+x}} \qquad (4\text{-}9)$$

For non-steady flow the right-hand side of eq [illegible] is given by an arbitrary function of space and time $v(x,t)$. Hence the vorticity distribution along the foil will also be a function of time and the inversion integral then becomes

$$\gamma_o(x,t) = \frac{1}{\pi} \sqrt{\frac{a-x}{a+x}} \int_{-a}^{a} \sqrt{\frac{a+x'}{a-x'}} \frac{v(x',t)}{x'-x} dx'$$

The total circulation around the foil is then

$$\Gamma_o(t) = \int_{-a}^{a} \gamma_o(x,t)dx$$

As seen from the above simple example, the [illegible] in arriving at an expression for the aerodynamic for[illegible] represent the foils by some vorticity distribution $\gamma(x,t)$ into account all neighboring velocity potentials. Th[illegible] applying the proper boundary conditions the unknown v[illegible] distributions can in principle be obtained from the de[illegible] relations. These procedures will now be applied to th[illegible] on hand.

V. RIGOROUS ANALYSIS OF PROPELLER-APPENDAGE SYSTEM

We are concerned here with the unsteady potential generated by a propeller rotating in the vicinity of a moving plane or appendage, as shown schematically in Fig. 1. The horizontal distance x_o of the blade from the appendage is a fixed quantity which can be either negative or positive while the vertical distance y_o is a variable. Thus the velocities and forces generated on both the appendage and propeller will be time dependent functions. A crucial element of the problem is that there is mutual interference between propeller and appendage. In addition, due to the unsteady circulation, wakes will be generated behind both propeller and appendage.

Mathematically the system can be represented by two flat plates at right angles to and at a continuously varying distance from each other, as shown in Fig. 5. We shall use

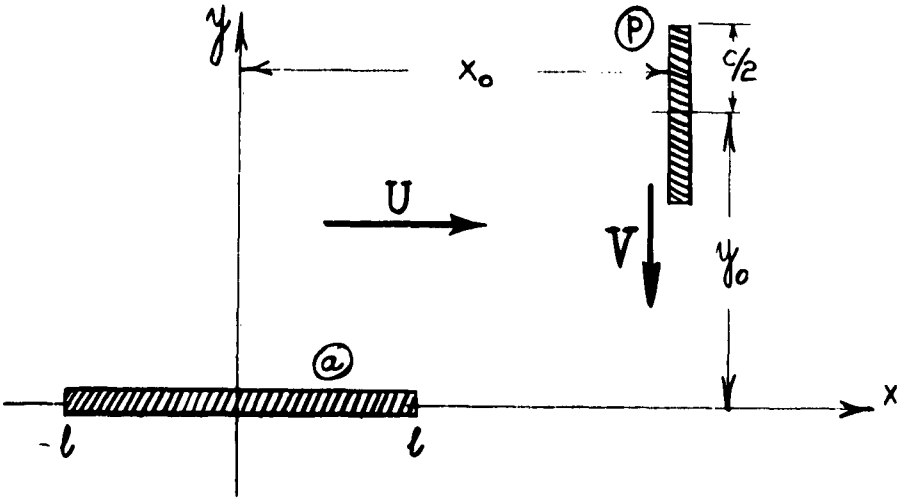

Figure 5.

Schematic Diagram of Propeller Appendage System

the following notation for the various vorticities involved:

$\gamma_{p\infty}(y)$ - vorticity distribution on propeller at infinity

$\gamma_{pi}(y)$ - vorticity distribution on propeller due to appendage interference

$\gamma_{op}(y)$ - quasi-steady vorticity on propeller

$\gamma'_{oa}(x)$ - vorticity distribution on appendage due to $\gamma_{pi}(y)$

$\gamma''_{oa}(x)$ - vorticity distribution on appendage due to $\gamma_{p\infty}(y)$

$\gamma_{oa}(x)$ - quasi-steady vorticity on appendage.

With the coordinate system fixed in the center of the appendage and the main flow parallel to x, i.e. $\alpha = 0$, we have from equ. (4-1)

$$w_o = - Uz + \frac{i}{2\pi}\int_{-\ell}^{\ell} \gamma_{oa}(x')\ell n(z-z')dx' + \frac{i}{2\pi}\int_{a_1}^{a_2} \gamma_{op}(y')\ell n(z-x_o-iy')dy' \tag{5-1}$$

The complex velocity potential is by differentiating (5-1).

$$\frac{dw_o}{dz} = - U + \frac{i}{2\pi}\int_{-\ell}^{\ell} \frac{\gamma_{oa}(x')dx'}{z-x'} + \frac{i}{2\pi}\int_{a_1}^{a_2} \frac{\gamma_{op}(y')dy'}{z-(x_o+iy')}$$

or after rationalizing the denominators

$$\frac{dw_o}{dz} = - U + \frac{i}{2\pi}\int_{-\ell}^{\ell} \gamma_{oa}(x')\ \frac{[(x-x')-iy']}{(x-x')^2+y^2}\ dx'$$

$$+ \frac{i}{2\pi}\int_{a_1}^{a_2} \gamma_{op}(y')\ \frac{[(x-x_o)-i(y-y')]}{(x-x_o)^2+(y+y')^2}\ dy'$$

The component velocities are thus

$$u = U - \frac{1}{2\pi}\left\{ y\int_{-\ell}^{\ell} \frac{\gamma_{oa}(x')dx'}{(x-x')^2+y^2} + \int_{a_1}^{a_2} \gamma_{op}(y')\ \frac{(y-y')dy'}{(x-x_o)^2+(y-y')^2}\right\} \quad (5\text{-}2a)$$

$$v = \frac{1}{2\pi}\left\{ \int_{-\ell}^{\ell} \frac{\gamma_{oa}(x')(x-x')dx'}{(x-x')^2+y^2} + \int_{a_1}^{a_2} \gamma_{op}(y')\ \frac{(x-x_o)dy'}{(x-x_o)^2+(y-y')^2}\right\} \quad (5\text{-}2b)$$

The boundary conditions to be satisfied are

1) On appendage: $v=0$ on $y=0$ $\quad -\ell \le x \le \ell$

2) On propeller: $u=0$ on $x=x_o$ $\quad yo - \frac{c}{2} \le y \le yo + \frac{c}{2}$

Thus

$$\int_{-\ell}^{\ell} \frac{\gamma_{oa}(x')dx'}{x'-x} = \int_{a_1}^{a_2} \frac{\gamma_{op}(y')(x-x_o)dy'}{(x-x_o)^2+(y')^2} \quad (5\text{-}3a)$$

$$U = \frac{1}{2\pi}\left\{ y\int_{-\ell}^{\ell} \frac{\gamma_{oa}(x')dx'}{(x_o-x')^2+y^2} + \int_{a_1}^{a_2} \frac{\gamma_{op}(y')dy'}{y-y'}\right\} \quad (5\text{-}3b)$$

Since $\gamma_{op}(y') = \gamma_{p\infty}(y') + \gamma_{pi}(y')$ we can rewrite the last integrals of the above two equations as follows:

$$(x-x_o)\int_{a_1}^{a_2}\frac{\gamma_{op}(y')dy'}{(x-x_o)^2+(y')^2} = (x-x_o)\left\{\int_{a_1}^{a_2}\frac{\gamma_{pi}(y')dy'}{(x-x_o)^2+(y')^2} + \int_{a_1}^{a_2}\frac{\gamma_{p\infty}(y')dy'}{(x-x_o)^2+(y')^2}\right\}$$

$$\frac{1}{2\pi}\int_{a_1}^{a_2}\frac{\gamma_{op}(y')dy'}{y-y'} = \frac{1}{2\pi}\int_{a_1}^{a_2}\frac{\gamma_{pi}(y')dy'}{y-y'} + \frac{1}{2\pi}\int_{a_1}^{a_2}\frac{\gamma_{p\infty}(y')dy'}{y-y'}$$

The last integral is of the form given in (4-4) where Usin α represents the cross flow, in our case merely U. Thus

$$\frac{1}{2\pi}\int_{a_1}^{a_2}\frac{\gamma_{p\infty}(y')dy'}{y-y'} = U \qquad (5\text{-}4)$$

Hence in Equ. (5-3b) the term U will be cancelled by the $\gamma_{p\infty}(y')$ portion of the second right hand integral. Furthermore, from Equ. (4-9) the value of $\gamma_{p\infty}(y')$ satisfying (5-4) is

$$\gamma_{p\infty}(y) = 2\,U\sqrt{\frac{y_o+\frac{c}{2}-y}{-y_o+\frac{c}{2}+y}} \qquad (5\text{-}5)$$

Thus after introducing the value of $\gamma_{p\infty}(y')$ into (5-3a) a portion of that integral will become after integration a known function of x alone. We can now rewrite (5-3) as follows

$$\int_{-\ell}^{\ell} \frac{\gamma_{oa}(x')dx'}{x'-x} = (x-x_o) \int_{a_1}^{a_2} \frac{\gamma_{pi}(y')dy'}{(x-x_o)^2+(y')^2} + f(x) \qquad (5\text{-}6a)$$

$$y \int_{-\ell}^{\ell} \frac{\gamma_{oa}(x')dx'}{(x_o-x')^2+y^2} = \int_{a_1}^{a_2} \frac{\gamma_{pi}(y')dy'}{y'-y} \qquad (5\text{-}6b)$$

Employing the inversion formula (4-7) for the above two integral equations with the Kutta condition applied at ℓ for the appendage and at a_2 on the propeller, we have

$$\gamma_{pi}(y) = -\frac{1}{\pi^2} \sqrt{\frac{a_2-y}{a_1-y}} \int_{a_1}^{a_2} \sqrt{\frac{a_1-y'}{a_2-y'}} \frac{y'}{y'-y} \int_{-\ell}^{\ell} \frac{\gamma_{oa}(x')dx'}{(x_o-x)+(y')^2} dy' \qquad (5\text{-}7)$$

$$\gamma_{oa}(x) = -\frac{1}{\pi^2} \sqrt{\frac{\ell-x}{\ell+x}} \int_{-\ell}^{\ell} \sqrt{\frac{\ell+s}{\ell-s}} \frac{(s-x_o)}{s-x} \int_{a_1}^{a_2} \frac{[\gamma_{pi}(y')+\gamma_{p\infty}(y')]dy'}{(x-x_o)^2+(y')^2} ds \qquad (5\text{-}8)$$

Breaking up the appendage vorticity $\gamma_{oa}(x)$ into a $\gamma'_{oa}(x)$ corresponding to $\gamma_{pi}(y)$, and a $\gamma''_{oa}(x)$ corresponding to $\gamma_{p\infty}(y)$ we can rewrite (5-8) as follows

$$\gamma'_{oa}(x) = -\frac{1}{\pi^2}\sqrt{\frac{\ell-x}{\ell+x}}\int_{-\ell}^{\ell}\sqrt{\frac{\ell+s}{\ell-s}}\frac{s-x_o}{s-x}\int_{a_1}^{a_2}\frac{\gamma_{ni}(y')dy'}{(s-x_o)^2+(y')^2}\,ds \qquad (5\text{-}9)$$

$$\gamma''_{oa}(x) = -\frac{1}{\pi^2}\sqrt{\frac{\ell-x}{\ell+x}}\int_{-\ell}^{\ell}\sqrt{\frac{\ell+s}{\ell-s}}\frac{s-x_o}{s-x}\int_{a_1}^{a_2}\frac{\gamma_{p\infty}(y')dy}{(s-x_o)^2+(y')^2}\,ds \qquad (5\text{-}10)$$

Integrating first with respect to s we are confronted with the following integral

$$I = \int_{-\ell}^{\ell}\sqrt{\frac{\ell+s}{\ell-s}}\,\frac{s-x_o}{s-x}\,\frac{ds}{(s-x_o)^2+y'^2} \qquad (5\text{-}11)$$

This integral which reappears several times later on is solved in general terms in the Appendix. The solution for the case of complex conjugate roots of the quadratic $(s-x_o)^2+y'^2$ is given by Equ. (A-9). For our case

$$k_1 = -x_o \qquad k_2 = x \qquad s_{1,2} = x_o \pm iy'$$

Thus

$$I = -\pi\,\mathrm{Re}\,\frac{1}{(x_o-x)+iy'}\sqrt{\frac{(x_o+\ell)+iy'}{(x_o-\ell)+iy'}} \qquad (5\text{-}12)$$

and

$$\gamma'_{oa}(x) = \frac{1}{\pi}\sqrt{\frac{\ell-x}{\ell+x}}\,\mathrm{Re}\int_{a_1}^{a_2}\frac{1}{(x_o-x)+iy'}\sqrt{\frac{(x_o+\ell)+iy'}{(x_o-\ell)-iy'}}\,\gamma_{pi}(y')dy' \qquad (5\text{-}13)$$

$$\gamma'_{oa}(x) = \frac{1}{\pi}\sqrt{\frac{\ell-x}{\ell+x}}\ \mathrm{Re}\int_{a_1}^{a_2}\frac{1}{(x_o-x)+iy'}\sqrt{\frac{(x_o+\ell)+iy'}{(x_o-\ell)-iy'}}\ \gamma_{p\infty}(y')dy' \qquad (5\text{-}14)$$

Evaluation of $\gamma'_{oa}(x)$

Introducing the value of $\gamma_{p\infty}(y)$ as given in Equ. (5-5) into (5-14) we have

$$\gamma'_{oa}(x) = \frac{2U}{\pi}\sqrt{\frac{\ell-x}{\ell+x}}\ \mathrm{Im}\int_{a_2}^{a_1}\sqrt{\frac{a_2-y'}{y'-a_1}}\sqrt{\frac{y'-b_1}{y'-b_2}}\ \frac{dy'}{y'-b}$$

where $b_1 = i(x_o+\ell)$ $\quad b_2 = i(x_o-\ell)$ $\quad b = i(x_o-x)$

The integration of

$$I_2 = \int_{a_1}^{a_2}\sqrt{\frac{a_2-y'}{y'-a_1}}\sqrt{\frac{y'-b_1}{y'-b_2}}\ \frac{dy'}{y'-b} \qquad (5\text{-}15)$$

is performed in the Appendix and its solution in terms of elliptic integrals is given by equ. (A-15) as

$$I_2 = \frac{2(1+\nu)}{(1-\nu a_{13})}\sqrt{\frac{1-\nu^2}{(a_{11}-\nu)(a_{12}-\nu)}}$$
$$\left\{(1-a_{11}\nu)K(k)+(1-\nu)(1-\nu a_{13})\,\Pi(\nu^2,k)+\frac{\nu(1-\nu)(a_{11}-a_{13})(1+a_{13})}{a_{13}-\nu}\right.$$
$$\left.\Pi(\beta^2,k)\right\} \qquad (5\text{-}16)$$

where K(k) is the complete elliptic integral of the 1st kind, $\Pi(\beta^2,k)$ the complete elliptic integral of the second kind and

$$\nu = \frac{1+a_{11}a_{12}}{a_{11}+a_{12}} \pm \sqrt{\left(\frac{1+a_{11}a_{12}}{a_{11}+a_{12}}\right)^2 - 1}$$

$$a_{11} = \frac{y_o - i(x_o+\ell)}{\frac{c}{2}} \qquad a_{12} = \frac{y_o - i(x_o-\ell)}{\frac{c}{2}}$$

$$a_{13} = \frac{y_o - i(x_o-x)}{\frac{c}{2}} \qquad k^2 = \frac{(1-a_{11}\nu)(a_{12}-1)}{(a_{11}-\nu)(a_{12}-\nu)}$$

$$\beta^2 = \left(\frac{1-\nu a_{13}}{a_{13}-\nu}\right)^2$$

The explicit expression for $\gamma'_{oa}(x)$ then becomes

$$\gamma'_{oa}(x) = \frac{4U}{\pi}\sqrt{\frac{\ell-x}{\ell+x}}\ \mathrm{Im}\frac{1+\nu}{\nu(1-\nu a_{13})}\sqrt{\frac{1-\nu^2}{(a_{11}-\nu)(a_{12}-\nu)}}\left\{(1-a_{11}\nu)K(k)\right.$$

$$\left.+(1-\nu)(1-\nu a_{13})\,\Pi(\nu^2,k) + \frac{\nu(1-\nu)(a_{11}-a_{13})(1+a_{13})}{a_{13}-\nu}\,\Pi(\beta^2,k)\right\} \qquad (5\text{-}17)$$

Evaluation of $\gamma_{pi}(y)$

The expression for $\gamma_{pi}(y)$ is given by Equ. (5-7). Since $\gamma_{oa}(x)$ is a function of x only we can rewrite it as follows:

$$\gamma_{pi}(y) = -\frac{1}{\pi^2}\sqrt{\frac{a_2-y}{y-a_1}}\int_{-\ell}^{\ell}\gamma_{oa}(x')\int_{a_1}^{a_2}\sqrt{\frac{a_1-y'}{y'-a_2}}$$

$$\frac{y'}{y'-y}\,\frac{dy'}{(x_o-x')^2+(y')^2}\,dx'$$

Writing $\zeta = \frac{y'-y_o}{\frac{c}{2}}$ the integral in y' reads

$$I = \frac{2}{c} \int_{-1}^{1} \sqrt{\frac{1+\zeta}{1-\zeta}} \; \frac{\zeta + \frac{2y_o}{c}}{\zeta - \frac{2(y-y_o)}{c}} \; \frac{d\zeta}{(\zeta-\zeta_1)(\zeta-\zeta_2)}$$

with $\zeta_{1,2} = -\frac{2}{c}\left[y_o \mp i(x_o-x')\right]$

We see that this integral is of the same form as (5-11) and its solution for complex conjugate roots is according to (A-9)

$$I = \pi \, \mathrm{Re} \, \frac{1}{y-i(x_o-x')} \sqrt{\frac{(y_o-\frac{c}{2})-i(x_o-x')}{(y_o+\frac{c}{2})-i(x_o-x')}}$$

We thus have

$$\gamma_{pi}(y) = -\frac{1}{\pi} \sqrt{\frac{a_2-y}{y-a_1}} \int_{-\ell}^{\ell} \mathrm{Re} \, \frac{\gamma_{oa}(x')}{y-i(x_o-x')} \sqrt{\frac{a_1-i(x_o-x')}{a_2-i(x_o-x')}} \, dx' \qquad (5\text{-}18)$$

Evaluation of $\gamma'_{oa}(x)$

Introducing now Equ. (5-18) into (5-14) we have for $\gamma'_{oa}(x)$ the following

$$\gamma'_{oa}(x) = \frac{1}{\pi} \sqrt{\frac{\ell-x}{\ell+x}} \int_{a_1}^{a_2} \mathrm{Re} \, \frac{1}{(x_o-x)+iy'} \sqrt{\frac{(x_o+\ell)+iy'}{(x_o-\ell)+iy'}} \left(-\frac{1}{\pi}\right) \sqrt{\frac{a_2-y'}{y'-a_1}}$$

$$\int_{-\ell}^{\ell} \mathrm{Re} \, \frac{1}{y-i(x_o-x')} \sqrt{\frac{a_1-i(x_o-x')}{a_2-i(x_o-x')}} \, \gamma_{oa}(x')dx'dy'$$

Since Re z_1 Re $z_2 = \frac{1}{2}$ (Re $z_1 z_2$ + Re $z_1 \bar{z}_2$) we have after multiplying top and bottom by -i and writing Im z=Re(-iz).

$$\gamma'_{oa}(x) = -\frac{1}{2\pi^2}\sqrt{\frac{\ell-x}{\ell+x}}\ \mathrm{Im}\left\{\int_{-\ell}^{\ell}\sqrt{\frac{a_1-i(x_o-x')}{a_2-i(x_o-x')}}\,\gamma_{oa}(x')\right.$$

$$\int_{a_1}^{a_2}\sqrt{\frac{a_2-y'}{y'-a_1}}\ \sqrt{\frac{y'-i(x_o+\ell)}{y'-i(x_o-\ell)}}\ \frac{1}{y'-i(x_o-x)}\,\frac{dy'}{y'-i(x_o-x')}\,dx'$$

$$+\int_{-\ell}^{\ell}\sqrt{\frac{a_1+i(x_o-x')}{a_2+i(x_o-x')}}\,\gamma_{oa}(x')\int_{a_1}^{a_2}\sqrt{\frac{a_2-y'}{y'-a_1}}\ \sqrt{\frac{y'-i(x_o+\ell)}{y'-i(x_o-\ell)}}$$

$$\left.\frac{1}{y'-i(x_o-x)}\,\frac{dy'}{y'+i(x_o-x')}\,dx'\right\} \qquad (5\text{-}19)$$

In abbreviated form the above reads

$$\gamma'_{oa}(x) = -\frac{1}{2\pi^2}\sqrt{\frac{\ell-x}{\ell+x}}\ \mathrm{Im}\left\{\int_{-\ell}^{\ell}\sqrt{\frac{a_1-i(x_o-x')}{a_2-i(x_o-x')}}\,\gamma_{oa}(x')I_b\,dx'\right.$$

$$\left.+\int_{-\ell}^{\ell}\sqrt{\frac{a_1+i(x_o-x')}{a_2+i(x_o-x')}}\,\gamma_{oa}(x')\ I_a\,dx'\right\}$$

with

$$I_a = \int_{a_1}^{a_2}\sqrt{\frac{a_2-y'}{y'-a_1}}\ \sqrt{\frac{y'-i(x_o+\ell)}{y'-i(x_o-\ell)}}\ \frac{1}{y'-i(x_o-x)}\,\frac{dy'}{y'+i(x_o-x')}$$

$$I_b = \int_{a_1}^{a_2} \sqrt{\frac{a_2-y'}{y'-a_1}} \sqrt{\frac{y'-i(x_o+\ell)}{y'-i(x_o-\ell)}} \frac{1}{y'-i(x_o-x)} \frac{dy'}{y'-i(x_o-x')}$$

By means of partial fractions I_a and I_b can be written as follows

$$I_a = \frac{1}{b+g} \int_{a_1}^{a_2} \sqrt{\frac{a_2-y}{y-a_1}} \sqrt{\frac{y-b_1}{y-b_2}} \frac{dy}{y-b} - \frac{1}{b+g} \int_{a_1}^{a_2} \sqrt{\frac{a_2-y}{y-a_1}} \sqrt{\frac{y-b_1}{y-b_2}} \frac{dy}{y+g} =$$

$$\frac{1}{b+g} I_{a1} - \frac{1}{b+g} I_{a2}$$

$$I_b = \frac{1}{b-g} \int_{a_1}^{a_2} \sqrt{\frac{a_2-y}{y-a_1}} \sqrt{\frac{y-b_1}{y-b_2}} \frac{dy}{y-b} - \frac{1}{b-g} \int_{a_1}^{a_2} \sqrt{\frac{a_2-y}{y-a_1}} \sqrt{\frac{y-b_1}{y-b_2}} \frac{dy}{y-g} =$$

$$\frac{1}{b-g} I_{a1} - \frac{1}{b-g} I_{b2}$$

where $b_1 = i(x_o+\ell)$ $\quad b_2 = i(x_o-\ell)$

$b = i(x_o-x)$ $\quad g = i(x_o-x')$

Integrals I_{a1}, I_{a2} and I_{b2} are of the same form as the integrals of Equ. (5-15) and their solution is given by Equ. (A-15) with

$$a_{14} = \frac{2}{c} [y_o+i(x_o-x')] \text{ replacing } a_{13} \text{ in } I_{a2}$$

$$a_{15} = \frac{2}{c} [y_o-i(x_o-x')] \text{ replacing } a_{13} \text{ in } I_{b2}$$

We thus have

$$I_{a1} = \frac{2(1+\nu)}{(1-\nu a_{13})} \sqrt{\frac{1-\nu^2}{(a_{11}-\nu)(a_{12}-\nu)}} \left\{ (1-a_{11}\nu)K(k) + \right.$$

$$\left. (1-\nu)(1-\nu a_{13}) \prod(\nu^2,k) + \frac{\nu(1-\nu)(a_{11}-a_{13})(1+a_{13})}{a_{13}-\nu} \prod(\beta^2,k) \right\}$$

$$I_{a2} = \frac{2(1+\nu)}{(1-\nu a_{14})} \sqrt{\frac{1-\nu^2}{(a_{11}-\nu)(a_{12}-\nu)}} \left\{ (1-a_{11}\nu)K(k) + \right.$$

$$\left. (1-\nu)(1-\nu a_{14}) \prod(\nu^2,k) + \frac{\nu(1-\nu)(a_{11}-a_{14})(1+a_{14})}{a_{14}-\nu} \prod(\gamma^2,k) \right\}$$

$$I_{b2} = \frac{2(1+\nu)}{(1-\nu a_{15})} \sqrt{\frac{1-\nu^2}{(a_{11}-\nu)(a_{12}-\nu)}} \left\{ (1-a_{11}\nu)K(k) + \right.$$

$$\left. (1-\nu)(1-\nu a_{15}) \prod(\gamma^2,k) + \frac{\nu(1-\nu)(a_{11}-a_{15})(1+a_{15})}{a_{15}-\nu} \prod(\delta^2,k) \right\}$$

Using these in the expressions for I_a and I_b and then in Equ. (5-19), we have for $\gamma'_{oa}(x)$ the following:

$$\gamma'_{oa}(x) = \frac{1}{\pi^2} \sqrt{\frac{\ell-x}{\ell+x}} \; \mathrm{Re} \sqrt{\frac{(1+\nu)^3(1-\nu)}{(a_{11}-\nu)(a_{12}-\nu)}}$$

$$\left\{ \int_{-\ell}^{\ell} \sqrt{\frac{a_1-i(x_o-x')}{a_2-i(x_o-x')}} \frac{\gamma_{oa}(x')}{x'-x} [k_4K(k) + k_2 \prod(\beta^2,k) - k_5 \prod(\delta^2,k)]dx' \right.$$

$$\left. + \int_{-\ell}^{\ell} \sqrt{\frac{a_1+i(x_o-x')}{a_2+i(x_o-x')}} \frac{\gamma_{oa}(x')}{x'-(2x_o-x)} [k_1K(k) + k_2 \prod(\beta^2,k) - k_3 \prod(\gamma^2,k)]dx' \right\} \tag{5-20}$$

or

$$\gamma'_{oa}(x) = \frac{1}{\pi^2}\sqrt{\frac{\ell+x}{\ell-x}}\,\mathrm{Re}\int_{-\ell}^{\ell}[\gamma'_{oa}(x')+\gamma''_{oa}(x')]$$

$$\left\{k_2\prod(\beta^2,k)\left[\frac{k_o}{x'-x}+\frac{\bar{k}_o}{x'-(2x_o-x)}\right]\right.$$

$$+K(k)\,\frac{k_4k_o}{x'-x}+\frac{k_1\bar{k}_o}{x'-(2x_o-x)}$$

$$\left.-\prod(\delta^2,k)\,\frac{k_5k_o}{x'-x}-\prod(\gamma^2,k)\,\frac{k_3\bar{k}_o}{x'-(2x_o-x)}\right\}\quad dx' \qquad (5\text{-}21)$$

Functionally Equ. (5-21) can be written as

$$\gamma'_{oa}(x) = \frac{1}{\pi^2}\sqrt{\frac{\ell-x}{\ell+x}}\,\mathrm{Re}\int_{-\ell}^{\ell}[\gamma'_{oa}(x')+\gamma''_{oa}(x')]\,f(x',x)dx'$$

which is a non-homogeneous integral equation in $\gamma'_{oa}(x)$ with $\gamma''_{oa}(x)$ given by Equ. (5-17).

VI. SIMPLIFIED ANALYSIS - METHOD OF SUBSTITUTION VORTICES

It is apparent from the above that the rigorous approach yields analytically unmanageable expressions. If at all feasible, the above integral equations would have to be solved numerically which because of the finite difference expressions and iteration procedures involved would appreciably affect the accuracy of the results. We shall therefore use a different approach to the problem which although involving certain initial simplifications permits us to obtain explicit analytical solutions with an accuracy perhaps higher than would have resulted from a numerical evaluation of the exact equations. While both the appendage and the propeller are treated as finite length plates with distributed vorticities, the effect that each of these plates has on its neighbor is assumed to be that of a concentrated vortex whose strength equals the total distributed strength of the respective plate. The method of evaluating the unknown strengths of the propeller and appendage will become clear in the course of the following analysis.

As explained previously the propeller experiences at infinity due to the cross flow U a vorticity $\gamma_{p_\infty}(y)$ given by equation (4.9). As the propeller approaches the appendage it begins to feel

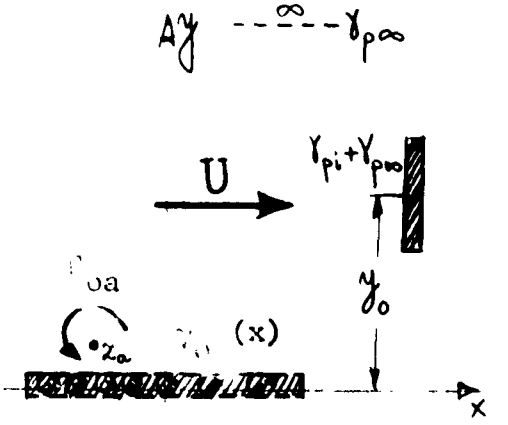

Fig. Representation of $\gamma_{ai}(x)$ by a concentrated vortex Γ_{ai}

the effect of $\gamma_{oa}(x)$, thus giving rise to an additional vorticity $\gamma_{pi}(y)$. Referring to Fig. 6 we shall now concentrate the distributed vorticity $\gamma_{oa}(x)$ of the appendage at some location z_a and call it Γ_{oa}. Since $\gamma_{p\infty}$ cancels the effect of the uniform stream U we have for the complex potential due to a concentrated vortex Γ_{oa} and a distributed vorticity γ_{pi} the following:

$$w = \frac{i\Gamma_{oa}}{2\pi} \ell n(z-z_a) + \frac{i}{2\pi} \int_{a_1}^{a_2} \gamma_{pi}(y') \ell n(z-x_o-iy')dy' \qquad (6\text{-}1)$$

From this

$$\frac{dw}{dz} = \frac{i\Gamma_{oa}}{2\pi(z-z_a)} + \frac{i}{2\pi} \int_{a_1}^{a_2} \frac{\gamma_{pi}(y')}{(z-x_o-iy')} dy'$$

Applying the condition

$$u = 0 \text{ at } x = x_o \qquad a_1 \leq y \leq a_2$$

$$\int_{a_1}^{a_2} \frac{\gamma_{pi}(y')}{y'-y} = \Gamma_{oa} \frac{(y-y_a)}{(x-x_a)^2+(y-y_a)^2}$$

This integral equation according to (4-7) yields

$$\gamma_{pi}(y) = -\frac{\Gamma_{oa}}{\pi^2} \sqrt{\frac{y_o + \frac{c}{2} - y}{y - y_o + \frac{c}{2}}} \int_{a_1}^{a_2} \sqrt{\frac{s - y_o + \frac{c}{2}}{y_o + \frac{c}{2} - s}} \frac{s}{(s-y_a)^2+(x_o-x_a)^2} \frac{ds}{s-y}$$

The circulation is given by

$$\Gamma_{op} = \int_{a_1}^{a_2} (\gamma_{p\infty} + \gamma_{pi})\, dy = 2U \int_{a_1}^{a_2} \sqrt{\frac{y_o + \frac{c}{2} - y}{y + \frac{c}{2} - y_o}}\, dy$$

$$- \frac{\Gamma_{oa}}{\pi^2} \int_{a_1}^{a_2} \sqrt{\frac{y_o + \frac{c}{2} - }{y - y_o + \frac{c}{2}}} \int_{a_1}^{a_2} \sqrt{\frac{s - y_o + \frac{c}{2}}{y_o + \frac{c}{2} - s}} \frac{s}{(s-y_a)^2 + (x_o - x_a)^2} \frac{ds}{s-y}\, dy$$

Using the substitution $\zeta = \frac{y - y_o}{\frac{c}{2}}$ we have for the first right-hand integral

$$\Gamma_{p\infty} = 2U \frac{c}{2} \int_{-1}^{1} \sqrt{\frac{1-\zeta}{1+\zeta}}\, d\zeta = \pi U c \qquad (6\text{-}2)$$

For the second integral, integrating first with respect to y

$$I_y = \int_{-1}^{1} \sqrt{\frac{1-\zeta}{1+\zeta}} \frac{d\zeta}{\frac{s - y_o}{\frac{c}{2}} - \zeta} = \pi$$

this being a Cauchy principal value integral. Now since

$$\frac{s - y_a}{(s-y_a)^2 + (x_o - x_a)^2} = \mathrm{Re} \frac{1}{s - [y_a + i(x_o - x_a)]}$$

and writing

$$\zeta = \frac{s - y_o}{\frac{c}{2}} \qquad p' = \frac{(y_o - y_a) + i(x_o - x_a)}{\frac{c}{2}}$$

we have

$$\Gamma_{p\infty} = -\frac{\Gamma_{oa}}{\pi} \mathrm{Re} \int_{-1}^{1} \sqrt{\frac{1+\zeta}{1-\zeta}} \frac{d\zeta}{\zeta - p'} \qquad (6\text{-}3)$$

The solution to the above integral is given by (A-7) and thus

$$\Gamma_{pi} = -\Gamma_{oa}\,\mathrm{Re}\left[1 - \sqrt{\frac{p'-1}{p'+1}}\,\right]$$

The total circulation is thus

$$\Gamma_{op} = \Gamma_{p\infty} + \Gamma_{pi} =$$

$$= \pi U c + \Gamma_{oa}\,\mathrm{Re}\left[\sqrt{\frac{(y_o-y_a-\frac{c}{2})+i(x_o-x_a)}{(y_o-y_a+\frac{c}{2})+i(x_o-x_a)}} - 1\right] \qquad (6\text{-}4)$$

To find $\gamma_{oa}(x)$ we treat $\gamma_{op}(y)$ as a concentrated vortex located at some appropriate coordinate z_p and write the complex potential as due to Γ_{op} and a distributed vorticity $\gamma_{oa}(x)$ along the appendage. We thus have

$$w = \frac{i\Gamma_{op}}{2\pi}\,\ell n(z-x_p-iy_p) + \frac{i}{2\pi}\int_{-\ell}^{\ell}\gamma_{oa}(x')\,\ell n(z-x')dx'$$

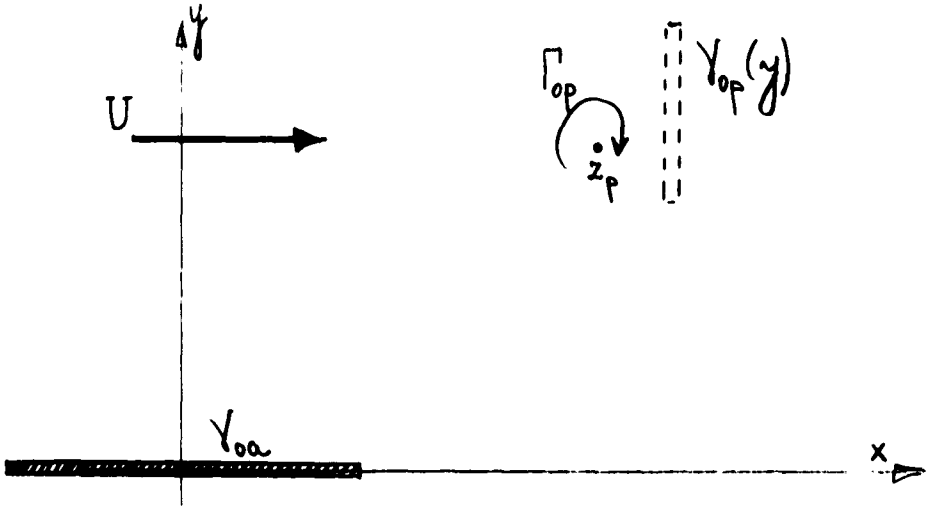

Figure 7.

Representation of $\gamma_{op}(y)$ by a concentrated vortex Γ_{op}

$$\frac{dw}{dz} = \frac{i\Gamma_{op}}{2\pi} \frac{1}{z-x_p-iy_p} + \frac{i}{2\pi} \int_{-\ell}^{\ell} \frac{\gamma_{oa}(x')dx'}{z-x'}$$

The condition of no normal velocity along the appendage requires

$$v = 0 \text{ on } y = 0 \quad -\ell \leq x \leq \ell$$

and thus

$$\int_{-\ell}^{\ell} \frac{\gamma_{oa}(x')dx'}{x'-x} = \frac{\Gamma_{op}(x-x_p)}{(x-x_p)^2+y_p^2}$$

Again using Equ.(4-7) for this integral equation we obtain

$$\gamma_{oa}(x) = -\frac{\Gamma_{op}}{\pi^2} \sqrt{\frac{\ell-x}{\ell+x}} \int_{-\ell}^{\ell} \sqrt{\frac{\ell+s}{\ell-s}} \frac{s-x_p}{(s-x_p)^2+y_p^2} \frac{ds}{s-x} \qquad (6\text{-}5)$$

Since

$$\Gamma_{oa} = \int_{-\ell}^{\ell} \gamma_{oa}(x)dx$$

we can write

$$\Gamma_{oa} = -\frac{\Gamma_{op}}{\pi^2} \int_{-\ell}^{\ell} \sqrt{\frac{\ell-x}{\ell+x}} \frac{dx}{s-x} \int_{-\ell}^{\ell} \sqrt{\frac{\ell+s}{\ell-s}} \frac{s-x_o}{(s-x_p)^2+y_p^2} ds$$

$$= -\frac{\Gamma_{op}}{\pi^2} \pi \int_{-\ell}^{\ell} \sqrt{\frac{\ell+s}{\ell-s}} \frac{s-x_o}{(s-x_p)^2+y_p^2} ds$$

By partial fractions the above integral can be broken up into a sum of two integrals of the form of I_{12} with their solution

given by (A-6). Thus

$$I = \pi \, \mathrm{Re} \left[1 - \sqrt{\frac{x_p+\ell+iy_p}{x_p-\ell+iy_p}}\right]$$

and

$$\Gamma_{oa} = \Gamma_{op} \, \mathrm{Re} \left[\sqrt{\frac{x_p+\ell+iy_p}{x_p-\ell+iy_p}} - 1\right] \tag{6-6}$$

Solving from expressions (6-4) and (6-6) for Γ_{op} and Γ_{oa} we obtain

$$\Gamma_{oa} = \pi U c \, \frac{\mathrm{Re}(A-1)}{1-\mathrm{Re}(A-1)\mathrm{Re}(B-1)} \tag{6-7}$$

$$\Gamma_{op} = \pi U c \, \frac{1}{1-\mathrm{Re}(A-1)\mathrm{Re}(B-1)} \tag{6-8}$$

where

$$A = \sqrt{\frac{(x_p+\ell)+iy_p}{(x_p-\ell)+iy_p}} \qquad B = \sqrt{\frac{(y_o-y_a-\frac{c}{2})+i(x_o-x_a)}{(y_o-y_a+\frac{c}{2})+i(x_o-x_a)}}$$

The method of determining x_p, y_p, x_a and y_a, the coordinates of the substitution vortices, is given in detail in the Appendix. The exact formulae for the four coordinates are given by equations (B.15), (B.18), (B.20) and (6-8). It can be verified either analytically or by sample calculations that $x_p = x_o$ and $y_a = 0$, i.e. that the substitution vortices lie on the plates, the only variation occurring along and not away from the appendage or propeller. We can thus rewrite A and B as

$$A = \sqrt{\frac{(x_o+\ell)+iy_p}{(x_o-\ell)+iy_p}} \qquad B = \sqrt{\frac{(y_o-\frac{c}{2})+i(x_o-x_a)}{(y_o+\frac{c}{2})+i(x_o-x_a)}} \tag{6-9}$$

VII. EXPRESSIONS FOR THE UNSTEADY FORCES

a) The Quasi-steady Forces

According to equ. (3-1) the quasi-steady forces are

$$\Gamma_{oa} = \rho U \Gamma_{oa}$$

$$F_{op} = \rho V \Gamma_{op}$$

or

$$\frac{rF_{oa}}{T} = \frac{Re(A-1)}{1-Re(A-1)Re(B-1)} \tag{7-1}$$

$$\frac{F_{op}}{T} = \frac{1}{1-Re(A-1)Re(B-1)} \tag{7-2}$$

where $T = \rho\pi cUV$ is the unperturbed propeller thrust. It will be noticed from the above that

$$F_{oa} = \frac{Re(A-1)}{r} F_{op} . \tag{7-3}$$

Also

$$\frac{F_{opi}}{T} = \frac{Re(A-1)Re(B-1)}{1-Re(A-1)Re(B-1)} \tag{7-4}$$

b) The Apparent-Mass Forces

As mentioned in Part III the determination of the apparent-mass forces involves the evaluation of the moment-of-momentum integrals namely

$$M_a = \int_{-\ell}^{\ell} x\gamma_{oa}(x)dx$$

and

$$M_p = \int_{a_1}^{a_2} y'\gamma_{op}(y')dy'.$$

Using for $\gamma_{oa}(x)$ the expression (6-5) we have

$$M_a = -\frac{\Gamma_{op}}{\pi^2} \int_{-\ell}^{\ell} x \sqrt{\frac{\ell-x}{\ell+x}} \int_{-\ell}^{\ell} \sqrt{\frac{\ell+s}{\ell-s}} \frac{s-x_o}{(s-x_p)^2+y_p^2} \frac{ds}{s-x} dx.$$

The s integral above has been solved previously, equ. (A-1), thus

$$M_a = \frac{\Gamma_{op}}{\pi} \text{Re} \sqrt{\frac{(x_p+\ell)+iy_p}{(x_p-\ell)+iy_p}} \int_{-\ell}^{\ell} \frac{x}{(x_p-x)+iy_p} \sqrt{\frac{\ell-x}{\ell+x}} dx$$

Let us consider the above integral with $z_p = x_p + iy_p$

$$I = \int_{-\ell}^{\ell} \frac{x}{z_p-x} \sqrt{\frac{\ell-x}{\ell+x}} dx \qquad (7\text{-}5)$$

Breaking it up by means of partial fractions

$$I = -\int_{-\ell}^{\ell} \sqrt{\frac{\ell-x}{\ell+x}} dx + z_p \int_{-\ell}^{\ell} \sqrt{\frac{\ell-x}{\ell+x}} \frac{dx}{z_p-x}$$

and using for the first integral the substitution $x = \cos\theta$ and for the second the solution given by equ. (A-7) we have

$$I = -\ell\pi + z_p\pi \left[1 - \sqrt{\frac{z_p-\ell}{z_p+\ell}} \right] \qquad (7\text{-}6)$$

Thus

$$M_a = \Gamma_{op} \text{Re} \left[\sqrt{(x_p+iy_p)^2-\ell^2} - (x_p+iy_p) \right] \qquad (7\text{-}7)$$

For M_p using the expression for γ_{op} we have

$$M_p = 2U \int_{a_1}^{a_2} (y-y_o) \sqrt{\frac{y_o+\frac{c}{2}-y}{y+\frac{c}{2}-y_o}}\, dy - \frac{\Gamma_{oa}}{\pi} \int_{a_1}^{a_2} (y-y_o) \sqrt{\frac{y_o+\frac{c}{2}-y}{y-y_o+\frac{c}{2}}} \frac{dy}{s-y} \int_{a_1}^{a_2} \frac{s-y_a}{(s-y_a)^2+(x_o-x_a)^2}\, ds$$

Writing $\frac{y-y_o}{\frac{c}{2}} = \zeta$ we have

$$M_p = 2U\left(\frac{c}{2}\right)^2 \int_{-1}^{1} \zeta \sqrt{\frac{1-\zeta}{1+\zeta}}\, d\zeta - \frac{\Gamma_{oa}}{\pi^2}\left(\frac{c}{2}\right) \int_{a_1}^{a_2} \int_{-1}^{1} \frac{\zeta-\zeta^2}{\sqrt{1-\zeta^2}} \frac{d\zeta}{\frac{s-y_o}{\frac{c}{2}}-\zeta} f(s)ds$$

$$= 2U\left(\frac{c}{2}\right)^2 \left(-\frac{\pi}{2}\right) - \frac{\Gamma_{oa}}{\pi^2} \int_{a_1}^{a_2} \pi\left[(s-y_o)-\frac{c}{2}\right] f(s)ds$$

$$= -\pi U\left(\frac{c}{2}\right)^2 + \frac{\Gamma_{oa}}{\pi} \int_{a_1}^{a_2} \sqrt{\left(\frac{c}{2}\right)^2-(s-y_o)^2}\ \mathrm{Re}\ \frac{ds}{s-[y_a-i(x_o-x_a)]}$$

Using the substitution $\frac{s-y_o}{\frac{c}{2}} = \zeta$ we have for the integral

$$I = \frac{c}{2} \int_{-1}^{1} \sqrt{1-\zeta^2}\ \frac{d\zeta}{\zeta-p'} = \frac{c}{2}\,\pi\left[-p' + \sqrt{p'^2-1}\ \right] \qquad (7\text{-}8)$$

where $$p' = \frac{(y_a-y_o)+i(x_a-x_o)}{\frac{c}{2}}$$

Thus

$$M_p = -\pi U\left(\frac{c}{2}\right)^2 + \Gamma_{oa}\mathrm{Re}\left\{(y_o-y_a)+i(x_o-x_a) - \sqrt{[(y_o-y_a)+i(x_o-x_a)]^2-\left(\frac{c}{2}\right)^2}\right\} \qquad (7\text{-}9)$$

The apparent mass forces are given by

$$F_{1a} = -\rho \frac{\partial}{\partial t} M_a$$

$$F_{1p} = -\rho \frac{\partial}{\partial t} M_p$$

Since $\frac{\partial}{\partial t} = \frac{\partial}{\partial y_o} \frac{\partial y_o}{\partial t} = - V \frac{\partial}{\partial y_o}$

$$F_{1a} = \rho V \frac{\partial}{\partial y_o} M_a$$

$$F_{1p} = \rho V \frac{\partial}{\partial y_o} M_p$$

Since $x_p = x_o$ and $y_a = 0$ we can rewrite the normalized expressions for F_{1a} and F_{1p} as follows:

$$\frac{F_{1a}}{T} = \frac{\partial}{\partial y_o} \bar{\Gamma}_{op} \text{ Re } [\sqrt{(\bar{x}_o+i\bar{y}_p)^2 - 1} \ -(\bar{x}_o+i\bar{y}_p)] \qquad (7\text{-}10)$$

$$\frac{F_{1p}}{T} = \frac{\partial}{\partial y_o} \bar{\Gamma}_{op} \text{ Re} \left\{ \bar{y}_o+i(\bar{x}_o-\bar{x}_a) - \sqrt{[\bar{y}_o+i(\bar{x}_o-\bar{x}_a)]^2-\bar{c}^2} \right\} \qquad (7\text{-}11)$$

In differentiating the above expressions it should be kept in mind that these in addition to y_o contain y_p and x_a, themselves functions of y_o as given by equs. (B.18) to (B.20) in Appendix B.

c) The Wake Forces

As mentioned in part III the unsteady circulation on both the appendage and propeller will cause the shedding of wake vortices and these in turn will induce an additional circulation round the two plates. For the appendage the circulation caused by a single concentrated vortex located at some distance x along the wake is by setting $c = y_p = 0$, $x_o = x$ in equ. (6-7) given by

$$\bar{\Gamma}_{oa}(x,o) = \left(\sqrt{\frac{\bar{x}+1}{\bar{x}-1}} - 1 \right) \tag{7-12}$$

Thus according to equs. (3-4) and (3-5) the integral equation for the wake vorticity $\gamma(\zeta)$ and the force induced by it on the appendage are

$$\int_1^{1+R} \gamma(\zeta,t) \sqrt{\frac{\zeta+1}{\zeta-1}}\, d\zeta = -\frac{\Gamma_a(t)}{\ell} \tag{7-13}$$

$$F_2 = \rho U \ell \int_1^{1+R} \frac{-\gamma(\zeta)\, d\zeta}{\sqrt{\zeta^2-1}} \tag{7-14}$$

Introducing the variable s, measured from the initial position of the appendage, $s = (1+R) - \zeta$, we have for equ (7-13) by writing $\mu(s) = \gamma(1+R-s)$

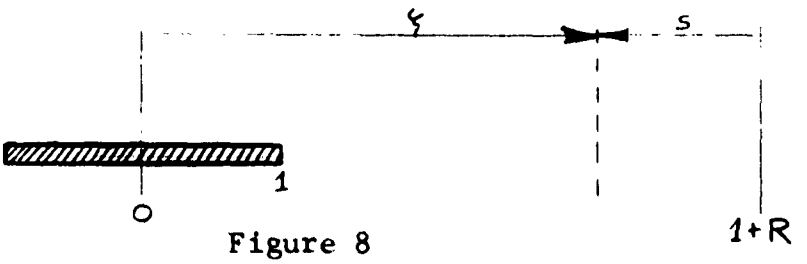

Figure 8

Coordinates of Wake Vorticity

$$\int_0^R \mu(s) \sqrt{\frac{2+R-s}{R-s}}\, ds = -\frac{\Gamma_{oa}}{\ell} \tag{7-15}$$

This integral equation is difficult to solve, particularly in view of the complexity of the expression for Γ_{oa}. We shall obtain a solution to (7-15) for a unit impulse i.e. for $\bar{\Gamma}_{oa} = 1$ and then sum the result by means of the Duhamel integral. For a unit impulse equ. (7-15) reads

$$\int_0^R \mu^{(1)}(s) \sqrt{\frac{2+R-s}{R-s}}\, ds = -\frac{1}{\ell} \tag{7-16}$$

and thus the unit force produced by this unit impulse is

$$F_2^{(1)} = \rho U \int_1^{1+R} \frac{\mu^{(1)}(1+R-\zeta)}{\sqrt{\zeta^2-1}}\, d\zeta \tag{7-17}$$

where $\mu^{(1)}$ is the solution to (7-16).

According to Garrick[6] the value of the integral in equ. (7-17) is within an accuracy of 2% given by

$$\int_1^{1+R} \frac{\mu^{(1)}(1+R-\zeta)}{\sqrt{\zeta^2-1}}\, d\zeta = -\frac{2}{4+R}$$

and thus

$$F_2^{(1)} = -\frac{2\rho U}{4+R} \quad (\text{unit circulation}) \tag{7-18}$$

The above is the force due to a unit impulse of magnitude $\bar{\Gamma}_{oa}=0$ at $t < 0$ and $\bar{\Gamma}_{oa}=1$ for $t \geq 0$. Using the Duhamel method of

superposition for any arbitrary input Γ_{oa} we have

$$\Delta F_2 = F_2^{(1)}(t-\tau)\Delta\Gamma_{oa}(\tau) + \Gamma_{oa}(0)F_2^{(1)}(t).$$

Since at $t=0$ $\Gamma_{oa}=0$ and $\Delta\Gamma_{oa}(\tau) = \frac{d\Gamma_{oa}}{d\tau}\, d\tau$.

$$F_{2a} = -\, 2\rho U \int_o^t \left(\frac{d\Gamma_{oa}(\tau)}{d\tau}\right) \frac{d\tau}{4 + \frac{U}{\ell}(t-\tau)} \tag{7-19}$$

Integrating by parts

$$F_{2a} = -\, 2\rho U \left\{ \Gamma_{oa} \frac{1}{4 + \frac{U}{\ell}(t-\tau)} \Bigg|_o^t - \int_o^t \Gamma_{oa} \frac{d(\frac{U}{\ell}\tau)}{4 + \frac{U}{\ell}(t-\tau)^2} \right.$$

Writing

$$\bar{\tau} = \frac{U\tau}{\ell}$$

$$F_{2a} = \rho\pi c U^2 \left\{ -\frac{1}{2}\bar{\Gamma}_{oa} + 2\int_o^R \frac{\bar{\Gamma}_{oa}(\bar{\tau})\,d\bar{\tau}}{(4+R-\bar{\tau})^2} \right\} \tag{7-20}$$

or

$$\frac{rF_{2a}}{T} = -\frac{1}{2}\left(\frac{rF_{oa}}{T}\right) + 2\int_o^R \frac{\bar{\Gamma}_{oa}(\bar{\tau})\,d\bar{\tau}}{(4+R-\bar{\tau})^2}$$

Eq. (7-20) tells us that the wake force is always equal to $-\frac{1}{2}\Gamma_{oa}$ or minus one-half of the quasi steady force plus a correction C given by

$$C = 2\int_o^R \frac{\bar{\Gamma}_{oa}(\bar{\tau})\,d\bar{\tau}}{(4+R-\bar{\tau})^2} \tag{7-21}$$

In the above

$$\bar{\Gamma}_{oa}(\bar{\tau}) = \frac{Re(A-1)}{1-Re(A-1)Re(B-1)}$$

where $\bar{y}_o = \bar{a}-rR$ with $\bar{\tau}$ replacing R for purposes of integration.

The constant a is the initial position of the propeller, later on to be pushed to infinity. In this expression t=0 implies that the propeller is at $y_o = a$ as shown in Figure 9. In order to have the propeller at y=0 at t=0 we shall employ a new time variable to be related to t by the expression

$$R = R_o + \frac{\bar{a}}{r}$$

with

$$R_o = \frac{Ut_o}{\ell}$$

Using this in (7-21) we have

$$C = 2 \int_0^{R_o + \frac{\bar{a}}{r}} \frac{\Gamma_{oa}(\bar{\tau})\, d\bar{\tau}}{(4+R_o+\frac{\bar{a}}{r}-\bar{\tau})^2} \qquad (7\text{-}22)$$

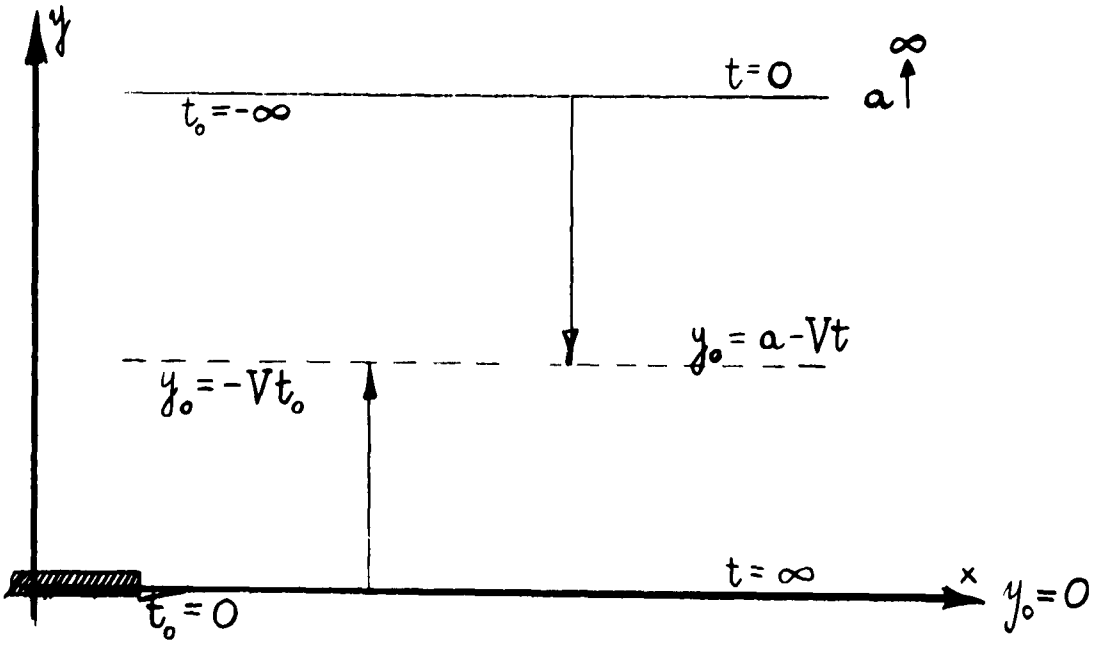

Figure 9

Time Coordinates for Propeller Position

Direct integration of (7-22) is difficult since $\Gamma_{oa}(\tau)$ in the numerator is a complicated function. However we can represent Γ_{oa} by a simpler function which by a suitable choice of constants can be made to give a fair approximation to the original expression.

Γ_{oa} in general has the shape of Figure 10 and we can write

$$\Gamma_{oa}(y_o) = \frac{q_a \Gamma_{am}}{(\bar{y}_o - \bar{y}_{om})^2 + q_a} \tag{7-23}$$

where q_a is a constant so chosen as to best approximate the exact Γ_{oa}. Since for large y_o $\Gamma_{op} \sim$ const., $\Gamma_{oa} = \Gamma_{op}$ Re(A-1) which when expanded and restricted to terms no higher than $\frac{1}{y_o^2}$ yields (for $y_p \sim y_o - \frac{c}{2}$)

$$\Gamma_{oa} = \frac{\bar{x}_o - \frac{1}{2}}{\bar{y}_o^2}$$

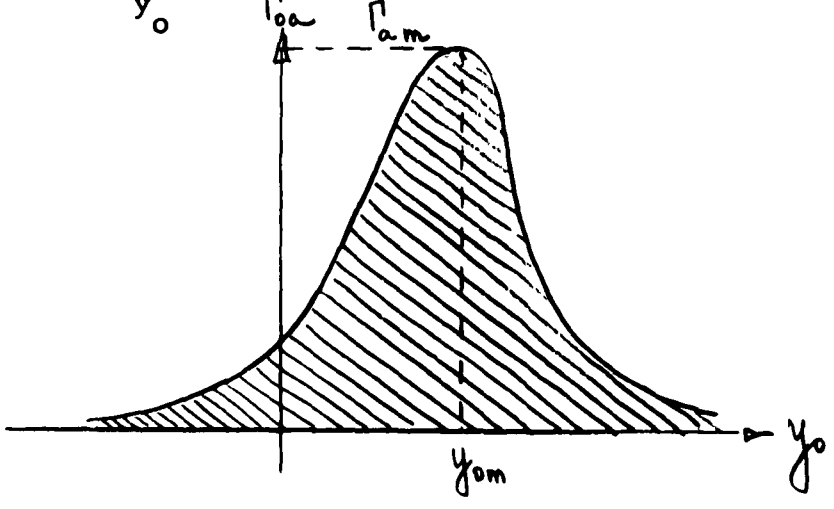

Figure 10.
Shape of $\Gamma_{oa}(y_o)$

Thus for large y_o we have $q_a\Gamma_{am} = \bar{x}_o - \frac{1}{2}$ and

$$q_a = \left(\frac{\bar{x}_o - \frac{1}{2}}{\Gamma_{am}}\right)$$

Introducing (7-23) and (7-22) and remembering that $\bar{y}_o = \bar{a} - r\bar{\tau}$

$$C = 2\, q_a\, \bar{\Gamma}_{am} \int_o^{R_o + \frac{\bar{a}}{r}} \frac{1}{(\bar{y}_{om} - \bar{a} + r\bar{\tau})^2 + q_a} \, d\bar{\tau}$$

To eliminate $\bar{a}$ from under the integral sign write

$$y_{om} - \bar{a} + r\bar{\tau} = -\zeta$$

and we have after letting $\bar{a} \to \infty$

$$C = 2rq_a\Gamma_{am} \int_{(y_o - y_{om})}^{\infty} \frac{d\zeta}{(\zeta^2 + q_a)(k+\zeta)^2} \qquad (7\text{-}24)$$

where $k = 4r - (\bar{y}_o - \bar{y}_{om})$

Breaking up (7-24) into partial fractions we have

$$C = \frac{2q_a r\, \bar{\Gamma}_{am}}{(k^2+q_a)^2} \left\{ -k \int_P^{\infty} \frac{2\zeta d\zeta}{\zeta^2+q_a} + (k^2 - q_a) \int_P^{\infty} \frac{d\zeta}{\zeta^2+q_a} \right.$$

$$\left. + (k^2+q_a) \int_P^{\infty} \frac{d\zeta}{(\zeta+k)^2} + 2k \int_P^{\infty} \frac{d\zeta}{\zeta+k} \right\}$$

where $P = (\bar{y}_o - \bar{y}_{om})$ These integrations are easily performed yielding

$$C = \frac{2q_a r\,\bar{\Gamma}_{am}}{[(4r-P)^2+q_a]^2} \left\{ (4r-P)\,\ell n\,\frac{(4r-P)^2+q_a}{16r^2} \right.$$

$$\left. + \frac{(4r-P)^2-q_a}{\sqrt{q_a}}\left(\frac{\pi}{2} - \tan^{-1}\frac{P}{\sqrt{q_a}}\right) + \frac{(4r-P)^2+q_a}{4r} \right\} \qquad (7\text{-}25)$$

Thus the force on the appendage due to the wake is

$$\frac{rF_{2a}}{T} = -\frac{1}{2}\left(\frac{rF_{oa}}{T}\right) + C \qquad (7\text{-}26)$$

For the propeller the effect of an arbitrary concentrated vortex located at some (x,y) is

$$\Gamma_{op} = C_o\ \mathrm{Re}\left(\sqrt{\frac{(\bar{y}_o-\bar{y}-\bar{c})+i(\bar{x}_o-\bar{x})}{(\bar{y}_o-\bar{y}+\bar{c})+i(\bar{x}_o-\bar{x})}} - 1\right)$$

Shifting the origin to (x_o, y_o) we obtain

$$\Gamma_{op} = C_o\ \mathrm{Re}\left(\sqrt{\frac{\zeta+\bar{c}+i\eta}{\zeta-\bar{c}+i\eta}} - 1 \right)$$

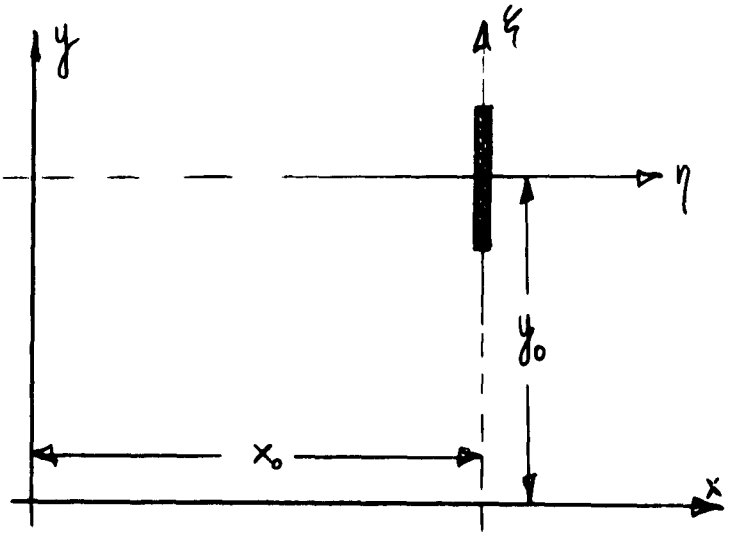

Figure 11.

Propeller Coordinates

In accordance with our original assumption of $V >> U$ the shed vortices in the wake are assumed to lie essentially along $\eta = 0$; thus

$$\Gamma_{op}(\zeta,o) = C_o \left(\sqrt{\frac{\zeta+\bar{c}}{\zeta-\bar{c}}} - 1 \right)$$

This is an expression similar to (7-12) and we can thus write down the expression for the wake force as

$$F_{2p} = \rho U \left(\frac{c}{2}\right) \int_1^{1+S} \frac{\gamma(\zeta)d}{\sqrt{\zeta^2-1}} \qquad (7\text{-}27)$$

where $S = \frac{Vt}{c/2}$.

The treatment of (7-27) is the same as that of (7-14) and thus

$$F_{2p} = -\frac{1}{2} F_{op} + 2\pi\rho UVc \int_0^S \frac{\bar{\Gamma}_{op}(\tau')d\tau'}{(4+S-\tau')^2}$$

where $\tau' = \frac{V\tau}{c/2}$ and all quantities in Γ_{op} have been normalized by $c/2$ instead of by ℓ, and

$$y_o' = a' - \tau'.$$

Using $S = S_o + a'$, a shift of variables to a new time t_o similar to that illustrated in Figure 9, we are now to evaluate

$$D = \int_o^{S_o+a'} \frac{\bar{\Gamma}_{op}(\tau')}{(4+S_o+a-\bar{\tau}')^2} d\tau'$$

The shape of $\Gamma_{op}(y_o)$ as shown later on is of the form given in Figure 12.

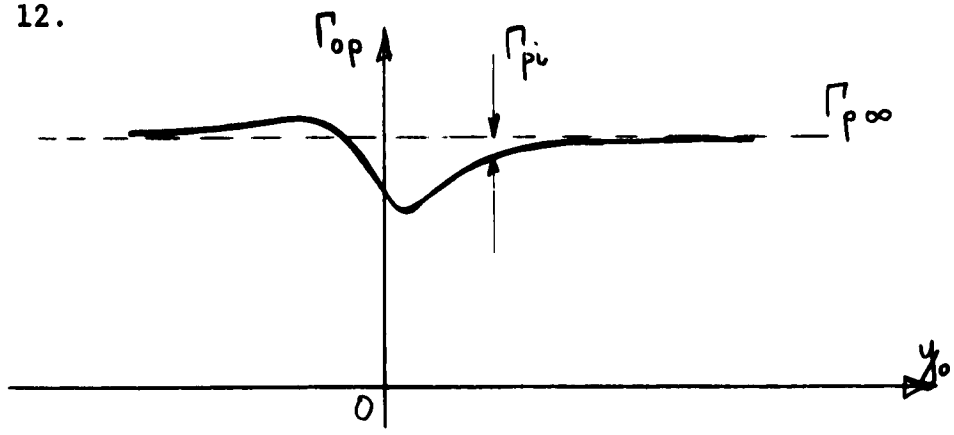

Figure 12.
Shape of $\Gamma_{op}(y_o)$

Thus $\Gamma_{op} = \Gamma_{p\infty} + \Gamma_{pi}$

and

$$F_{2p} = -\frac{1}{2} F_{op} + 2\pi\rho UVc \int_o^{S_o+a'} \frac{\bar{\Gamma}_{p\infty} + \bar{\Gamma}_{pi}}{(4+S_o+a'-\tau')^2} d\tau'$$

$$= -\frac{1}{2} F_{op} + \frac{1}{2} F_{p\infty} + 2\pi\rho UVc \int_o^{S_o+a'} \frac{\bar{\Gamma}_{pi}}{(4+S_o+a'-\tau')^2} d\tau'$$

or

$$\frac{F_{2p}}{T} = -\frac{1}{2} F_{opi}/T + 2 \int_o^{S_o+a'} \frac{\bar{\Gamma}_{pi}(a-\tau')}{(4+S_o+a'-\tau')^2} d\tau'$$

Thus since Γ_{pi} is the only varying component of the total circulation the wake force is equal to $-\frac{1}{2} F_{opi}$ plus a correction term given by

$$D = 2 \int_{o}^{S_o+a'} \frac{\bar{\Gamma}_{pi}(a'-\tau')}{(4+S_o+a'-\tau')^2} \, d\tau' \qquad (7\text{-}28)$$

In the above

$$\bar{\Gamma}_{pi}(y_o) = \frac{Re(A-1)Re(B-1)}{1-Re(A-1)Re(B-1)}$$

where, for large values of y_o, $\bar{\Gamma}_{pi}$ can be shown to vary as

$$\frac{\bar{c}(\bar{x}_o - \frac{1}{2})}{\bar{y}_o^3} \quad .$$

To eliminate a' from under the integral sign we write

$$a'-\tau' = \xi$$

and since $- S_o = y_o$

$$D = - 2 \int_{a'}^{y_o} \frac{\bar{\Gamma}_{pi}(\xi)d\xi}{(4-y_o' + \xi)^2}$$

Letting $a' \longrightarrow \infty$ we have

$$D = 2 \int_{y_o'}^{\infty} \frac{\bar{\Gamma}_{pi}(\xi)}{(4-y_o' + \xi)^2} \, d\xi \qquad (7\text{-}29)$$

VIII NUMERICAL EVALUATION OF FORCES

By summing the three component forces we have for the resultant force on the appendage

$$\frac{rF_a}{T} = \frac{rF_{oa}}{T} + \frac{F_{1a}}{T} - \frac{1}{2}\left(\frac{rF_{oa}}{T}\right) + C$$

or

$$\frac{rF_a}{T} = \frac{1}{2}\left(\frac{rF_{oa}}{T}\right) + \frac{F_{1a}}{T} + C \qquad (8\text{-}1)$$

This expression is implicitly dependent on r and is then a function of four parameters $\bar{y}_o$, x_o, c and r. The total force on the propeller is

$$\frac{F_p}{T} = \frac{F_{op}}{T} + \frac{F_{1p}}{T} - \frac{1}{2}\frac{F_{pi}}{T} + D$$

or since $F_{op} = F_{p\infty} + F_{pi} = T + F_{pi}$

$$\frac{F_p}{T} = 1.0 + \frac{1}{2}\frac{F_{pi}}{T} + \frac{F_{1p}}{T} + D \qquad (8\text{-}2)$$

The force on the propeller due to neglecting second order effects is independent of r.

Equations (8-1) and (8-2) were evaluated on an IBM 7090 digital computer using the expressions derived in Section VII. Expression D as given by Eq. (7-29) was the only unevaluated integeral and it has been integrated numerically using Simpson's rule. The following discrete values of the involved parameters were used

$\bar{y}_o$	from + 5.0 to -5.0 in intervals of 0.1
$\bar{c}$	0, .1, .2, .3, .5
$\bar{x}_o$	$\pm$1.6, $\pm$1.4, $\pm$1.2 $\pm$ 1.05
r	2, 3, 4.

The values for both the component and total forces are available in tabular form and the essential results of these calculations are plotted in Figures 13 through 51. In these all forces are plotted in terms of the unperturbed propeller thrust T_∞ or $F_{p\infty}$, whereas all distances and the propeller half-chord c/2 have been normalized by the appendage half-chord ℓ.

IX. DISCUSSION

The various expressions for the component and total forces given in the preceding sections contain the propeller-appendage length ratio $\bar{c} = c/2\ell$ as a parameter. When in these expressions we set $\bar{c} = 0$, the forces on both propeller and appendage disappear. However, in spite of this disappearance, the dimensionless ratios F/T approach definite non-zero limits as $\bar{c} \longrightarrow 0$. The curves for the case $\bar{c} = 0$ are therefore to be interpreted as plots of these limiting values. These $\bar{c} = 0$ curves are, [illegible] identical with the curves of Breslin who obtained the forces on the appendage by making the simplifying assumption that the propeller has both a constant non-zero circulation and zero chord.

In the discussion to follow we shall first describe the effect of varying x_o, r and $\bar{c}$ on the nature and magnitude of the hydrodynamic forces and then draw some conclusions with regard to optimum design features of propeller-appendage assemblies.

Rudder Position ($+x_o$)

Effects on Appendage - Figures 13 through 16 show sample plots of the component forces indicating that while the apparent-mass forces go up more than proportionately with c, the [illegible] wake forces change less than proportionately with c. The complex way in which these component forces make up the total force is shown in a sample plot of Fig. 17. Figs. 19 through 29 show the variations of the total forces and these can be summarized as follows:

a) The forces are predominantly positive, i.e., they act in a direction opposite to propeller motion. For reasonable spacings, $\bar{x}_o > 1.1$, a minimum in the value of F_a/T occurs around $\bar{c} = .15$ for $r = 2$ and around $\bar{c} = .1$ for $r = 4$.

b) The maximum force occurs before the propeller center passes the appendage, $0 < y_{om} < \ell$, with y_{om} moving closer towards 0 with a decrease in $\bar{c}$.

c) After the propeller has passed the appendage the forces are usually negative and negligible

d) The maximum forces decrease with an increase in propeller velocity. F_{am} is reduced by about 25% in going from $r = 2$ to $r = 4$

e) As shown in Figs. 31 and 33 the forces go up drastically with a decrease in x_o. F_{am} increases 2-1/2 times in going from $x_o = 1.6$ to $x_o = 1.2$.

Effects on Propeller

The apparent mass forces and also usually the wake force go up, according to Figs. 35 through 37, more than proportionately with $\bar{c}$ while the quasi steady forces go up less than proportionately with $\bar{c}$. Fig. 38 shows how the three component forces make up the total force. It should be noticed that the line Fa/T = 1 represents the force on the propeller at infinity or the unperturbed thrust Thus the plots in Figs. 40 to 45 in addition to the actual forces on the propeller also represent the ratio of the actual force to that without interference. The variation of the total force can be viewed as a small or moderate perturbation round $F_{p\infty}/T = 1$ and thus the propeller force always acts in the same direction F_p is independent

of r and its dependence on x_o and $\bar{c}$ can be summarized as follows:

a) The effect of appendage interference is in general to yield forces less than the unperturbed propeller thrust. This reduction increases with $\bar{c}$.

b) The propeller force reaches a minimum before it passes the appendage in the region of $0 < \bar{y}_o < .6$

c) A measurable maximum as shown in Fig. 47, is reached by F_p only at $\bar{x}_o < 1.2$.

d) After the propeller has passed the appendage the forces on it are slightly higher than the unperturbed thrust.

From an analytical point of view it is interesting to note in Figures 49 and 51 the rather wide scatter of the coordinates of the substitution vortices. The value of $\bar{x}_a$ even fails to approach the expected quarter-chord position as $\bar{y}_o \longrightarrow \infty$

Skeg Position ($-x_o$)

Effects on Appendage - For the case where the propeller is upstream of the appendage both the quasi-steady forces and the wake forces increase more than proportionately with an increase in $\bar{c}$. However, the apparent mass forces exhibit a fairly complex behaviour. The depressions occuring at $\bar{y}_o < 0$ were unexpected and their influence can be noticed in the shape of the total force as exemplified in Fig. 18. From the succeeding plots of the total appendage force for a skeg position the following general comments can be made.

a) Except for $\bar{x}_o \geq -1.2$ the forces are predominantly negative acting in the direction of propeller motion. The ratio F_a/T seems to

increase with an increase in $\bar{c}$. Thus with an increase in propeller chord the value of F_a will increase both by virtue of an increase in c as well as an increase in the coefficient F_a/T.

b) The maximum (negative) force occurs before the propeller center passes the appendage and this occurs in the fairly narrow range, $.1 < \bar{y}_o < .5$.

c) After the propeller has passed the appendage the forces are usually positive and negligible.

d) The maximum (negative) forces decrease with an increase in propeller velocity.

e) The forces go up drastically with a decrease in $\bar{x}_o$.

f) The peak forces for a skeg arrangement are quantitatively about the same and of opposite sign as the peak forces for a rudder arrangement.

Effects on Propeller - The apparent mass forces go up less than proportionately with an increase in $\bar{c}$ while the quasi-steady and wake forces go up more than linearly with $\bar{c}$. From Figs. 40 to 45 the following emerges:

a) The effect of appendage interference is to increase the propeller force above that of the unperturbed thrust.

b) As shown in Fig. 48b F_p reaches a maximum in the region $.3 < \bar{y}_o < 1.0$

c) As shown in Fig. 47 the value of the maximum force increases with a decrease in $\bar{x}_o$ and an increase in $\bar{c}$.

d) After the propeller has passed the appendage the forces on it are slightly below the value of the unperturbed thrust.

As shown in Fig. 50 the scatter of the substitution vortices is here smaller than for the propeller-rudder arrangement and for large values of $\bar{y}_o$ they approach the quarter-chord position on both propeller and appendage.

X. CONCLUSIONS

1. Spacing closer than $\bar{x}_o = |1.2|$ between propeller and appendage should be avoided for at least two reasons; at $\bar{x}_o < |1.2|$ there are two cycles of stress reversals; and the peak forces become excessive.

2. For a given propeller chord size c there exists an optimum ratio $\bar{c}$ which will produce the smallest peak force on the appendage. These values are $2\ell \approx 7c$ for low propeller speeds (r = 2); and $2\ell = 10c$ for high propeller speeds (r = 4). The above, of course, applies to the practical range of $\bar{c}$ values, $.1 < \bar{c} < .5$ and excludes the case of $\ell = 0$ when the force on the appendage would be zero.

3. Peak forces on both appendage and propeller always occur before the propeller center passes the appendage; the forces are negligible after the propeller has passed the appendage.

4 The peak forces on the appendage do not differ appreciably for either skeg or rudder arrangement.

5. The peak forces on the propeller for a rudder arrangement are essentially equal to the unperturbed thrust; for a skeg arrangement they are measurably higher.

6. On the appendage the peak forces increase less than proportionately with an increase in V; on the propeller they are proportional to its velocity.

REFERENCES

1. Lewis, F.M. "Propeller Vibration", Trans. of Soc. of Naval Arch. and Mar. Eng., Vol. 43, pp. 252-285, 1935.
2. Lewis, F.M. "Propeller Vibration", Trans. of Soc. of Naval Arch. and Mar. Eng., Vol. 44, pp. 501-519, 1936.
3. Breslin, J.P. "The Unsteady Pressure Field Near A Ship Propeller and the Nature of the Vibratory Forces Produced On An Adjacent Surface", Stevens Inst. of Tech. Exp. Towing Tank, Report No. 609, June 1956.
4. Karman von Th. and Sears, W.R. "Airfoil Theory for Non-Uniform Motion" Jour. of Aeronautical Sciences", Vol. 5, No. 10, August 1938.
5. Cheng, H.K. and Rott, N. " Generalizations of The Inversion Formula of Thin Airfoil Theory", Journal of Rational Mechanics and Analysis, Indiana University, Vol. 3, No. 3, p. 377, 1954.
6. Garrick, I.E. "On Some Reciprocal Relations in The Theory of Non-Stationary Flows", NASA Report No. 629, 1938.
7. L.M. Milne-Thompson, Theoretical Aerodynamics , Macmillan and Co., Ltd., 3rd Edition, 1958, p. 153ff.

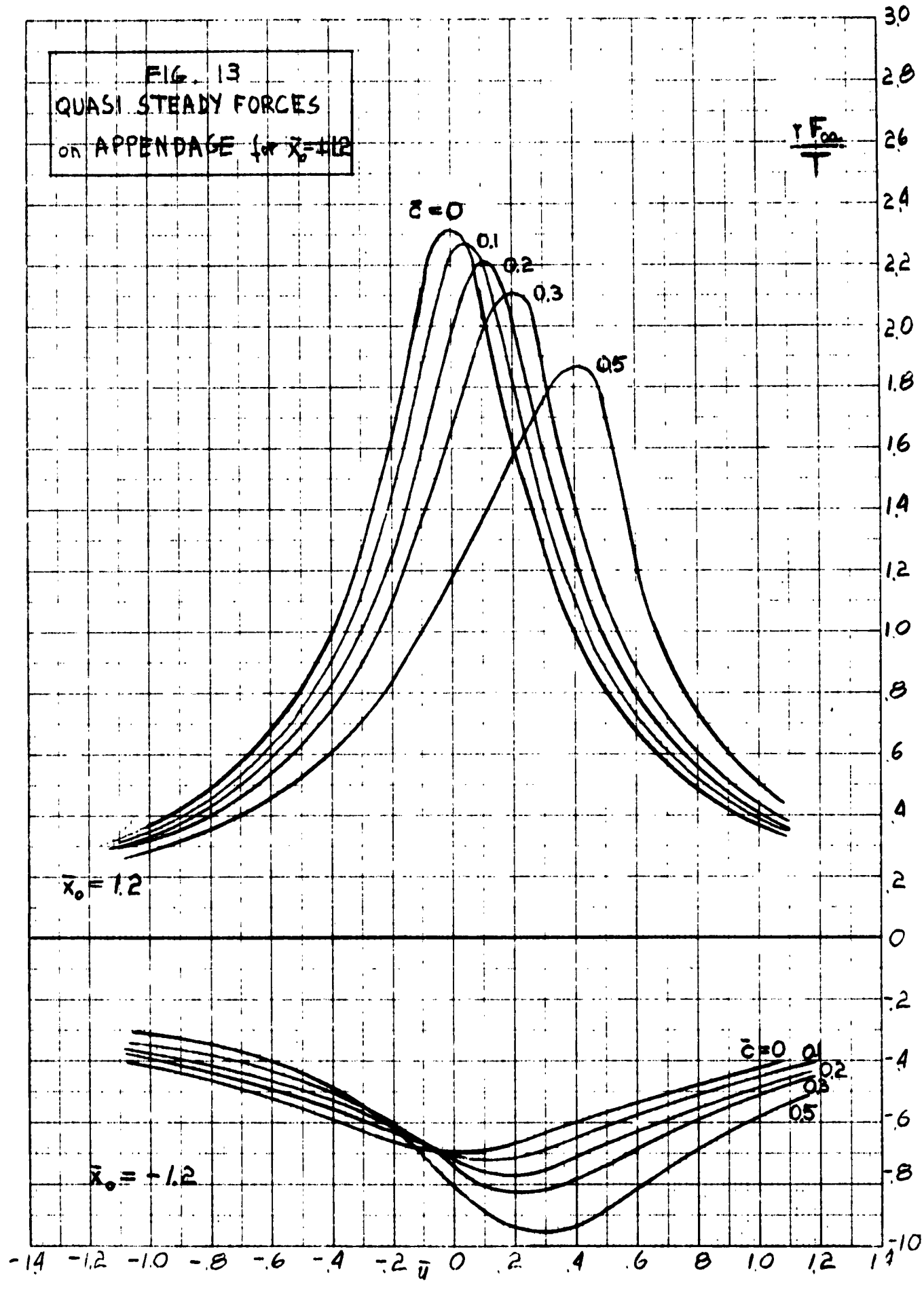
FIG. 13
QUASI STEADY FORCES
ON APPENDAGE for $\bar{X}_0 = \pm 1.2$
$\frac{\tau F_{00}}{T}$
$\bar{c} = 0$
0.1
0.2
0.3
0.5
$\bar{X}_0 = 1.2$
$\bar{X}_0 = -1.2$
$\bar{u}$
3.0
2.8
2.6
2.4
2.2
2.0
1.8
1.6
1.4
1.2
1.0
.8
.6
.4
.2
0
-.2
-.4
-.6
-.8
-1.0
-1.4 -1.2 -1.0 -.8 -.6 -.4 -.2 0 .2 .4 .6 .8 1.0 1.2 1.4

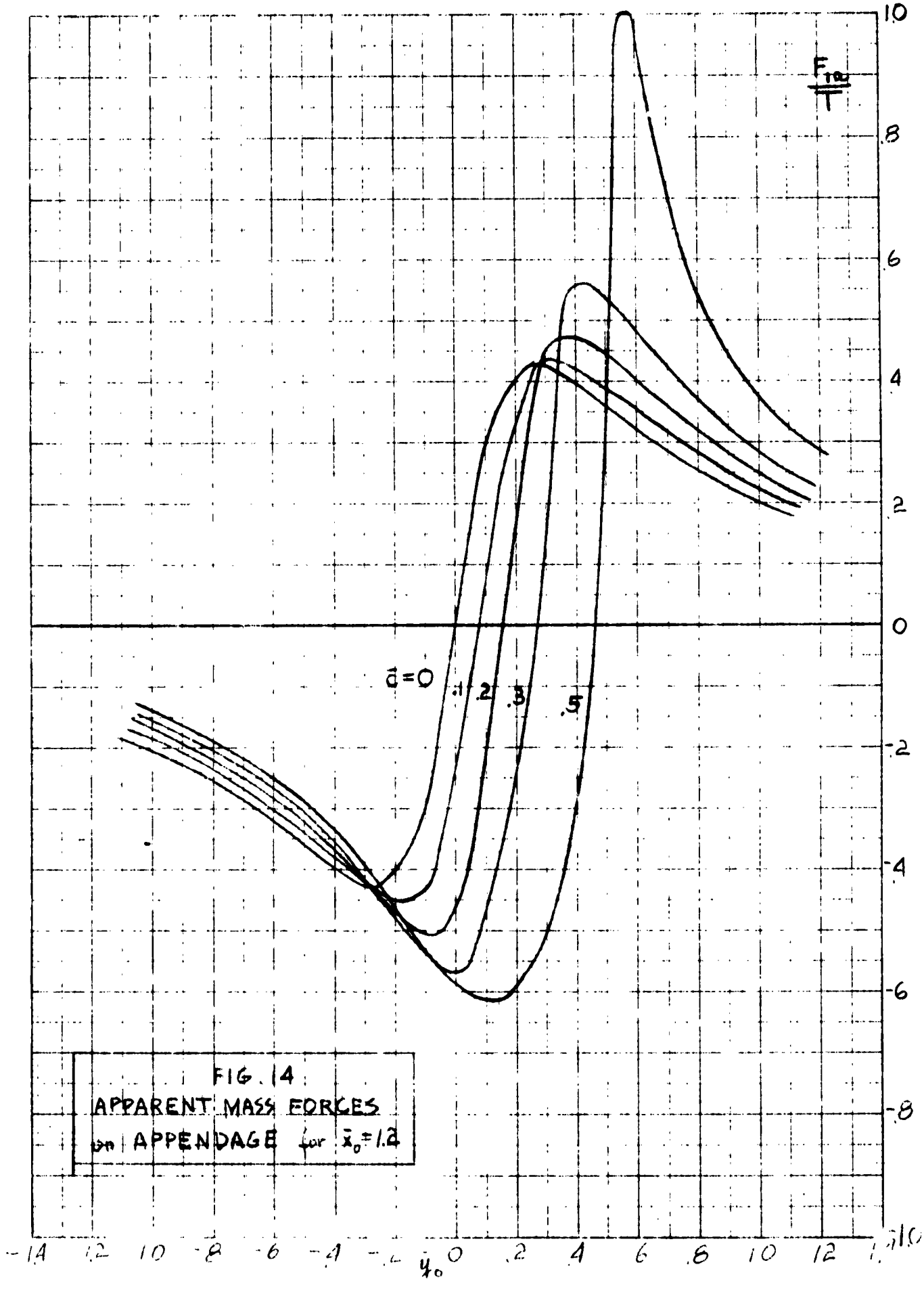

FIG. 14
APPARENT MASS FORCES
on APPENDAGE for $\bar{x}_0 = 1.2$

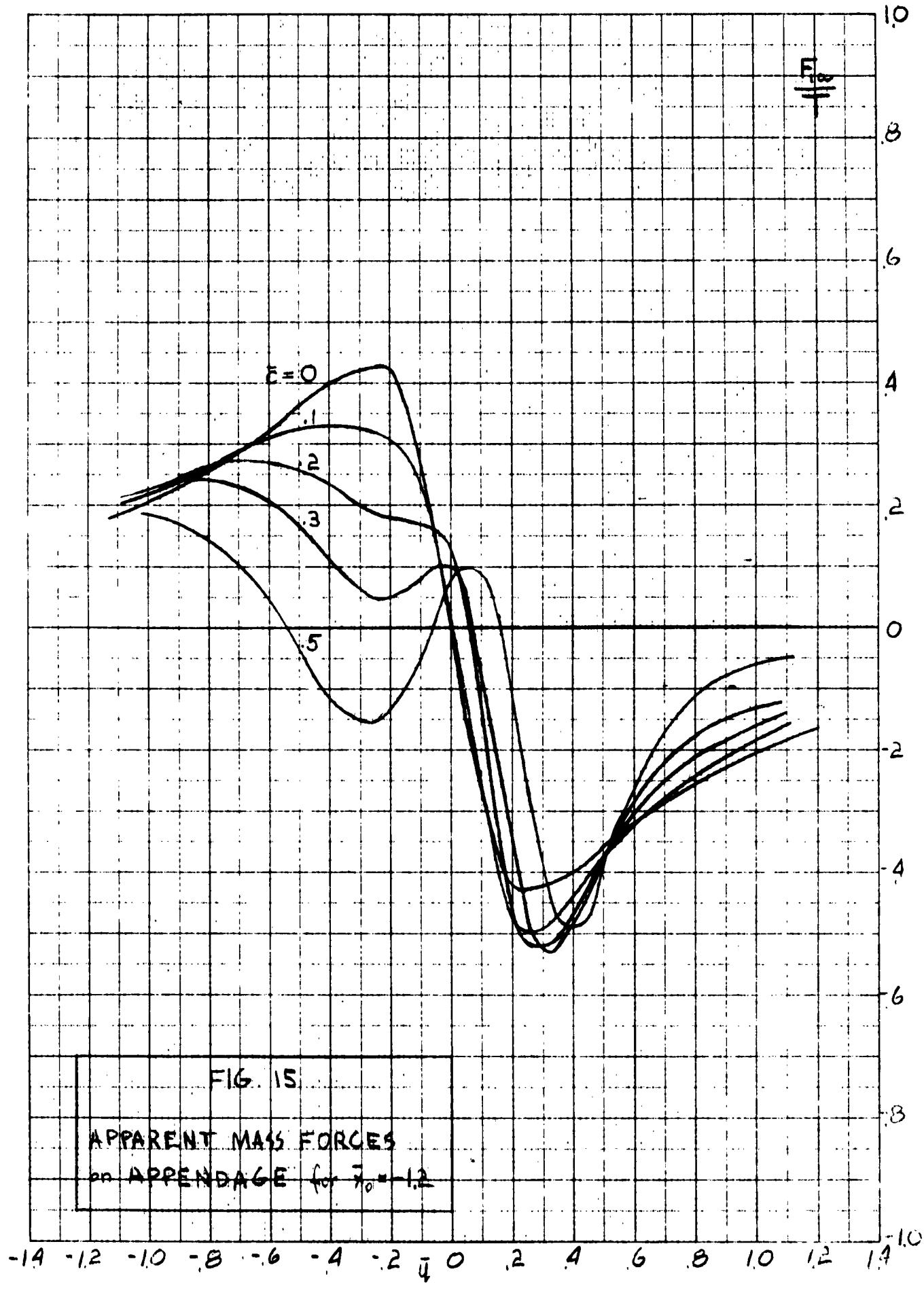

FIG. 15

APPARENT MASS FORCES on APPENDAGE for $\bar{x}_0 = -1.2$

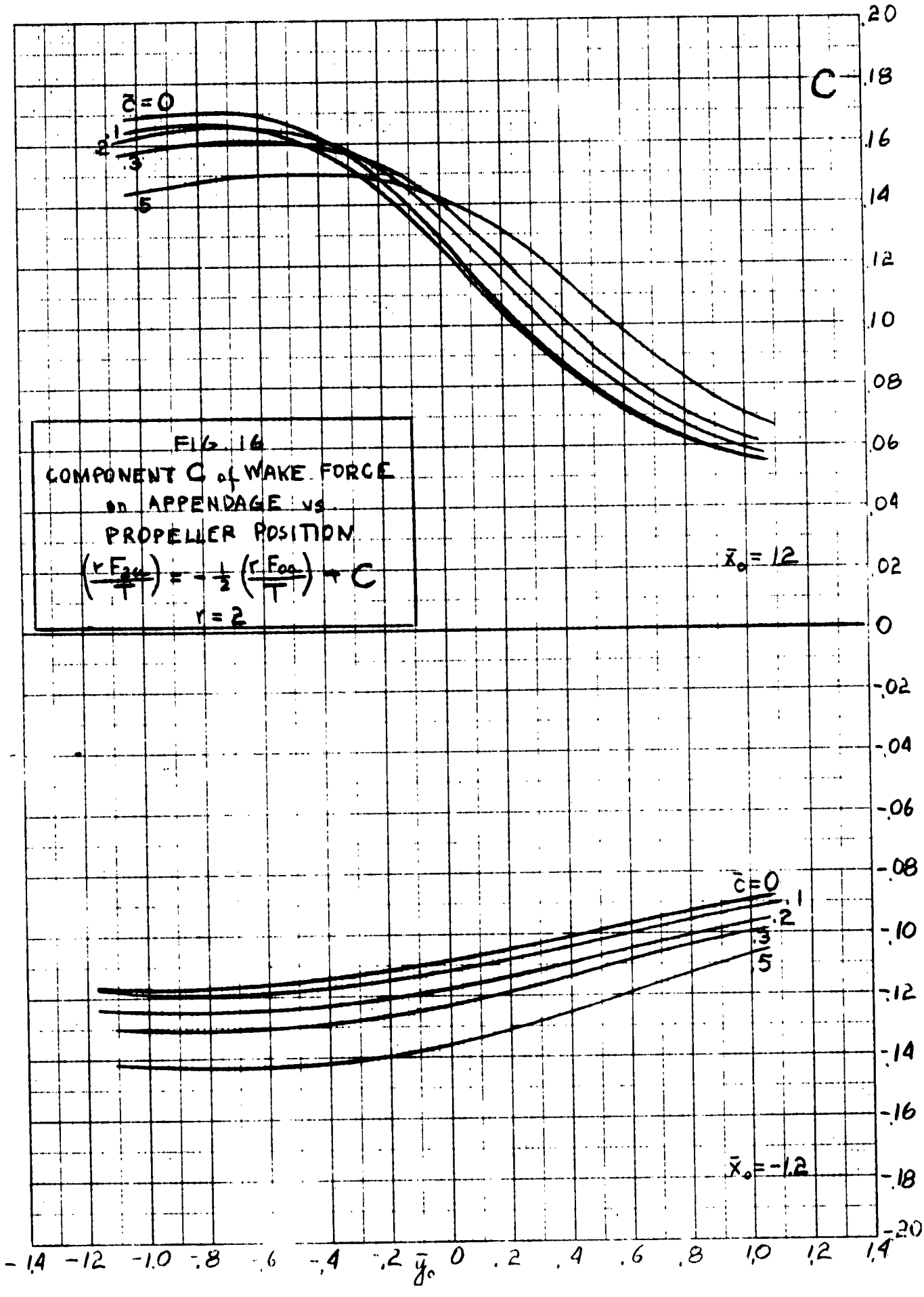

FIG. 16
COMPONENT C of WAKE FORCE
on APPENDAGE vs.
PROPELLER POSITION

$$\left(\frac{r F_{zc}}{T}\right) = -\frac{1}{2}\left(\frac{r F_{oa}}{T}\right) + C$$

$r = 2$

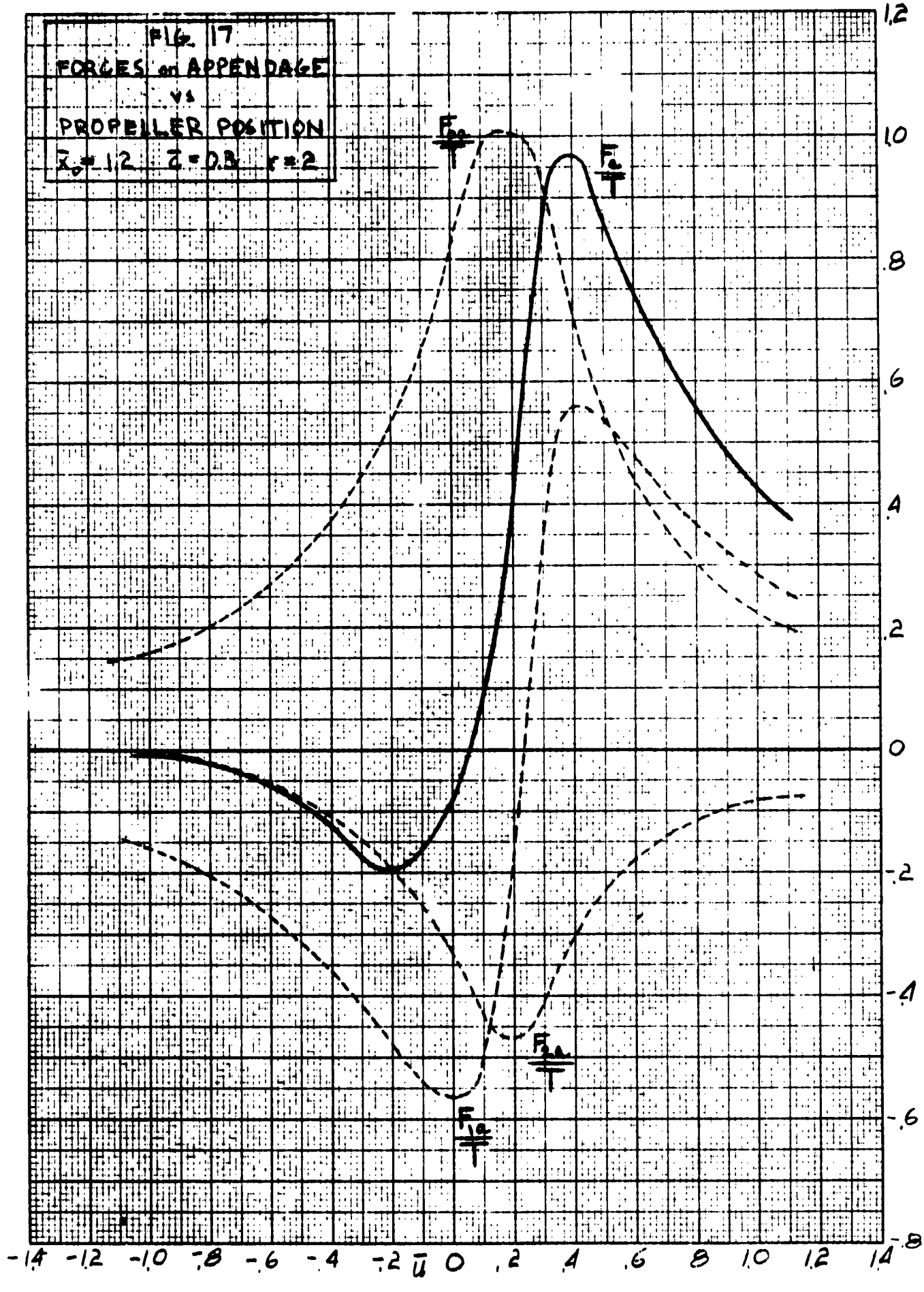
FIG. 17
FORCES on APPENDAGE
vs
PROPELLER POSITION
$\bar{x}_0 = 1.2$ $\bar{z} = 0.3$ $r = 2$
$\frac{F_{pa}}{T}$
$\frac{F_a}{T}$
$\frac{F_{ia}}{T}$
$\frac{F_{ra}}{T}$
1.2
1.0
.8
.6
.4
.2
0
-.2
-.4
-.6
-.8
-1.4 -1.2 -1.0 -.8 -.6 -.4 -.2 $\bar{u}$ 0 .2 .4 .6 .8 1.0 1.2 1.4

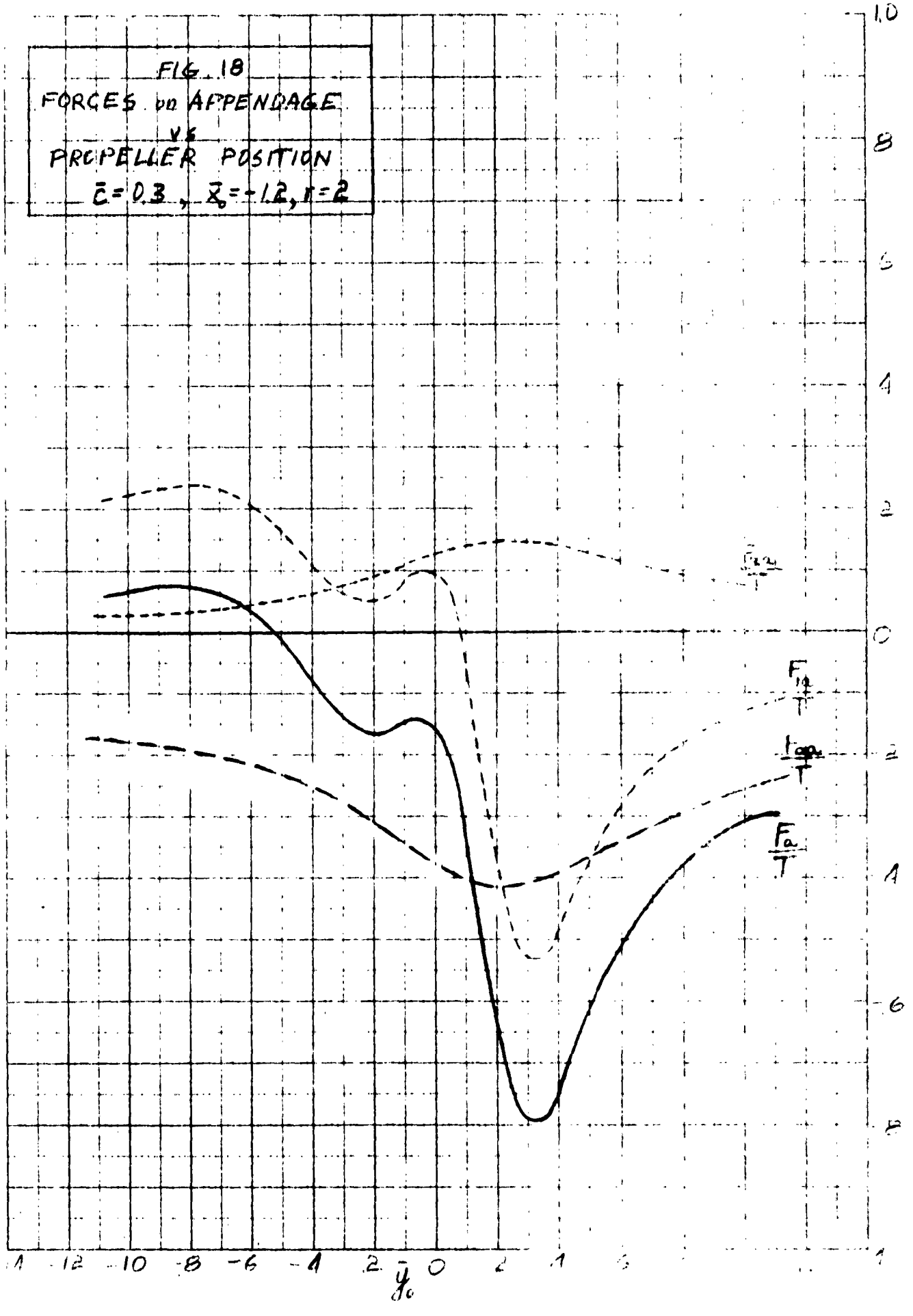
FIG. 18
FORCES on APPENDAGE
vs
PROPELLER POSITION
$\bar{c} = 0.3$, $\bar{x}_0 = -1.2$, $t = 2$
$\frac{F_{1a}}{T}$
$\frac{F_{2a}}{T}$
$\frac{F_a}{T}$
1.0
.8
.6
.4
.2
0
.2
.4
.6
.8
1.0
-1.4 -1.2 -1.0 -.8 -.6 -.4 -.2 0 .2 .4 .6
$\bar{y}_0$

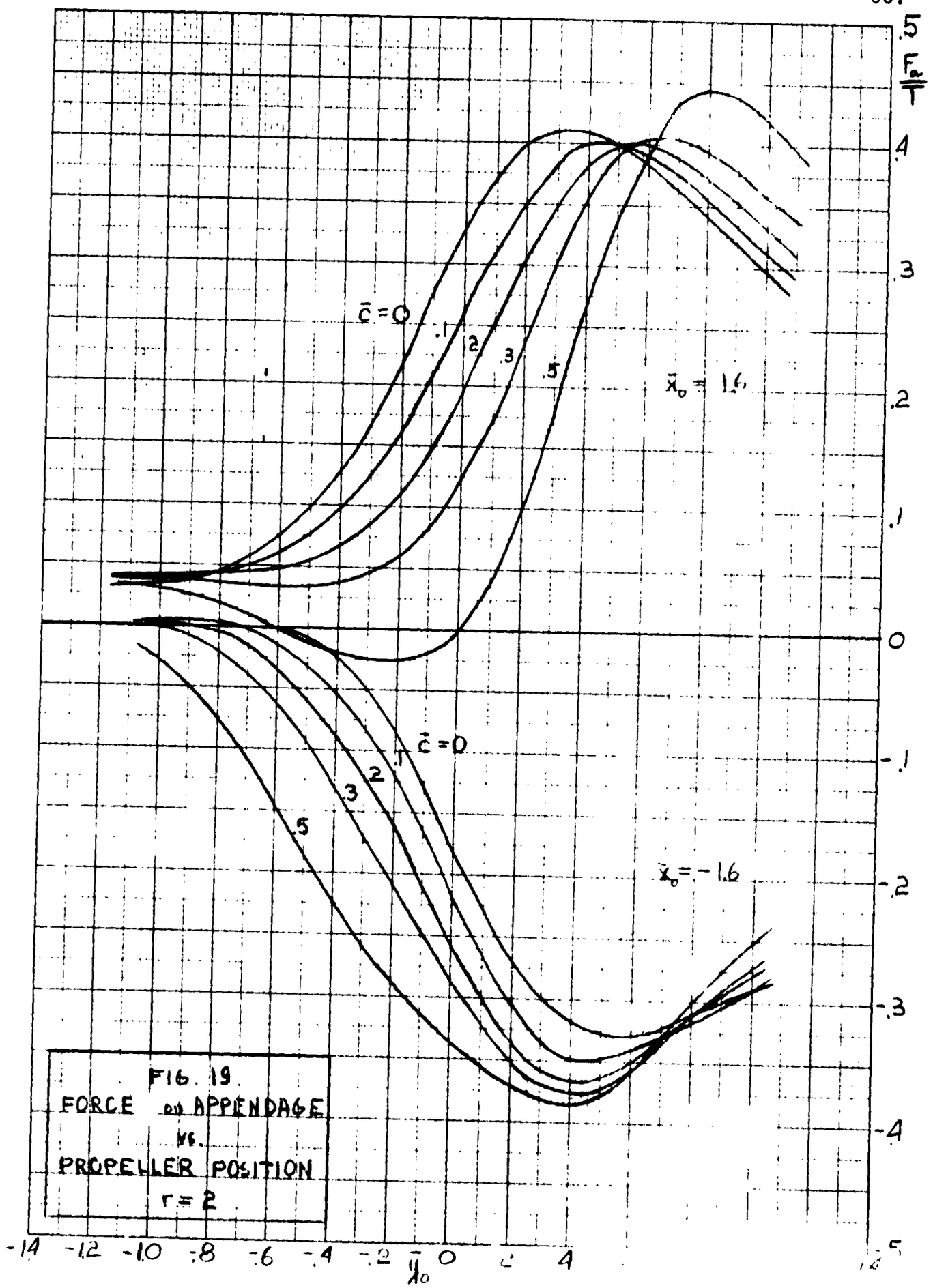

FIG. 19
FORCE on APPENDAGE
vs.
PROPELLER POSITION
r = 2

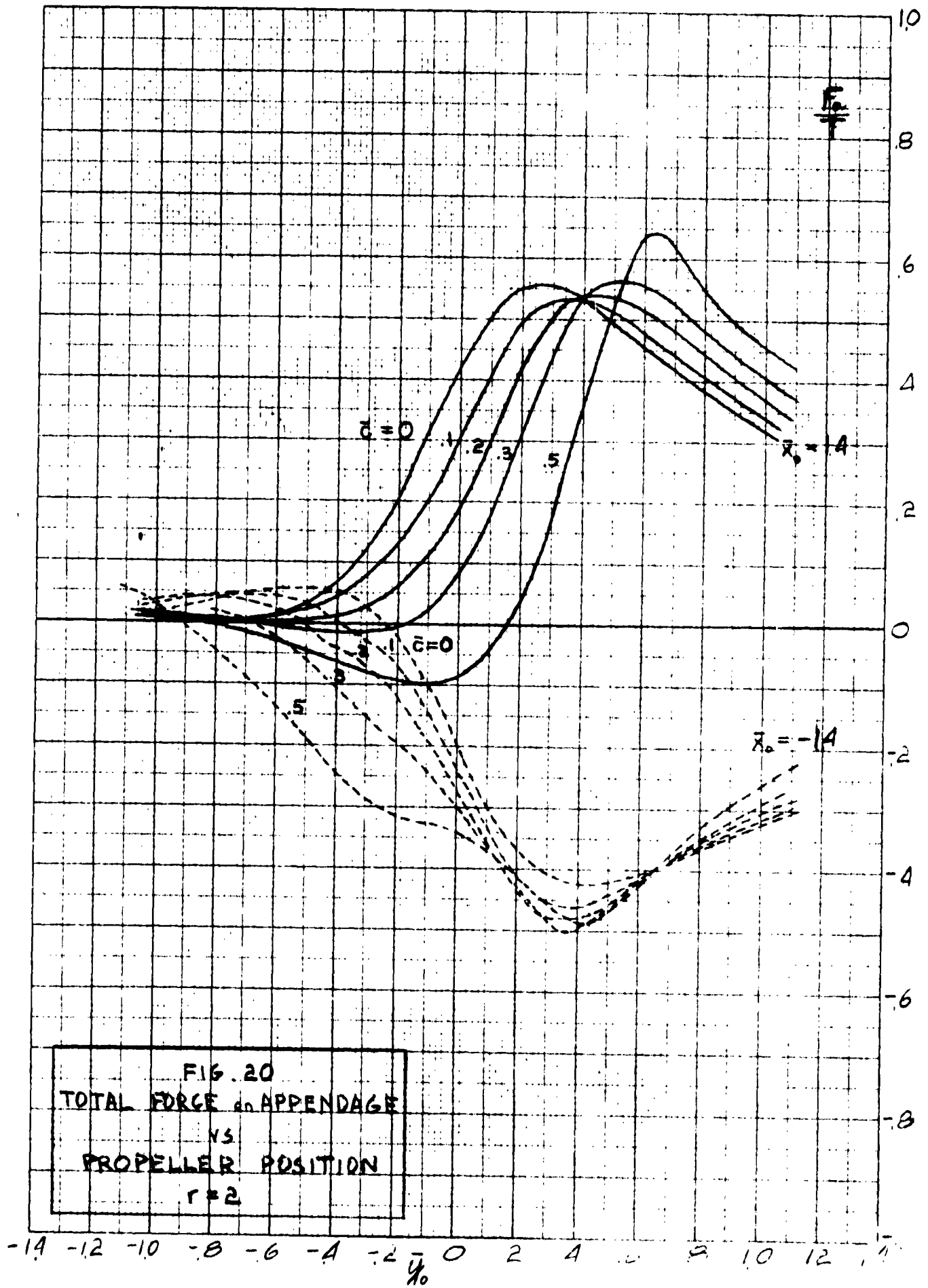

FIG. 20
TOTAL FORCE on APPENDAGE
VS
PROPELLER POSITION
r = 2

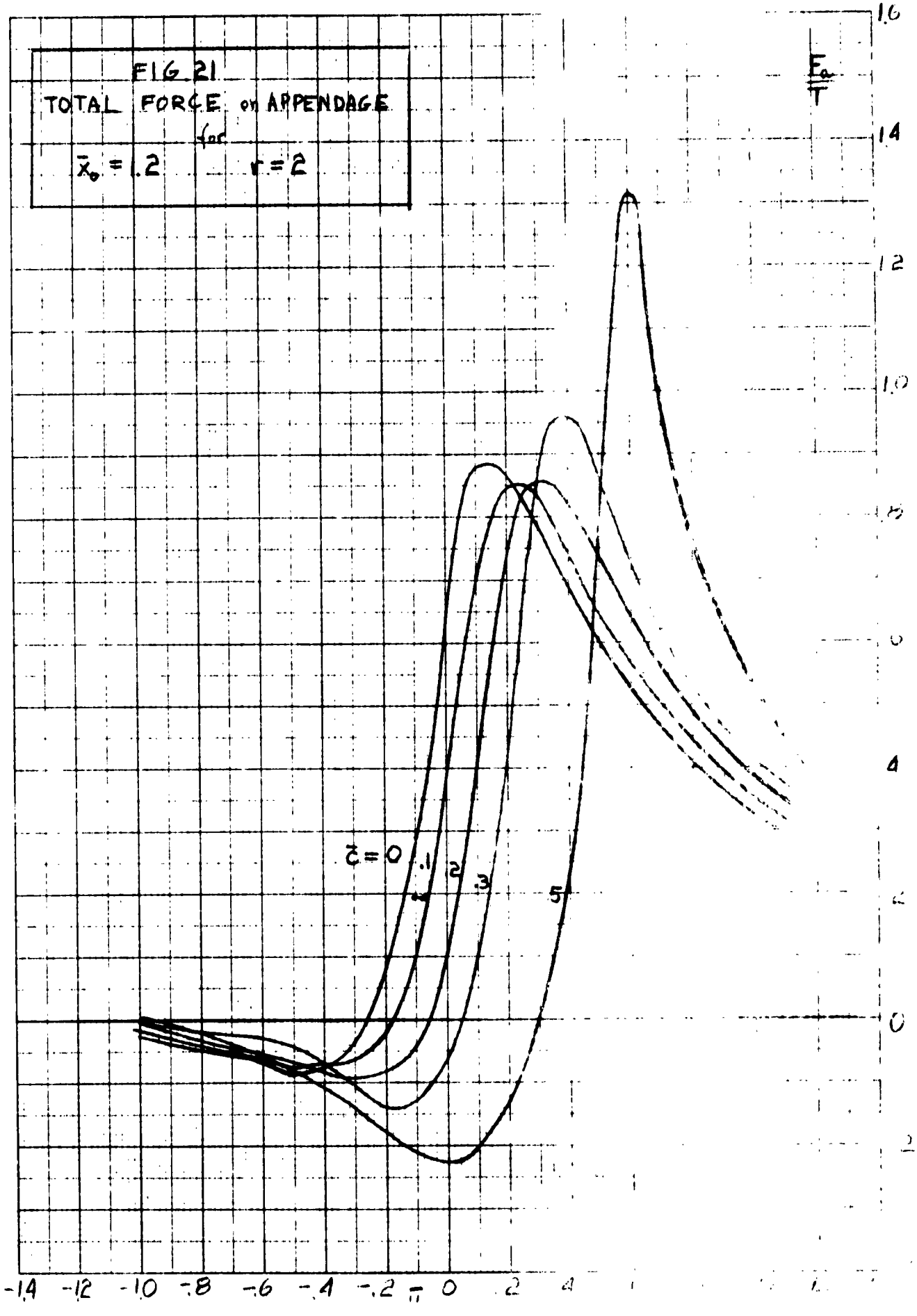
FIG 21
TOTAL FORCE on APPENDAGE
for
$\bar{x}_0 = 1.2$ $r = 2$
$\frac{F_a}{T}$
1.6
1.4
1.2
1.0
.8
.6
.4
.2
0
$\bar{c} = 0$ .1 .2 .3 .4 5
-1.4 -1.2 -1.0 -.8 -.6 -.4 -.2 π 0 .2

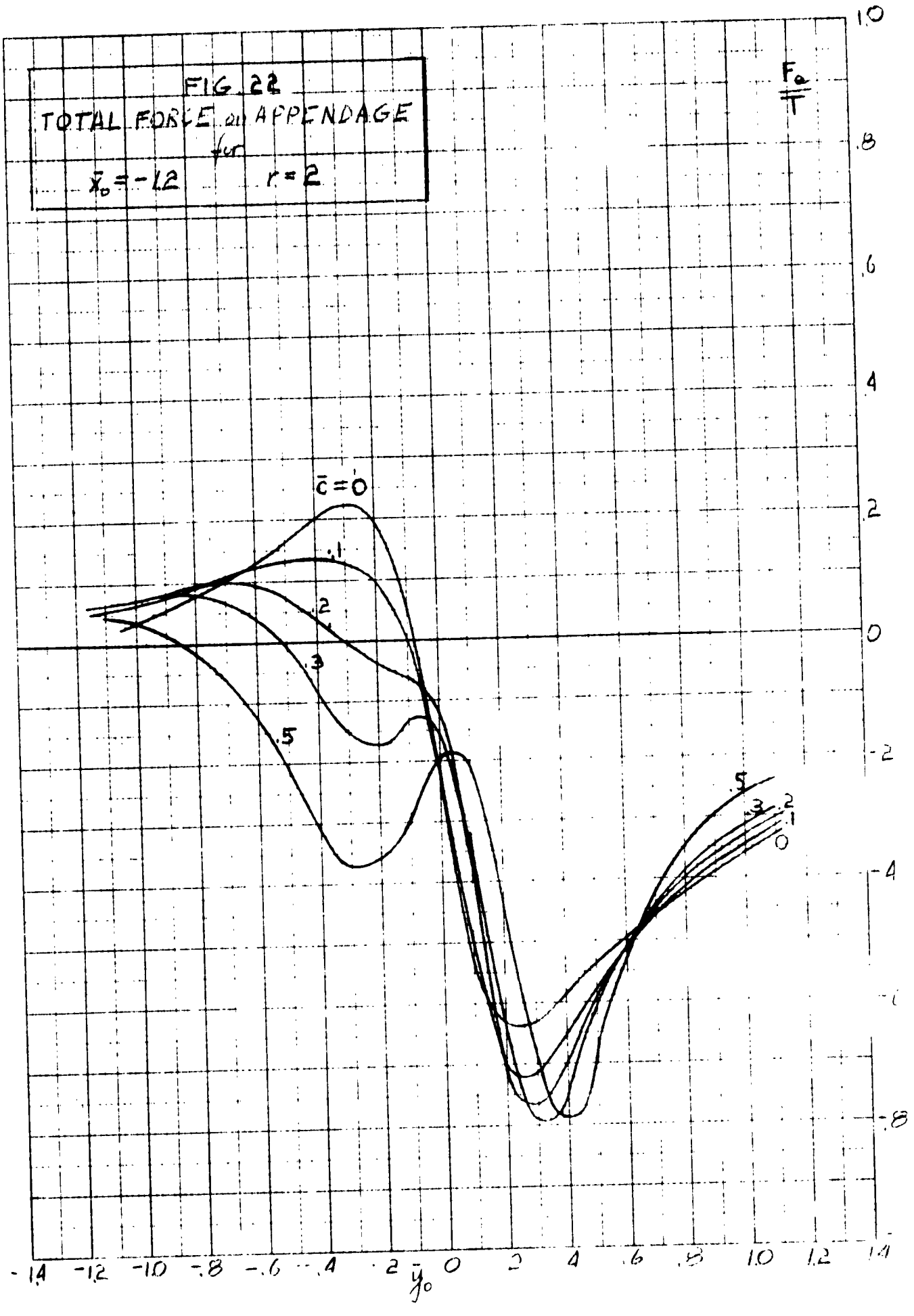
FIG. 22
TOTAL FORCE on APPENDAGE
for
$\bar{x}_0 = -1.2$ $r = 2$
$\frac{F_a}{T}$
$\bar{c} = 0$
.1
.2
.3
.5
1.0
.8
.6
.4
.2
0
-.2
-.4
-.8
-1.4 -1.2 -1.0 -.8 -.6 -.4 -.2 0 .2 .4 .6 .8 1.0 1.2 1.4
$\bar{y}_0$

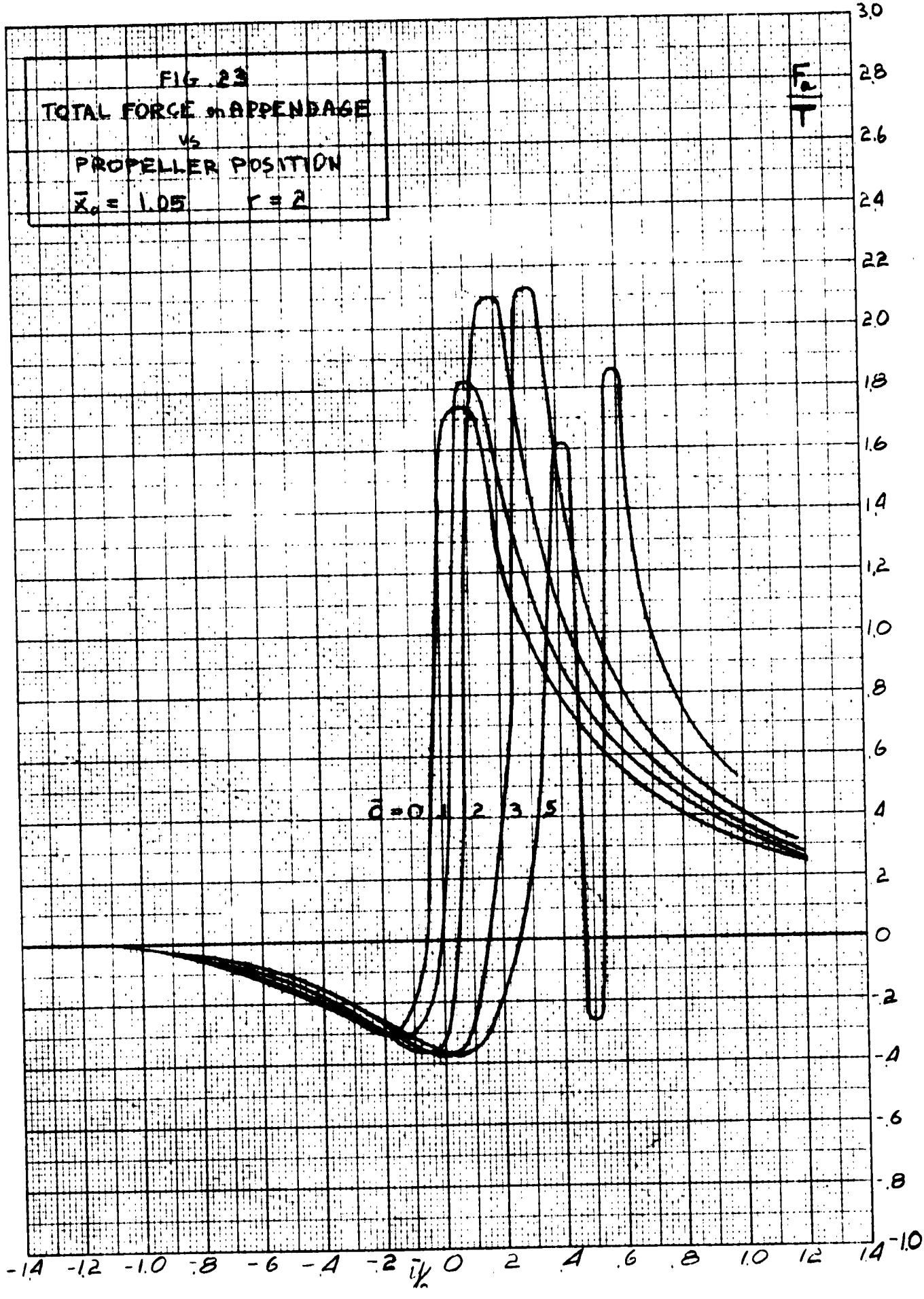
FIG. 23
TOTAL FORCE on APPENDAGE
vs
PROPELLER POSITION
$\bar{X}_d$ = 1.05 r = 2
$\frac{F_a}{T}$
3.0
2.8
2.6
2.4
2.2
2.0
1.8
1.6
1.4
1.2
1.0
.8
.6
.4
.2
0
-.2
-.4
-.6
-.8
-1.0
$\bar{d}$ = 0 1 2 3 5
-1.4 -1.2 -1.0 -.8 -.6 -.4 -.2 i_p 0 .2 .4 .6 .8 1.0 1.2 1.4

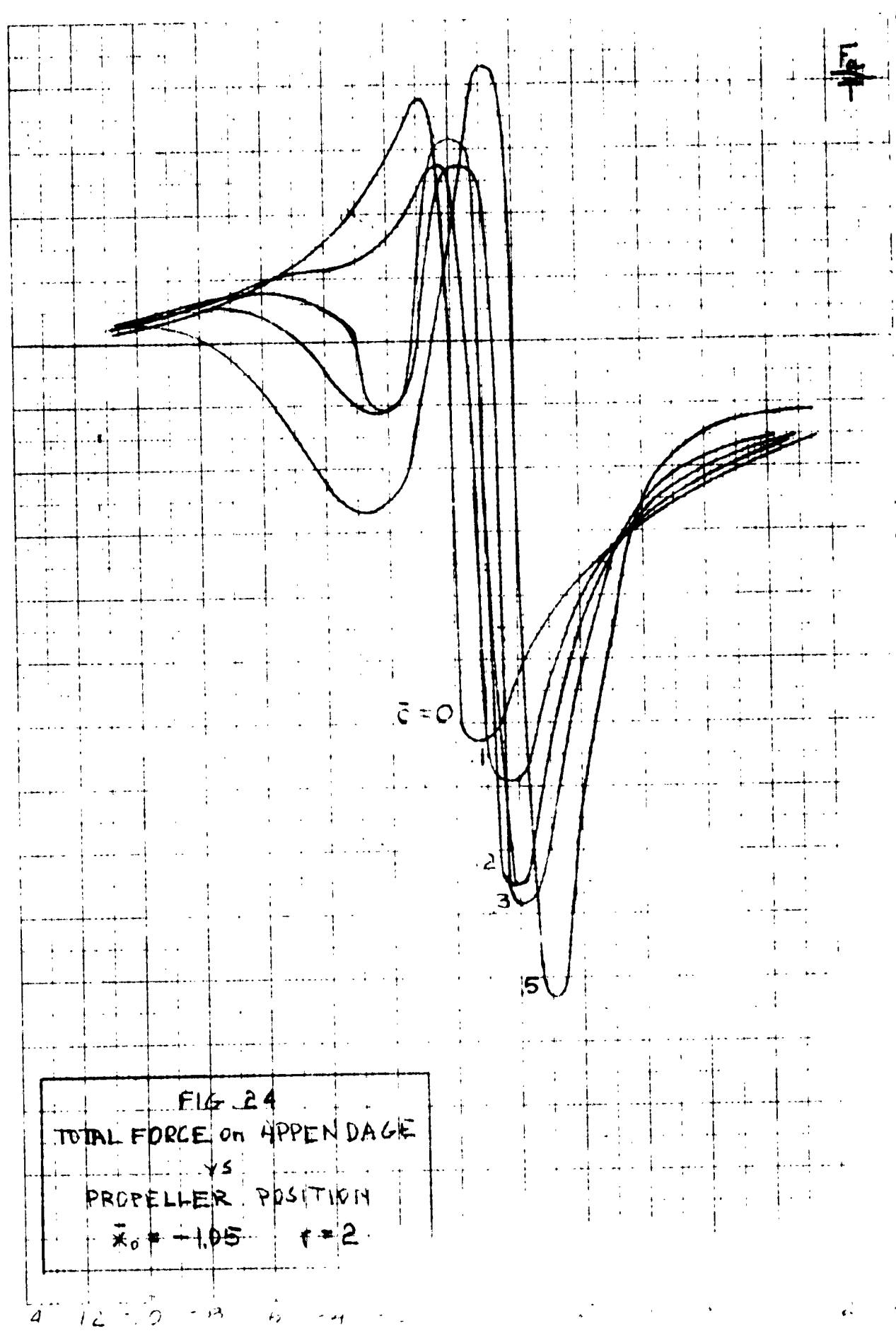

FIG 24
TOTAL FORCE on APPENDAGE
vs
PROPELLER POSITION
$\bar{x}_0 = -1.05$ $t = 2$

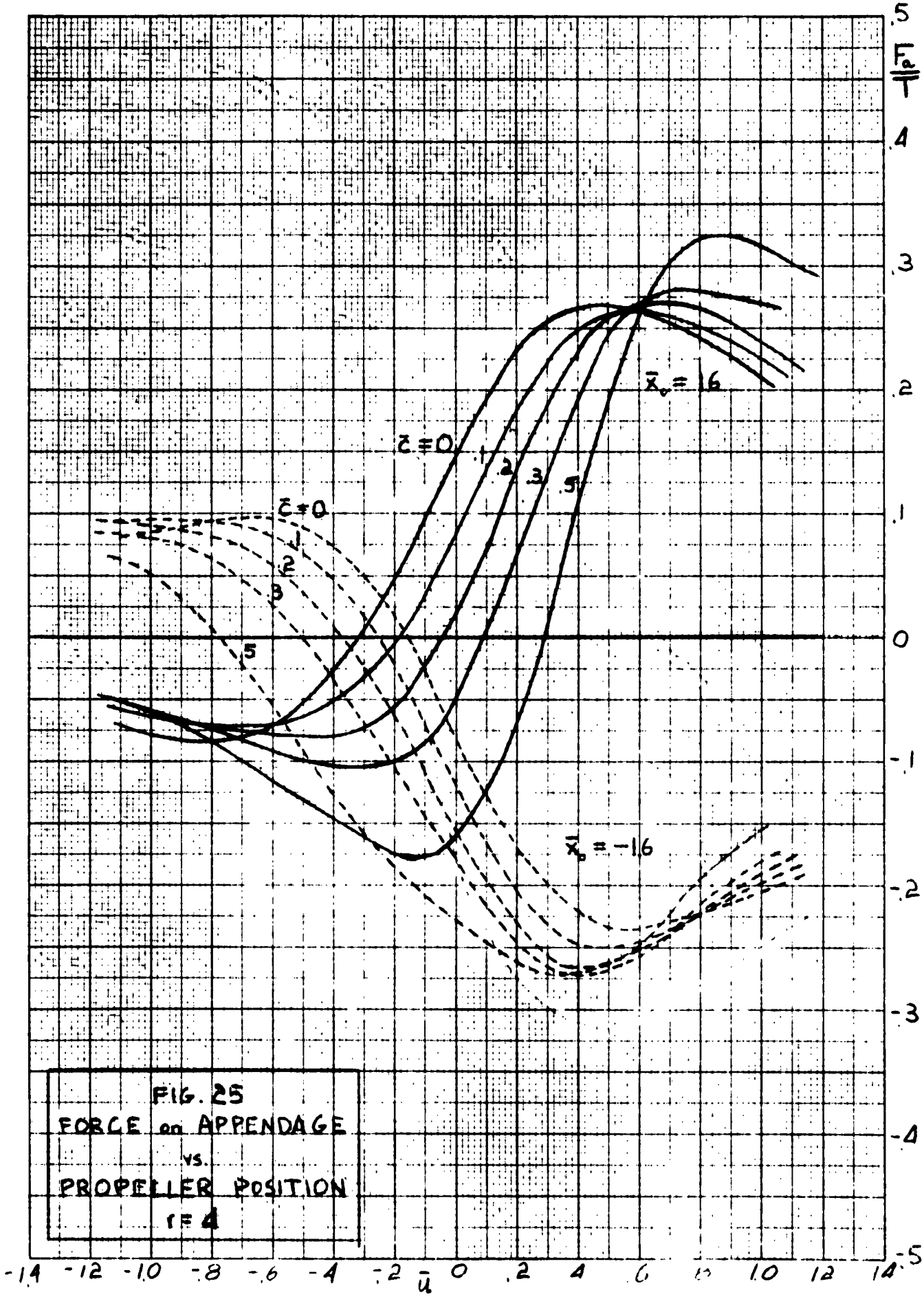

FIG. 25
FORCE on APPENDAGE
vs.
PROPELLER POSITION
r = 4

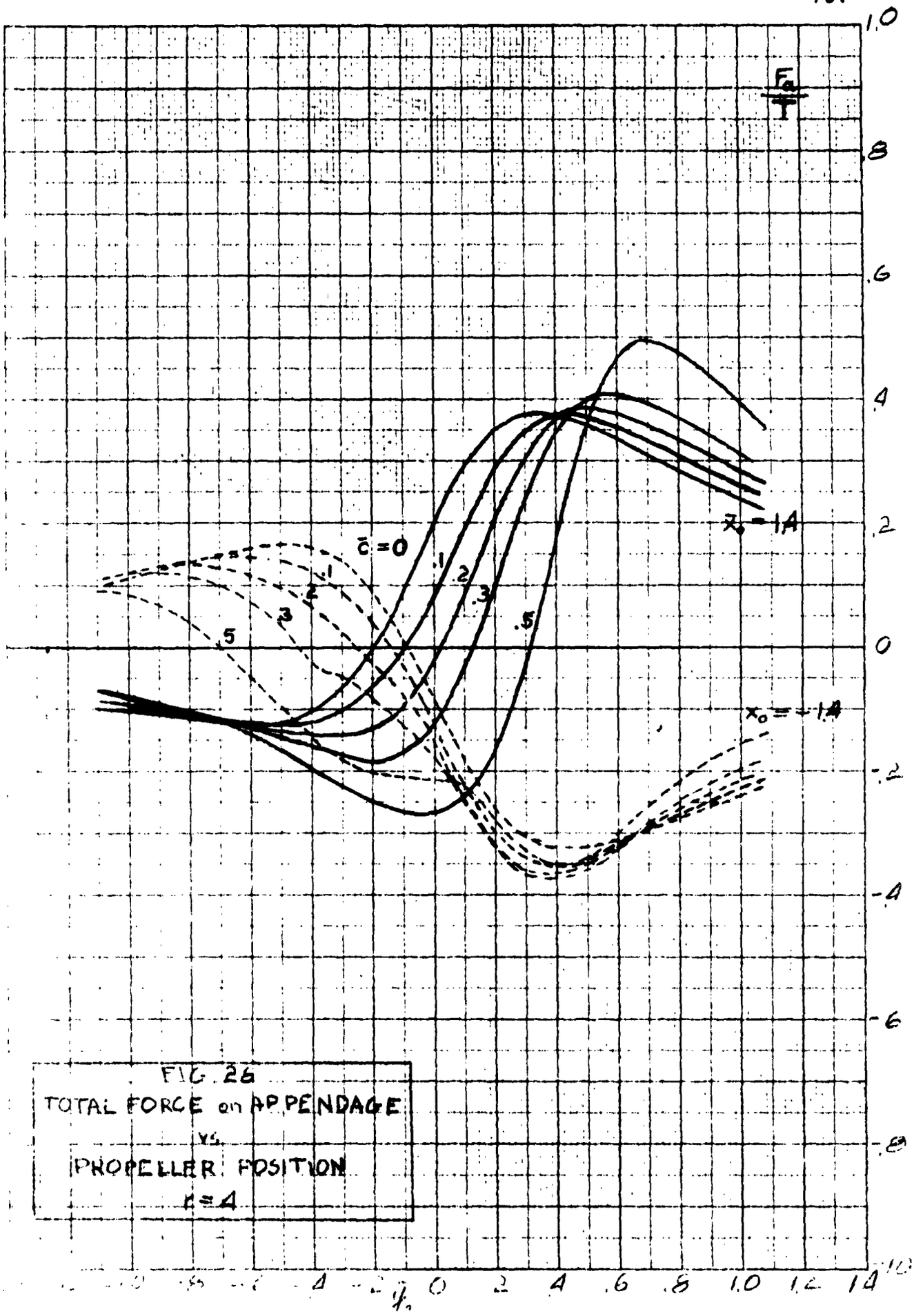

FIG. 26
TOTAL FORCE on APPENDAGE
vs.
PROPELLER POSITION
$r=4$

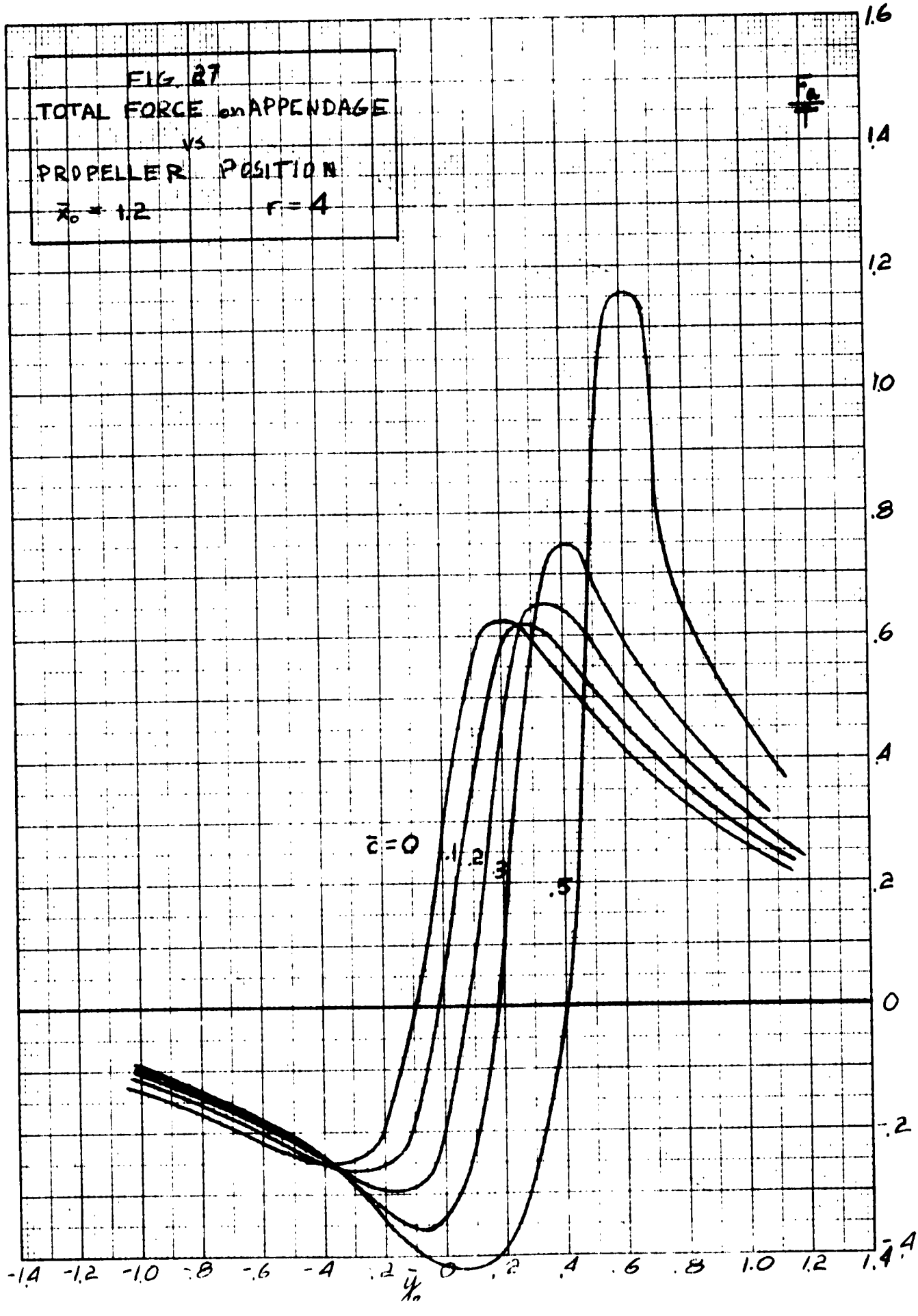
FIG. 27
TOTAL FORCE on APPENDAGE
vs
PROPELLER POSITION
$\bar{x}_0 = 1.2$ r = 4
$\bar{F}_a$
1.6
1.4
1.2
1.0
.8
.6
.4
.2
0
-.2
-.4
$\bar{c} = 0$
.1
.2
.3
.5
-1.4 -1.2 -1.0 -.8 -.6 -.4 -.2 0 .2 .4 .6 .8 1.0 1.2 1.4
$\bar{y}_0$

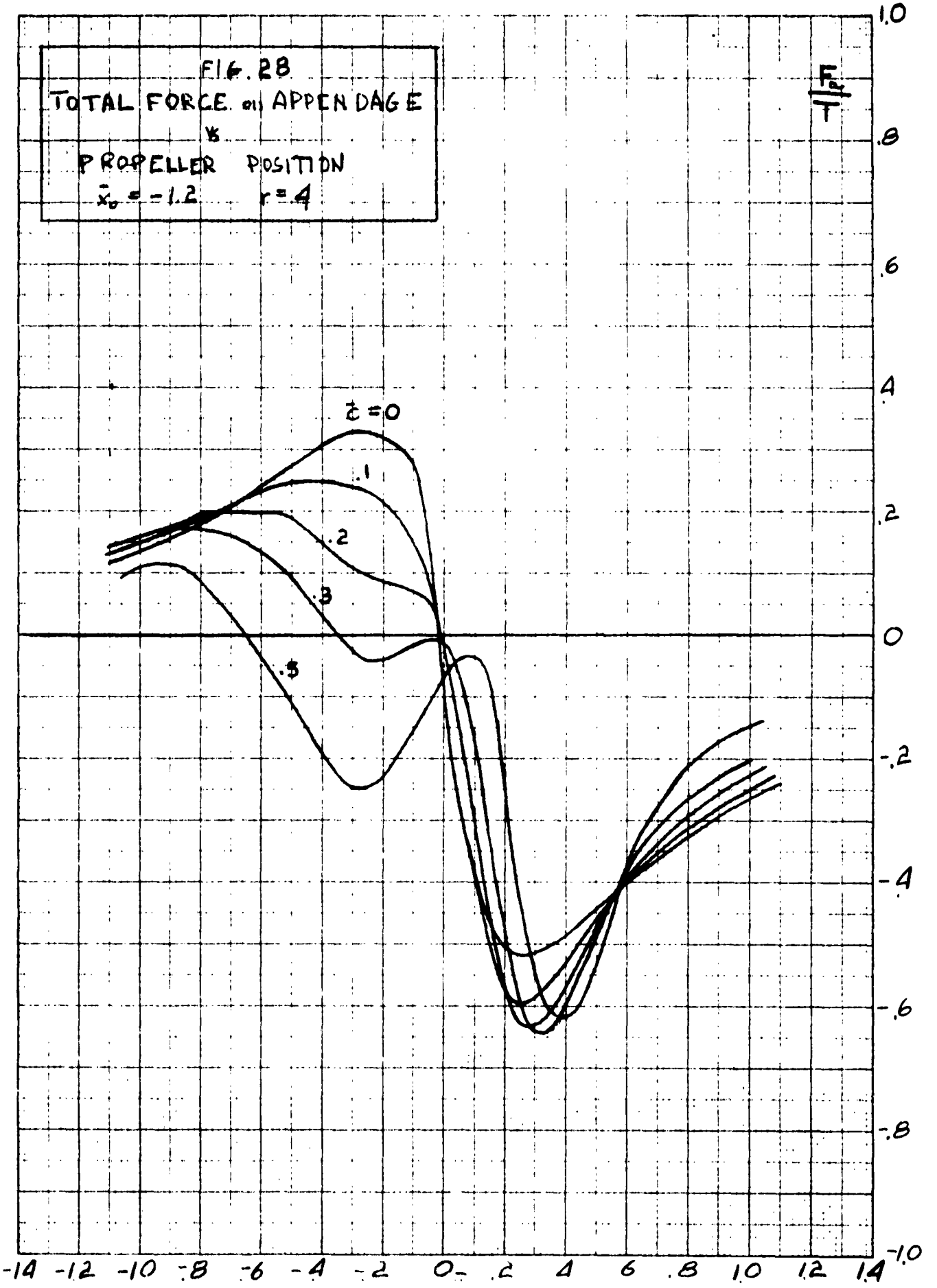
FIG. 28
TOTAL FORCE on APPENDAGE
vs
PROPELLER POSITION
$\bar{x}_0 = -1.2$ $r = .4$
$\frac{F_x}{T}$
$\bar{z} = 0$
.1
.2
.3
.5
1.0
.8
.6
.4
.2
0
-.2
-.4
-.6
-.8
-1.0
-1.4 -1.2 -1.0 -.8 -.6 -.4 -.2 0 .2 .4 .6 .8 1.0 1.2 1.4

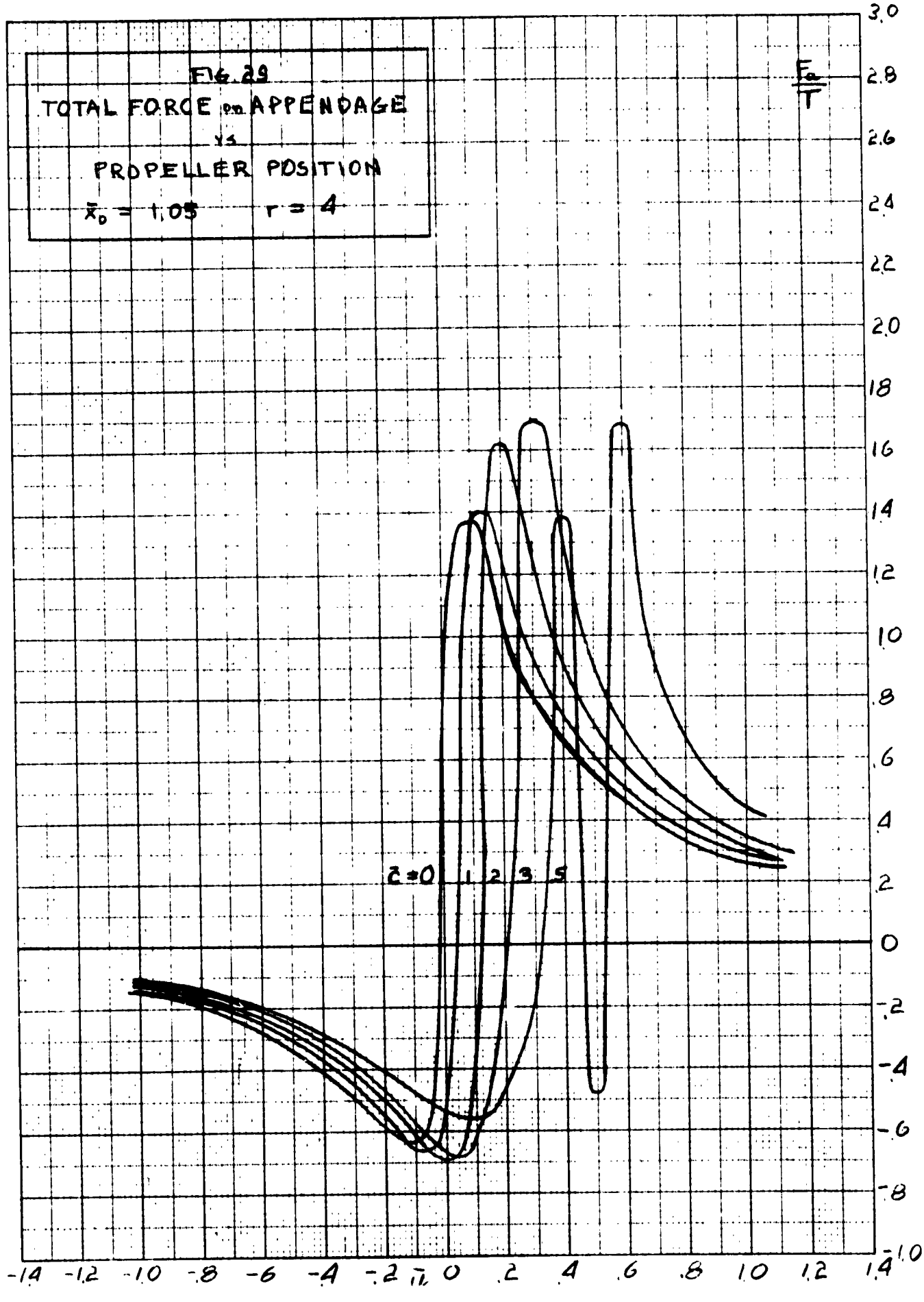
FIG. 29
TOTAL FORCE on APPENDAGE
vs
PROPELLER POSITION
$\bar{x}_0 = 1.05$ r = 4
$\frac{F_a}{T}$
3.0
2.8
2.6
2.4
2.2
2.0
1.8
1.6
1.4
1.2
1.0
.8
.6
.4
.2
0
-.2
-.4
-.6
-.8
-1.0
$\bar{z}$ = 0 1 2 3 5
-1.4 -1.2 -1.0 -.8 -.6 -.4 -.2 0 .2 .4 .6 .8 1.0 1.2 1.4
$\bar{x}$

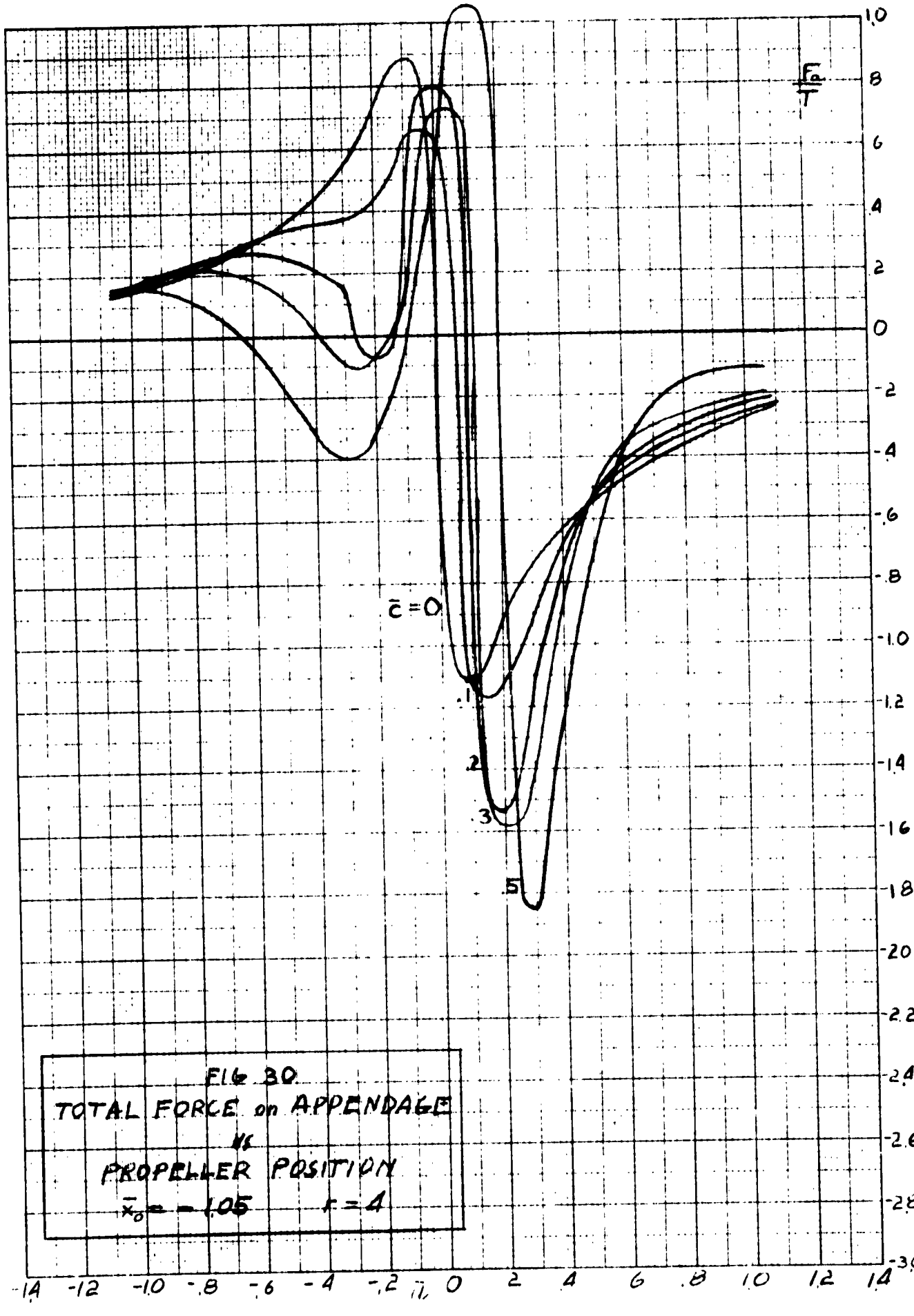

FIG 30
TOTAL FORCE on APPENDAGE
VS
PROPELLER POSITION
$\bar{x}_o = -1.05$ $r = 4$

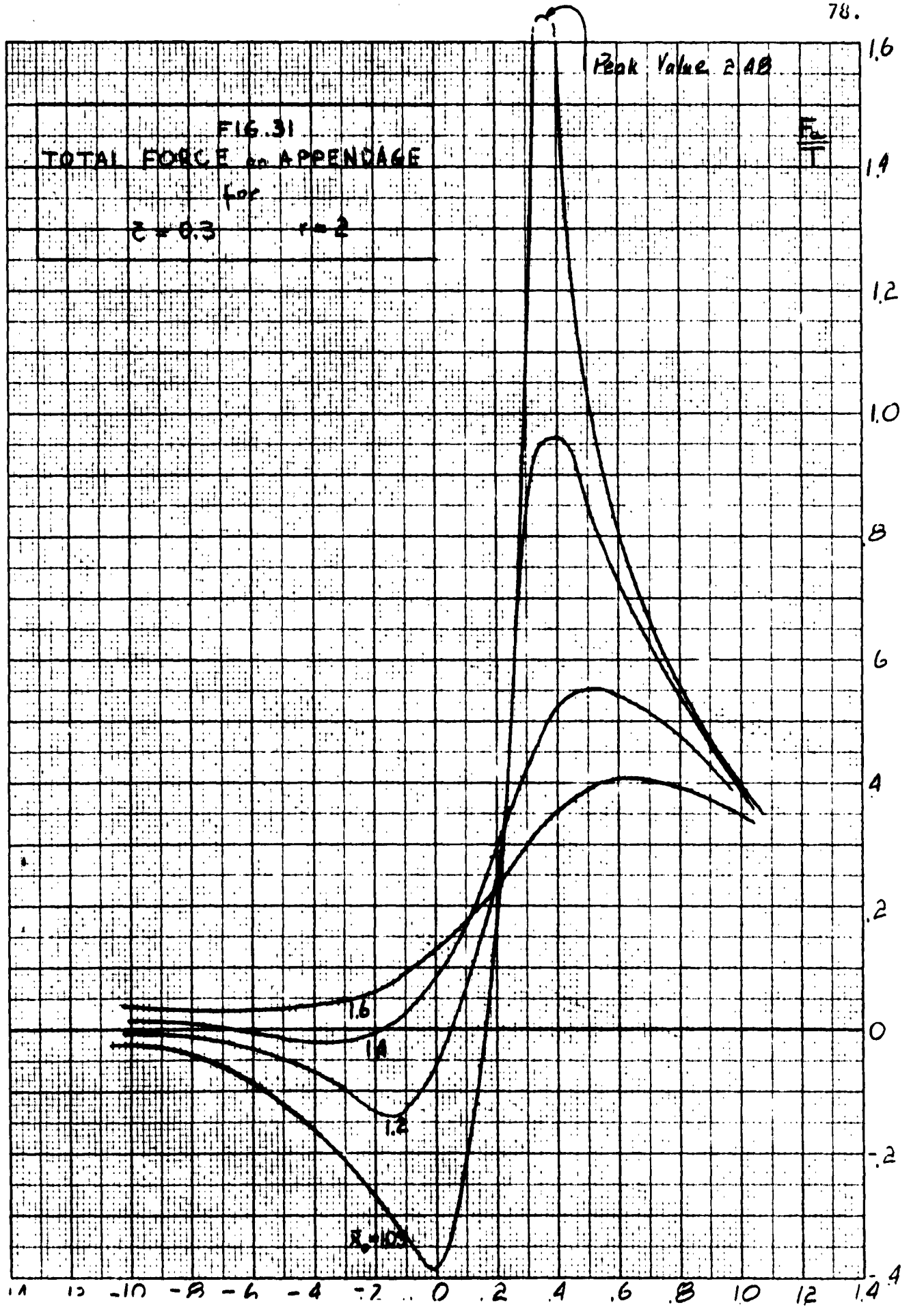

FIG. 31
TOTAL FORCE on APPENDAGE
for
$\zeta = 0.3$ $r = 2$

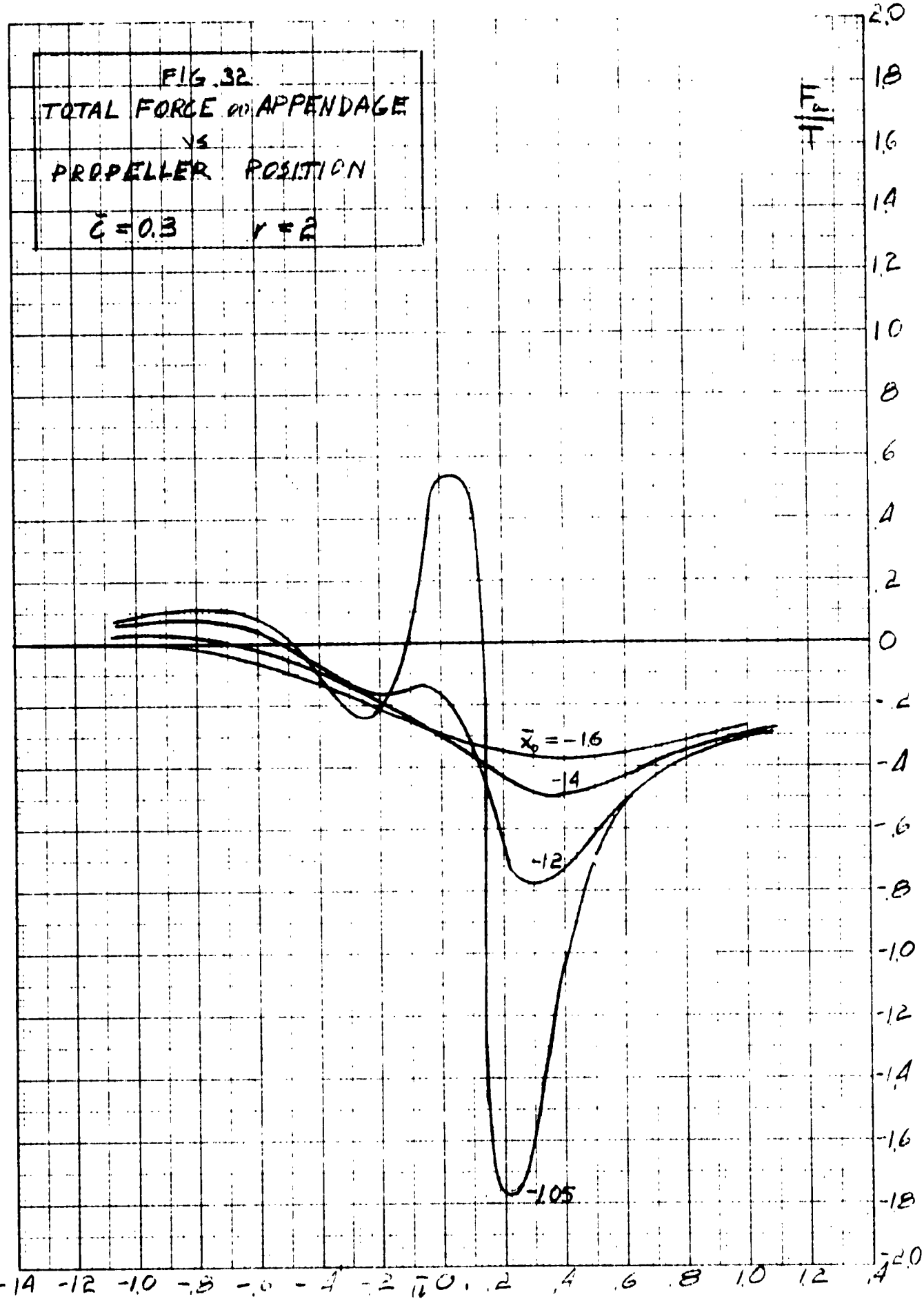
FIG. 32
TOTAL FORCE ON APPENDAGE
VS
PROPELLER POSITION
$\bar{C} = 0.3$ $r = 2$
$\frac{F_x}{T}$
$\bar{x}_0 = -1.6$
-1.4
-1.2
-1.05
2.0
1.8
1.6
1.4
1.2
1.0
.8
.6
.4
.2
0
-.2
-.4
-.6
-.8
-1.0
-1.2
-1.4
-1.6
-1.8
-2.0
-1.4 -1.2 -1.0 -.8 -.6 -.4 -.2 0 .2 .4 .6 .8 1.0 1.2 1.4

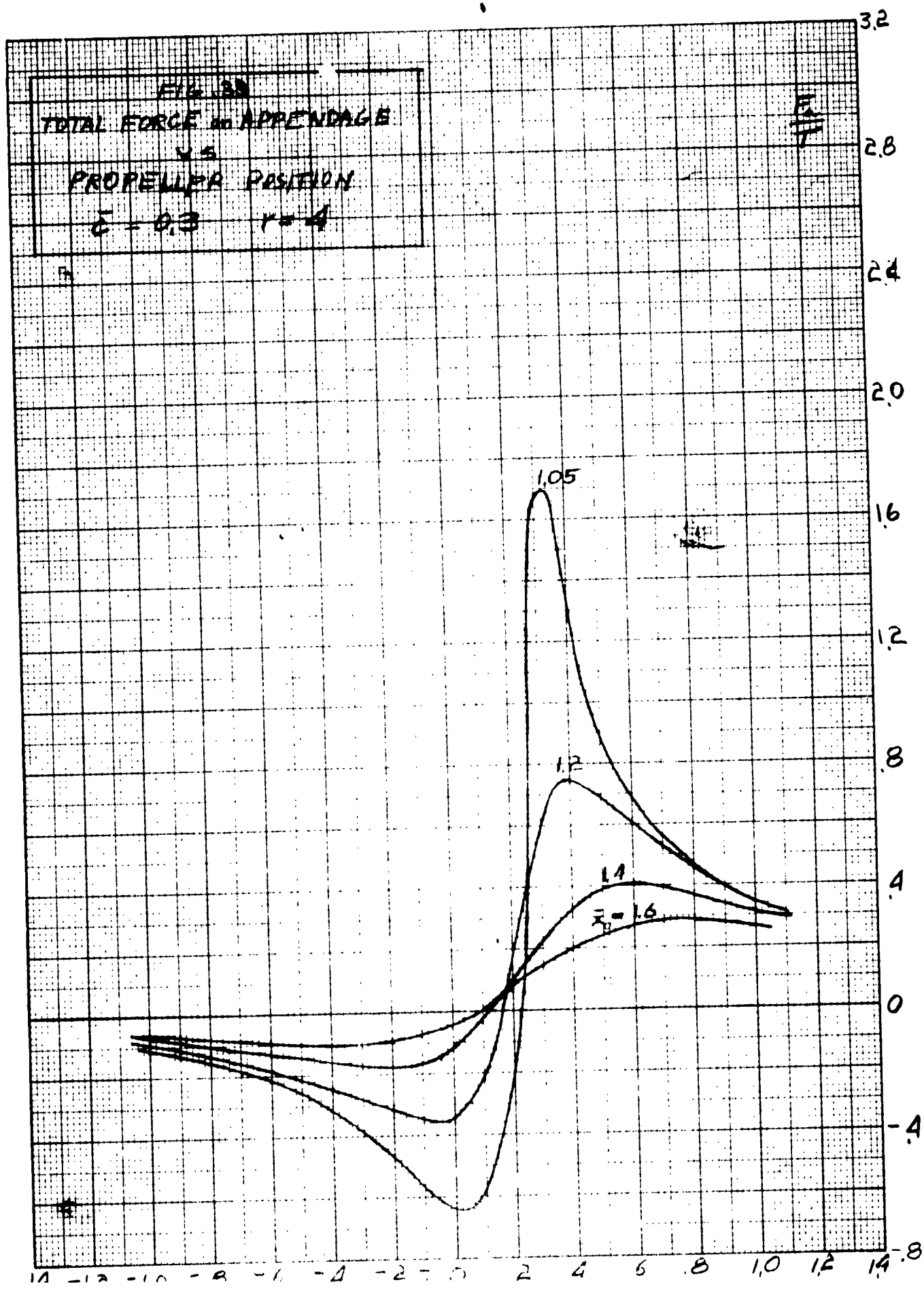
FIG. 38
TOTAL FORCE on APPENDAGE
vs
PROPELLER POSITION
$\bar{c} = 0.3$ $r = 4$
$\frac{F_n}{T}$
3.2
2.8
2.4
2.0
1.6
1.2
.8
.4
0
-.4
-.8
1.05
1.2
1.4
$\bar{x}_0 = 1.6$
-1.4 -1.2 -1.0 -.8 -.6 -.4 -.2 0 .2 .4 .6 .8 1.0 1.2 1.4

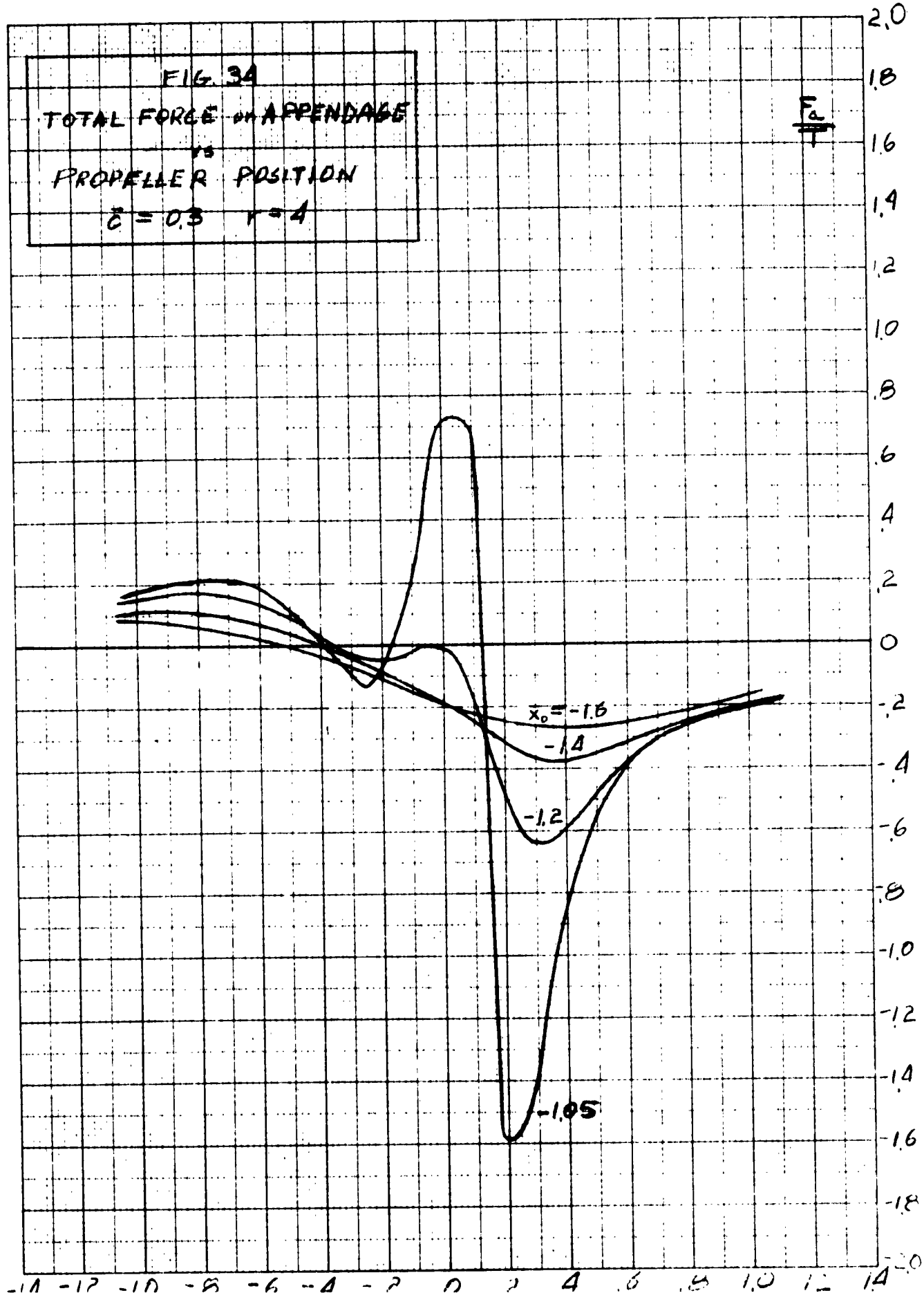
FIG. 34
TOTAL FORCE on APPENDAGE
vs
PROPELLER POSITION
$\bar{c} = 0.3$ $r = 4$
$\frac{F_a}{T}$
$\bar{x}_0 = -1.6$
-1.4
-1.2
-1.05
2.0
1.8
1.6
1.4
1.2
1.0
.8
.6
.4
.2
0
-.2
-.4
-.6
-.8
-1.0
-1.2
-1.4
-1.6
-1.8
-2.0
-1.4 -1.2 -1.0 -.8 -.6 -.4 -.2 0 .2 .4 .6 .8 1.0 1.2 1.4

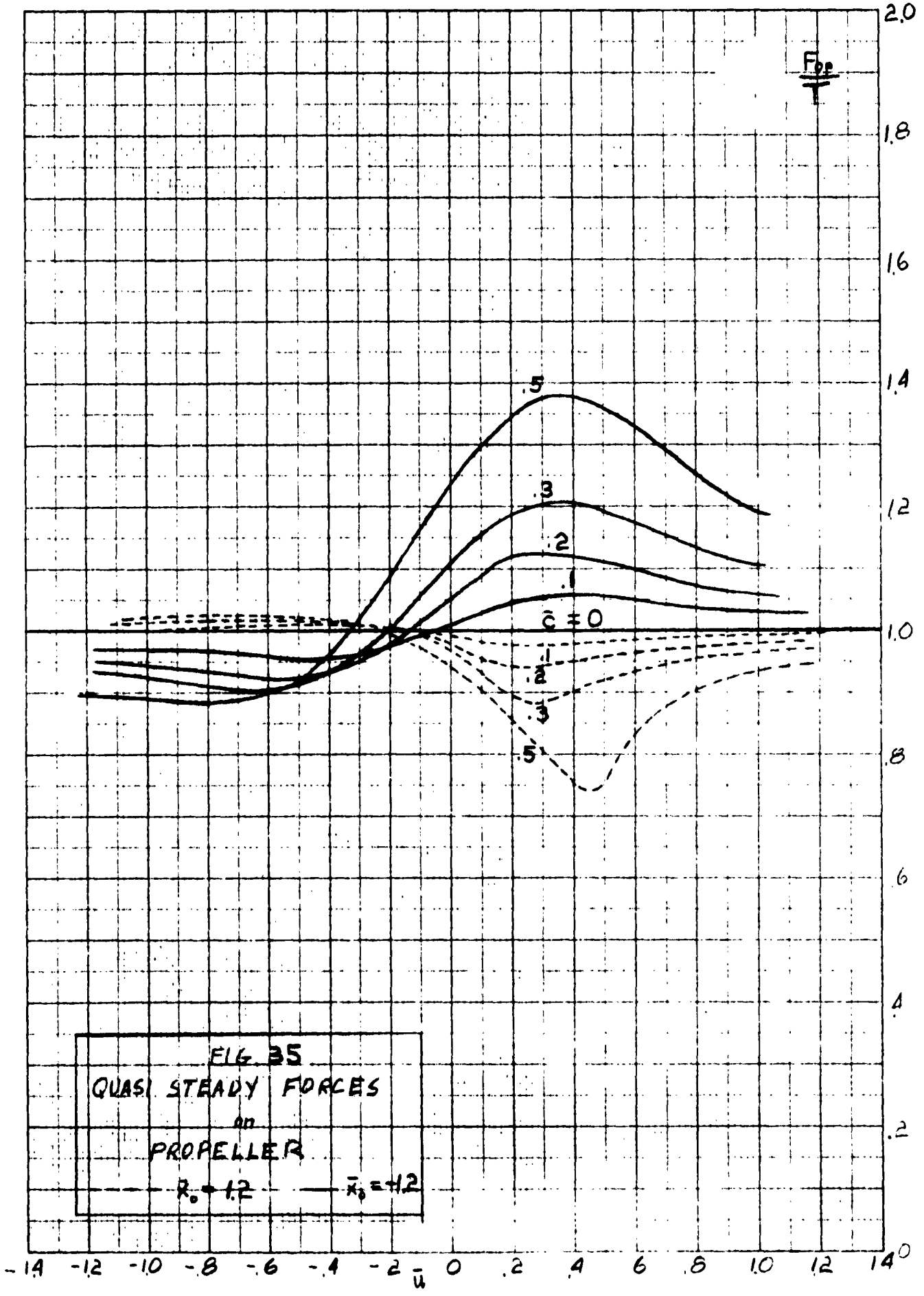

FIG. 35
QUASI STEADY FORCES
on
PROPELLER
$R_0 = 1.2$ — $\bar{x}_0 = -1.2$

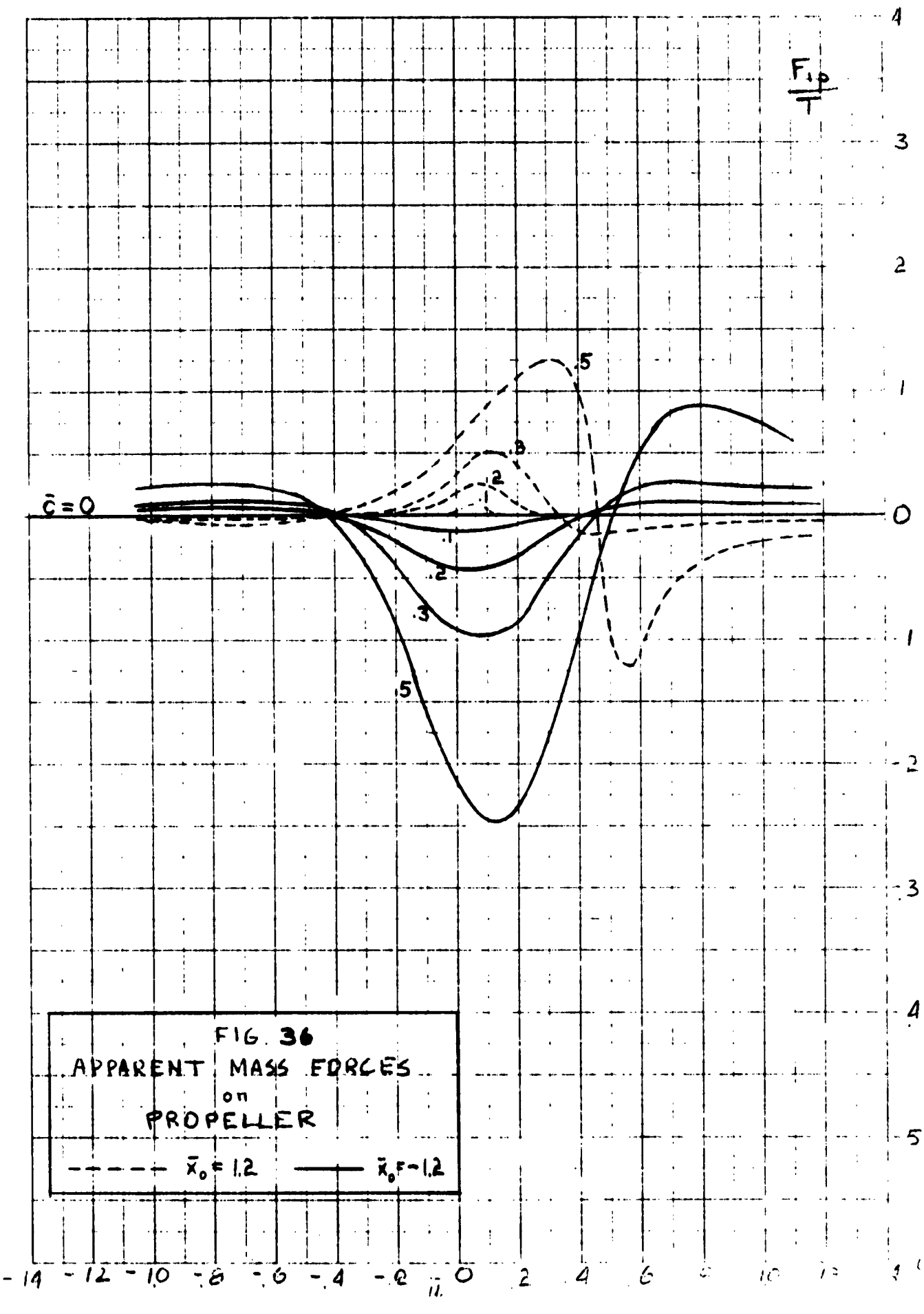

FIG. 36
APPARENT MASS FORCES
on
PROPELLER

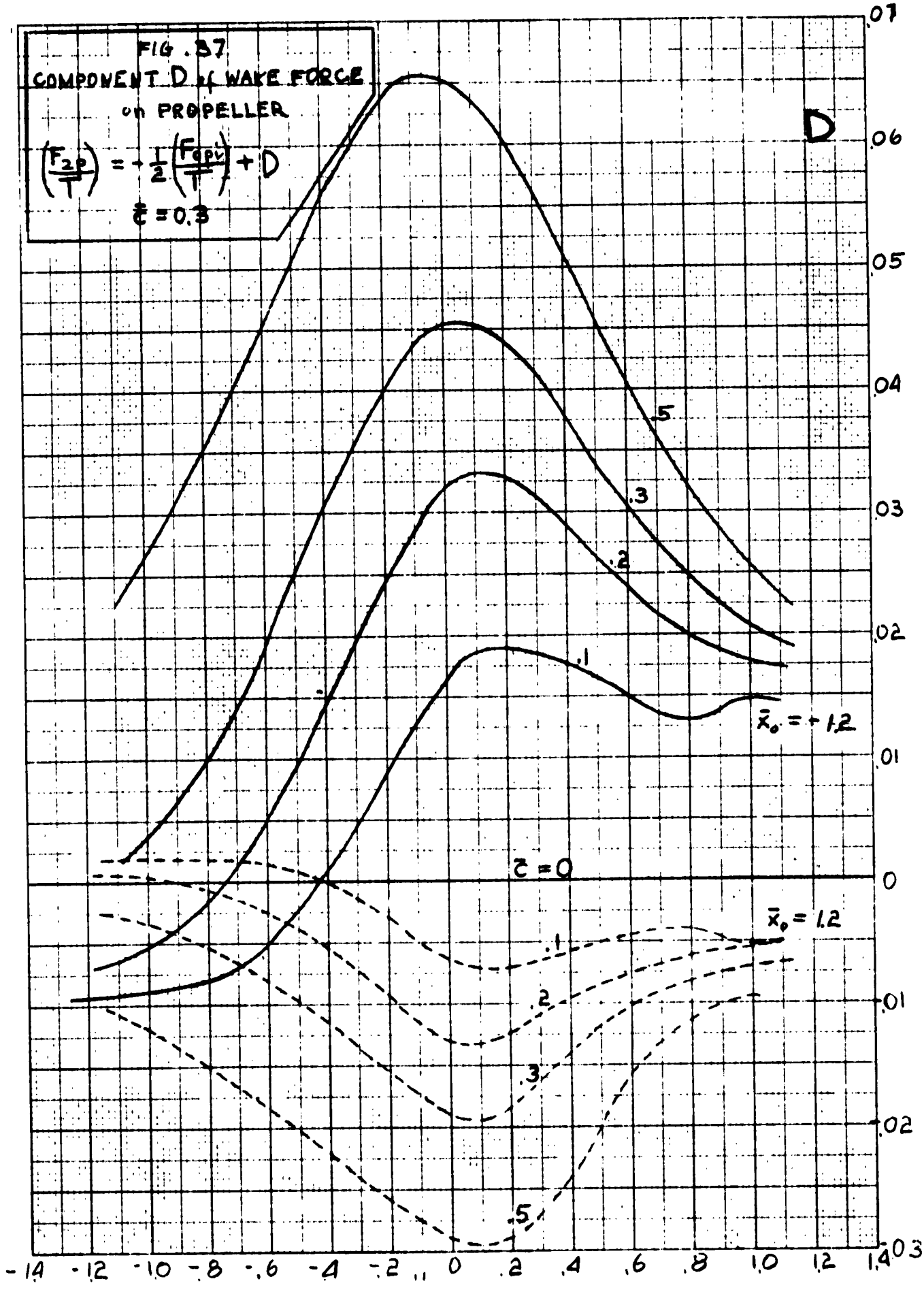
FIG. 37
COMPONENT D of WAKE FORCE
on PROPELLER
$\left(\frac{F_{2p}}{T}\right) = -\frac{1}{2}\left(\frac{F_{opv}}{T}\right) + D$
$\bar{c} = 0.3$
D
.07
.06
.05
.04
.03
.02
.01
0
.01
.02
.03
.5
.3
.2
.1
$\bar{x}_0 = +1.2$
$\bar{c} = 0$
$\bar{x}_0 = 1.2$
.1
.2
.3
.5
-.14 -.12 -.10 -.8 -.6 -.4 -.2 0 .2 .4 .6 .8 1.0 1.2 1.4

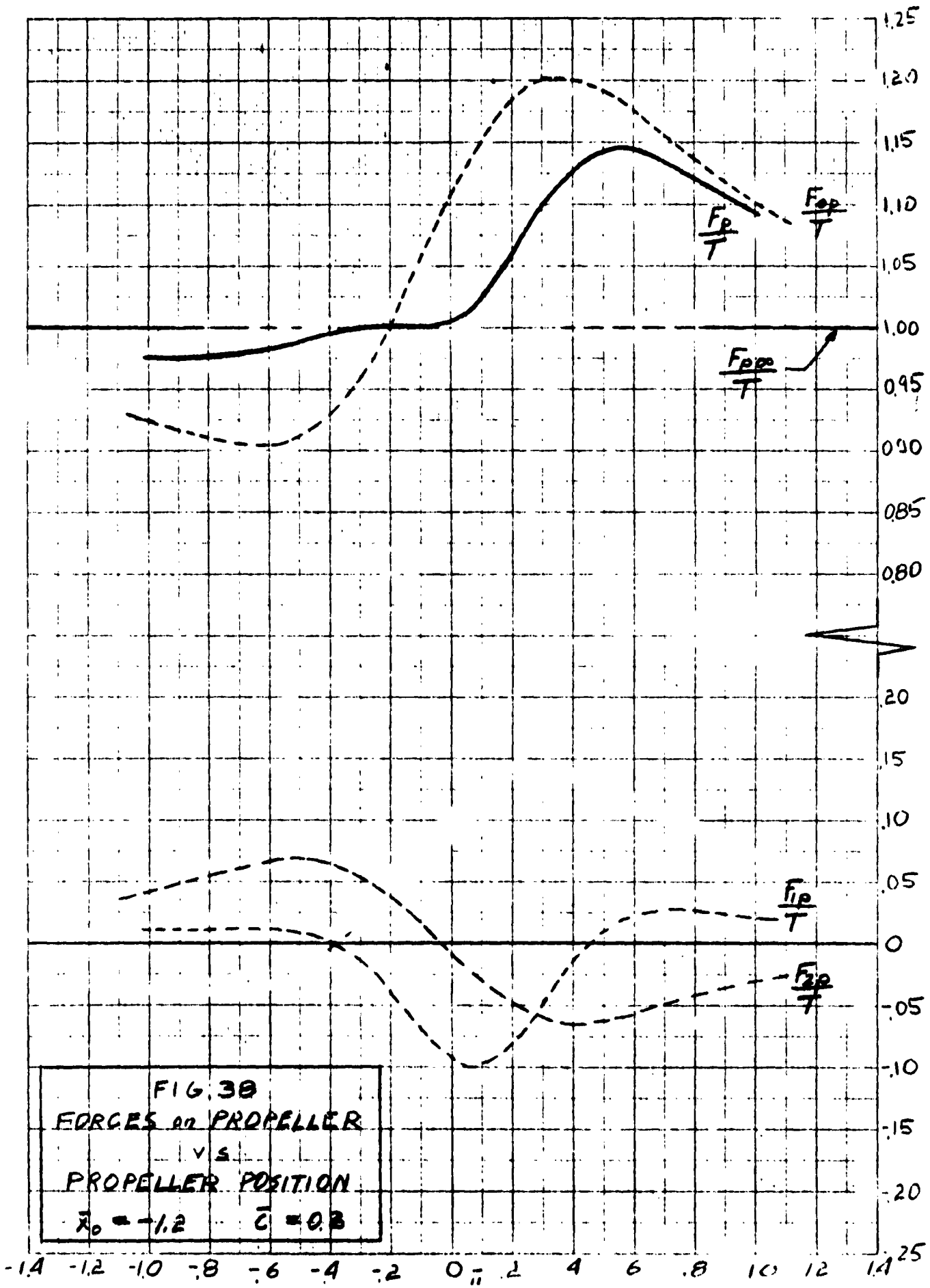

FIG. 38
FORCES on PROPELLER
vs
PROPELLER POSITION
$\bar{x}_0 = -1.2 \quad \bar{c} = 0.2$

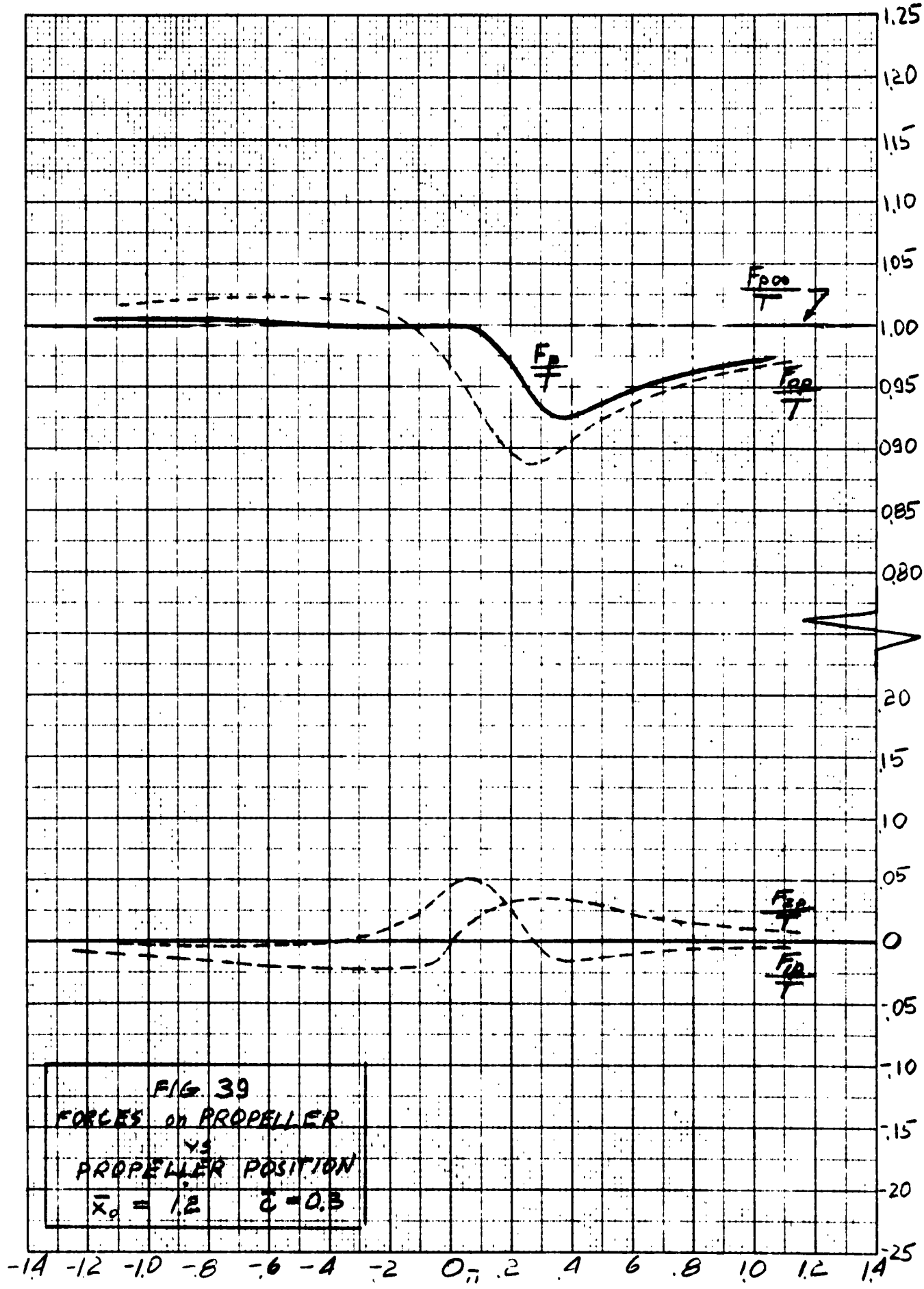

FIG. 39
FORCES on PROPELLER
vs
PROPELLER POSITION
$\bar{x}_0 = 1.2$ $\bar{c} = 0.3$

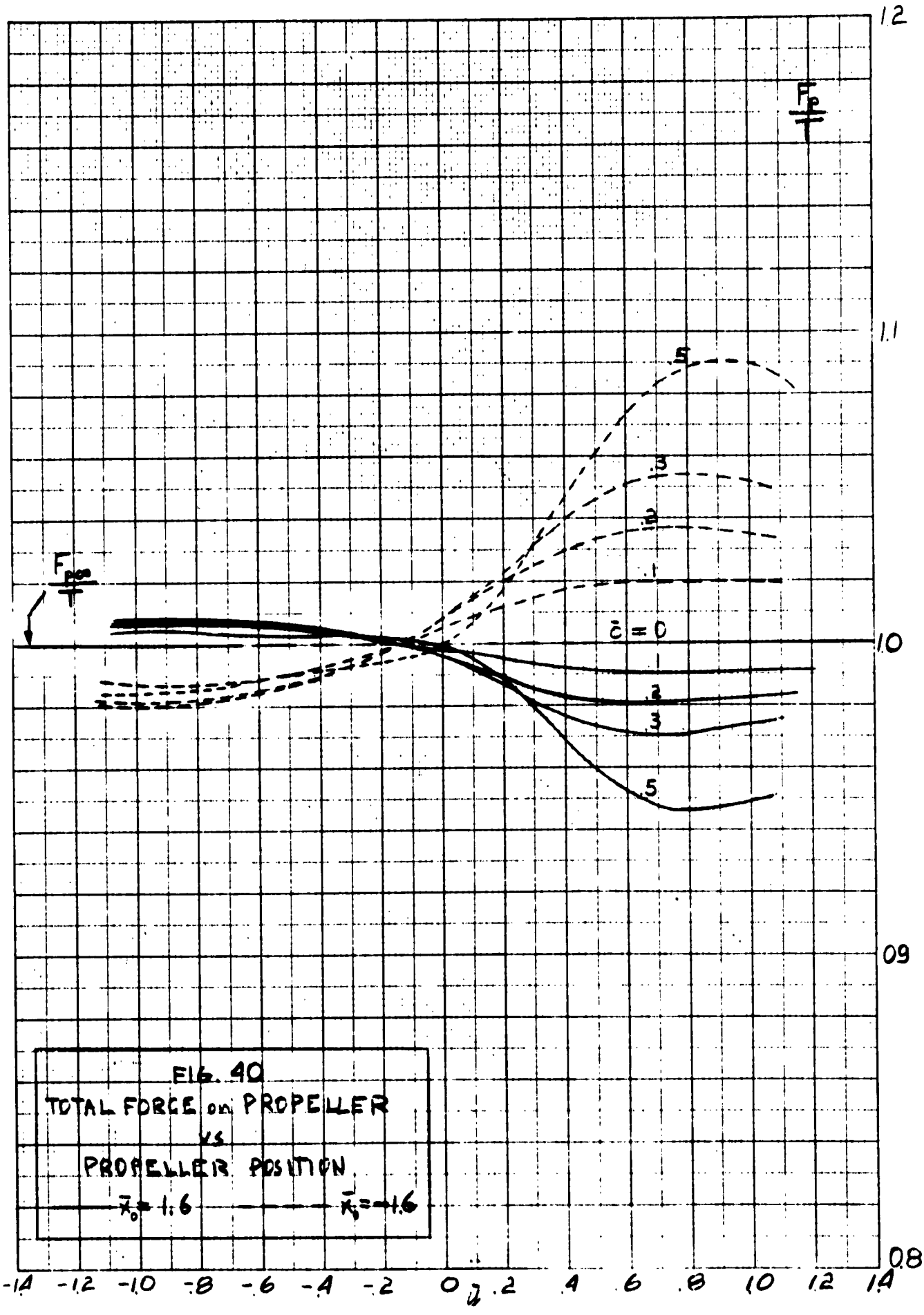

FIG. 40
TOTAL FORCE on PROPELLER
vs
PROPELLER POSITION
$\bar{x}_0 = 1.6$ $\bar{x}_1 = -1.6$

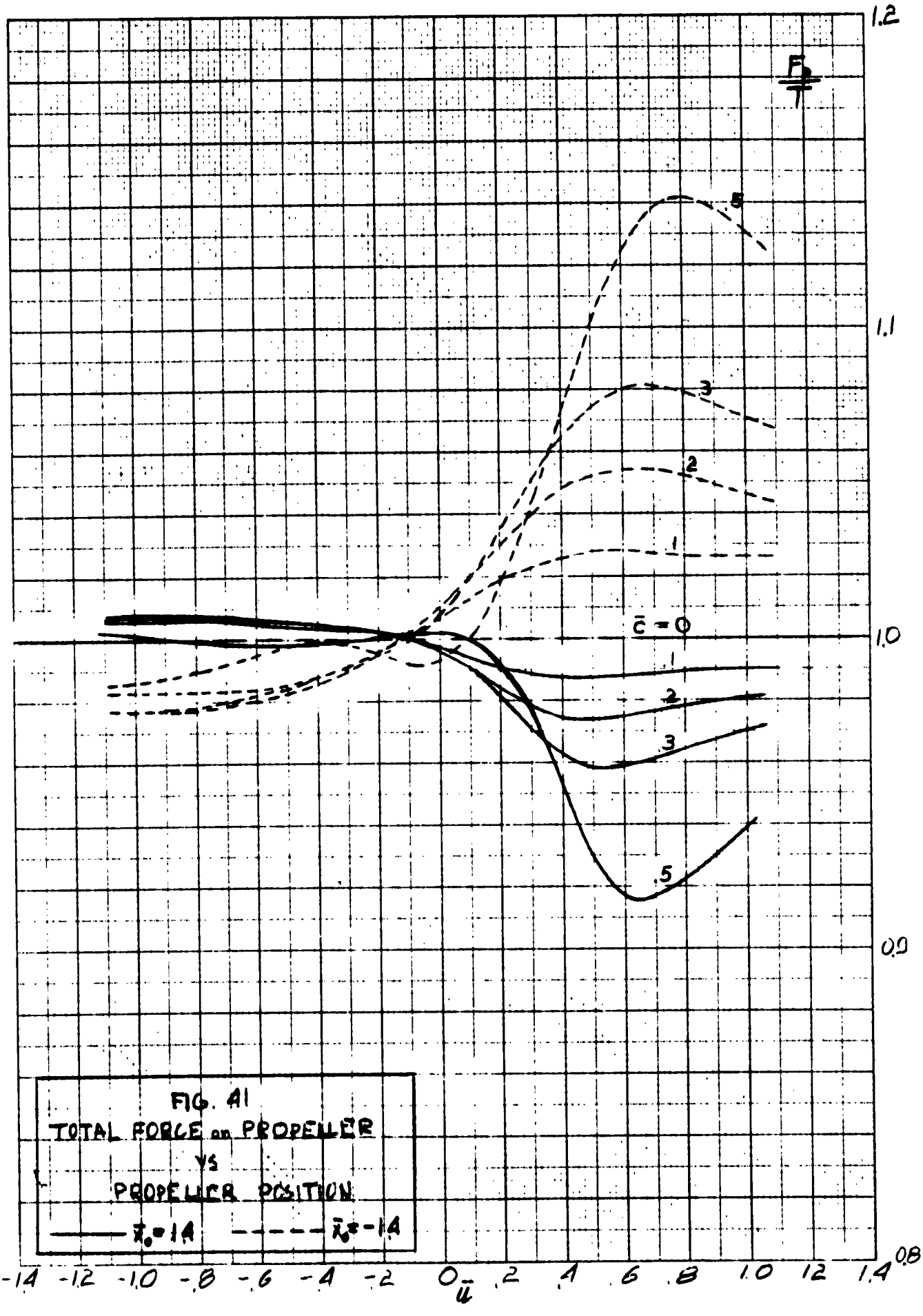

FIG. 41
TOTAL FORCE on PROPELLER
VS
PROPELLER POSITION
—— $\bar{x}_0 = 1.4$ - - - - $\bar{x}_0 = -1.4$

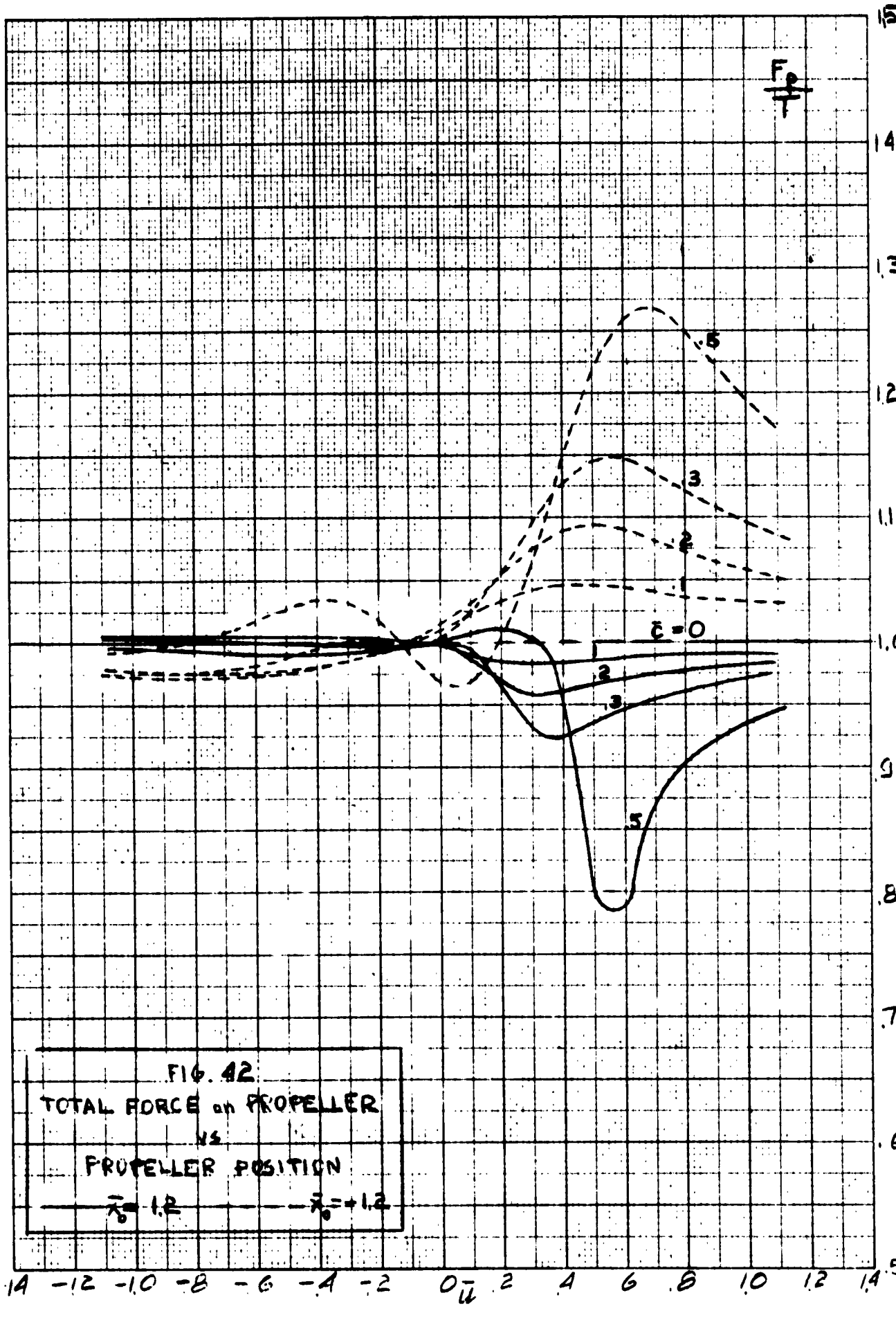

FIG. 42

TOTAL FORCE on PROPELLER

VS

PROPELLER POSITION

—— $\bar{x}_0 = 1.2$ — — — $\bar{x}_0 = +1.2$

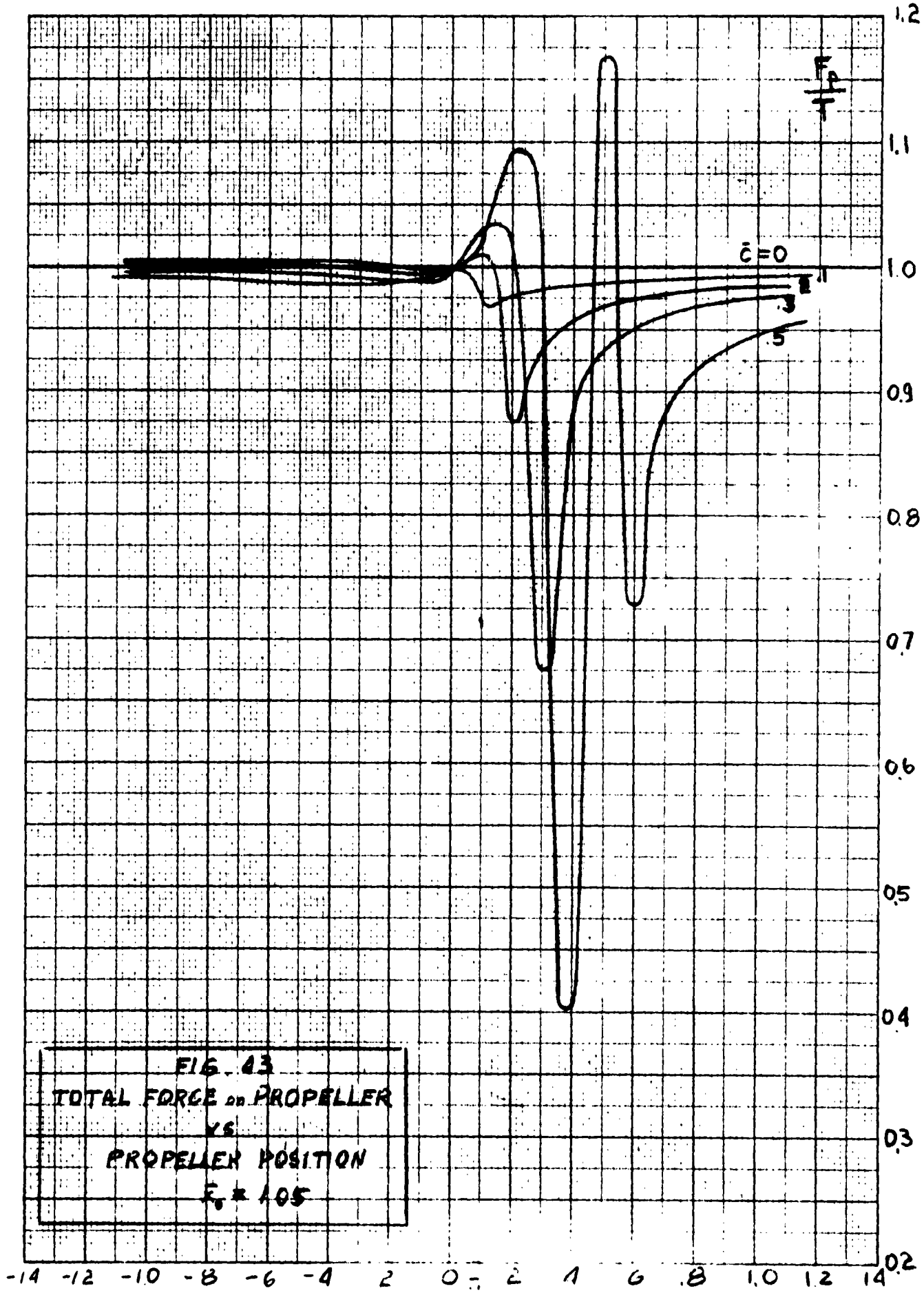

FIG. 43
TOTAL FORCE on PROPELLER
vs
PROPELLER POSITION
$F_0 * .105$

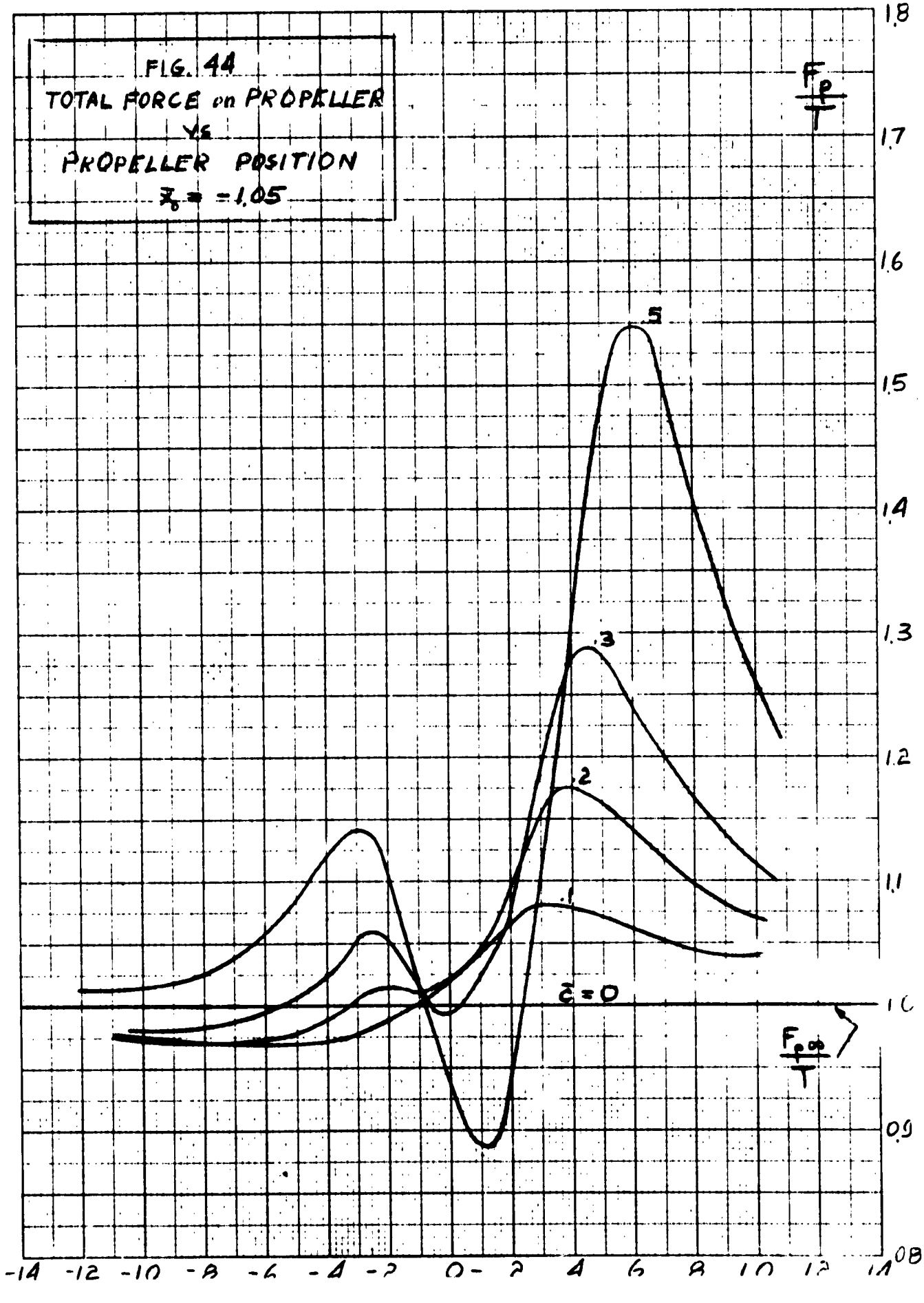
FIG. 44
TOTAL FORCE on PROPELLER
vs
PROPELLER POSITION
$\bar{x}_0 = -1.05$
$\frac{F_p}{T}$
1.8
1.7
1.6
1.5
1.4
1.3
1.2
1.1
1.0
0.9
0.8
.5
.3
.2
.1
$\bar{c} = 0$
$\frac{F_{p\infty}}{T}$
-14 -12 -10 -8 -6 -4 -2 0 2 4 6 8 10 12 14

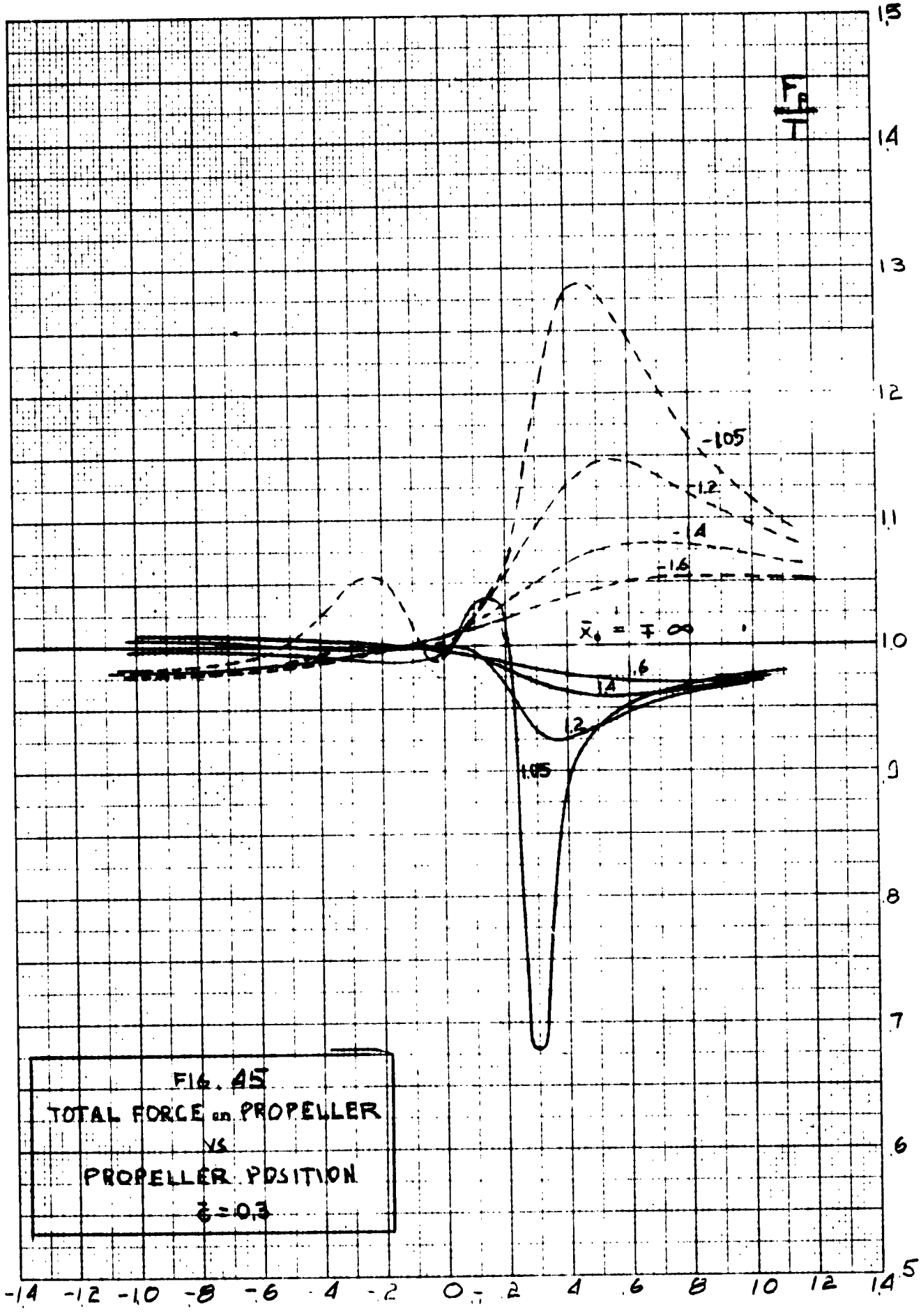

FIG. 45
TOTAL FORCE on PROPELLER
vs
PROPELLER POSITION
$\bar{z} = 0.3$

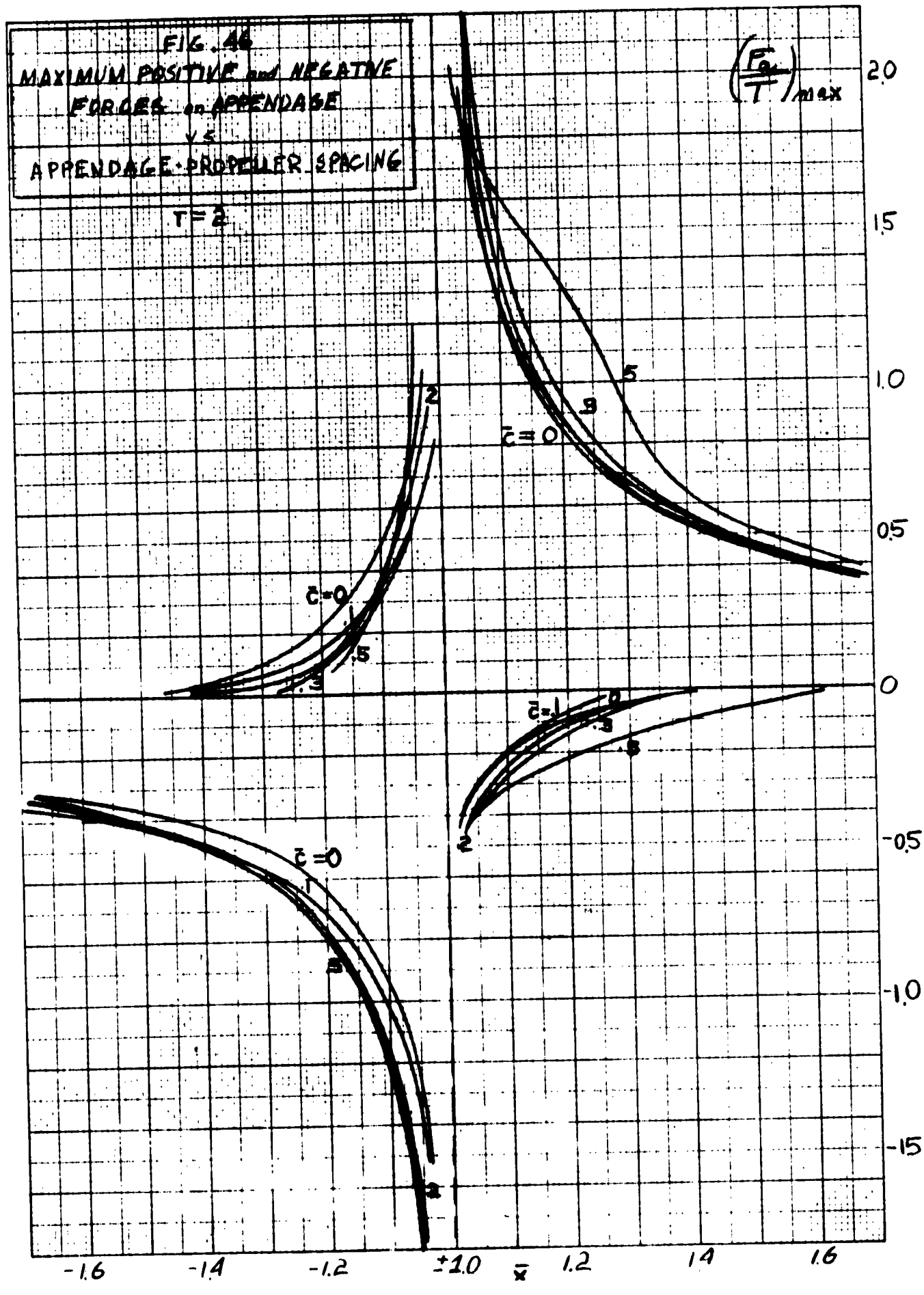
FIG. 46
MAXIMUM POSITIVE and NEGATIVE FORCES on APPENDAGE
vs
APPENDAGE-PROPELLER SPACING
T = 2
$\left(\frac{F_a}{T}\right)_{max}$
2.0
1.5
1.0
0.5
0
-0.5
-1.0
-1.5
$\bar{c}=0$
.5
1
2
3
5
$\bar{c}=1$
$\bar{c}=0$
-1.6
-1.4
-1.2
±1.0
1.2
1.4
1.6
$\bar{x}$

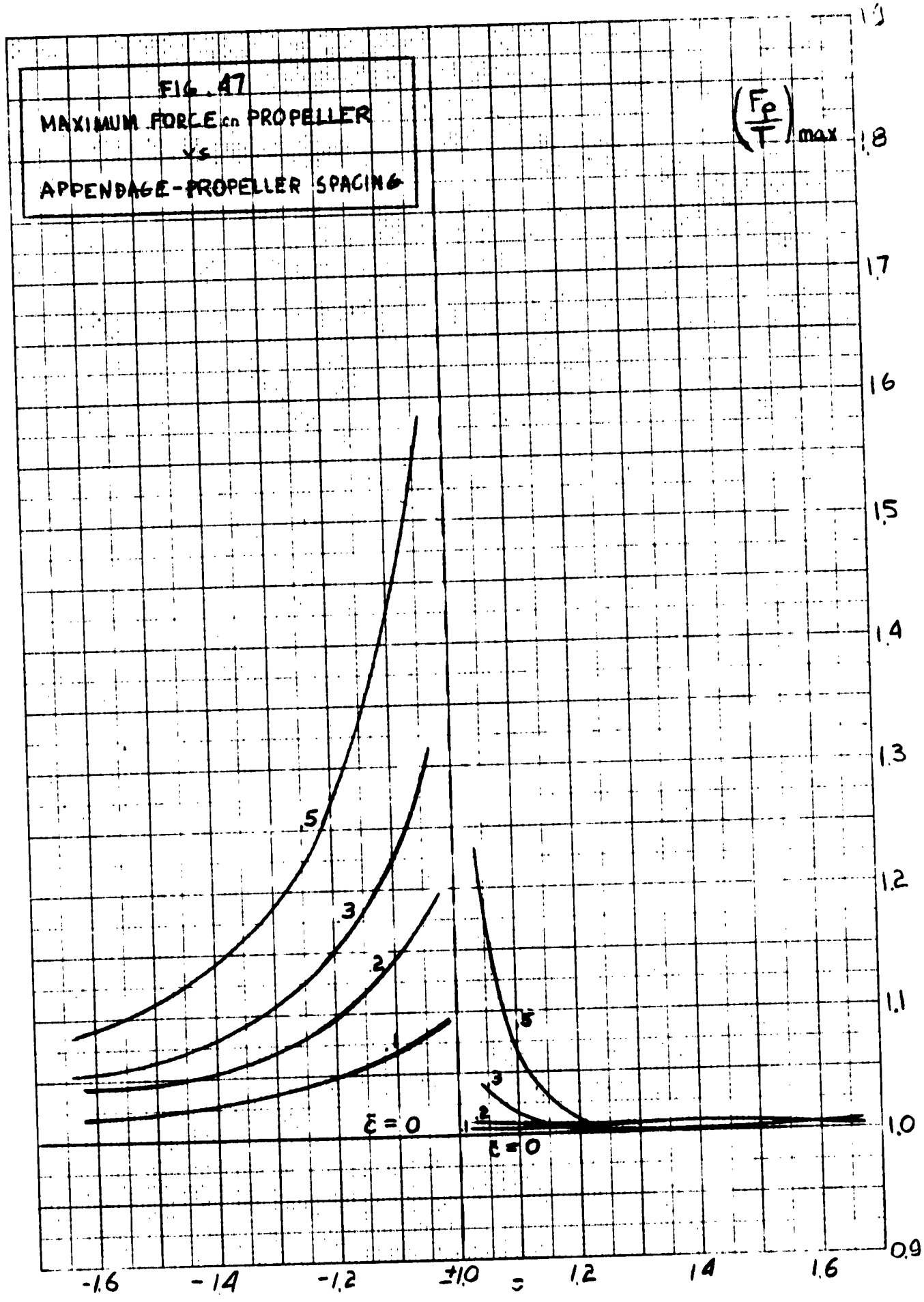
FIG. 47
MAXIMUM FORCE on PROPELLER
vs
APPENDAGE-PROPELLER SPACING
$\left(\frac{F_e}{T}\right)_{max}$
1.8
1.7
1.6
1.5
1.4
1.3
1.2
1.1
1.0
0.9
.5
.3
.2
$\bar{\epsilon} = 0$
.5
.3
.2
$\bar{\epsilon} = 0$
-1.6
-1.4
-1.2
-1.0
1.2
1.4
1.6

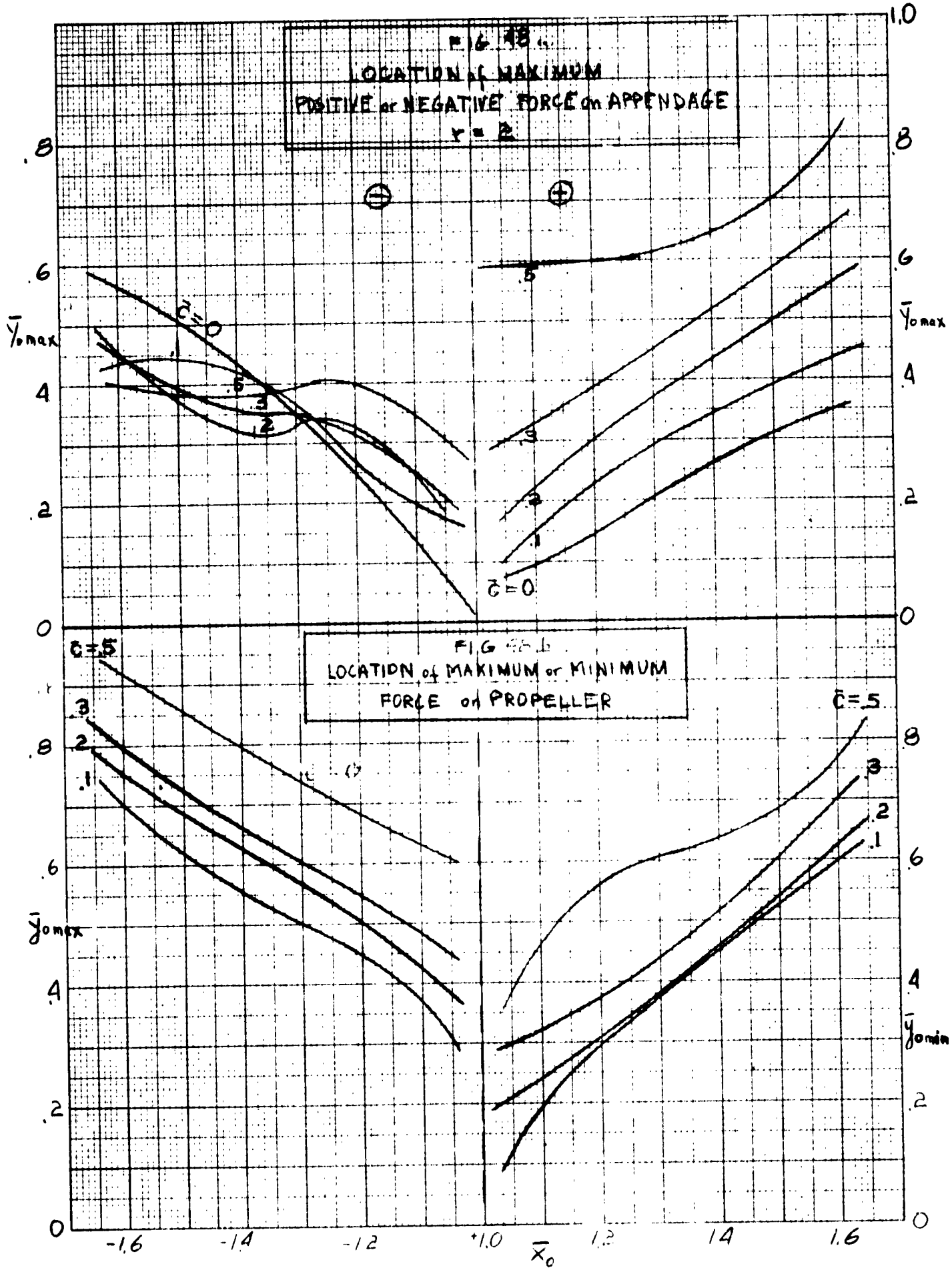
FIG 4a
LOCATION of MAXIMUM
POSITIVE or NEGATIVE FORCE on APPENDAGE
r = 2
⊖
⊕
$\bar{y}_{o\,max}$
$\bar{c}=0$
.5
.3
.2
.1
$\bar{c}=0$
FIG 4b
LOCATION of MAXIMUM or MINIMUM
FORCE on PROPELLER
$\bar{c}=.5$
.3
.2
.1
$\bar{y}_{o\,max}$
$\bar{c}=.5$
.3
.2
.1
$\bar{y}_{o\,min}$
0
.2
.4
.6
.8
1.0
-1.6
-1.4
-1.2
+1.0
1.2
1.4
1.6
$\bar{x}_o$

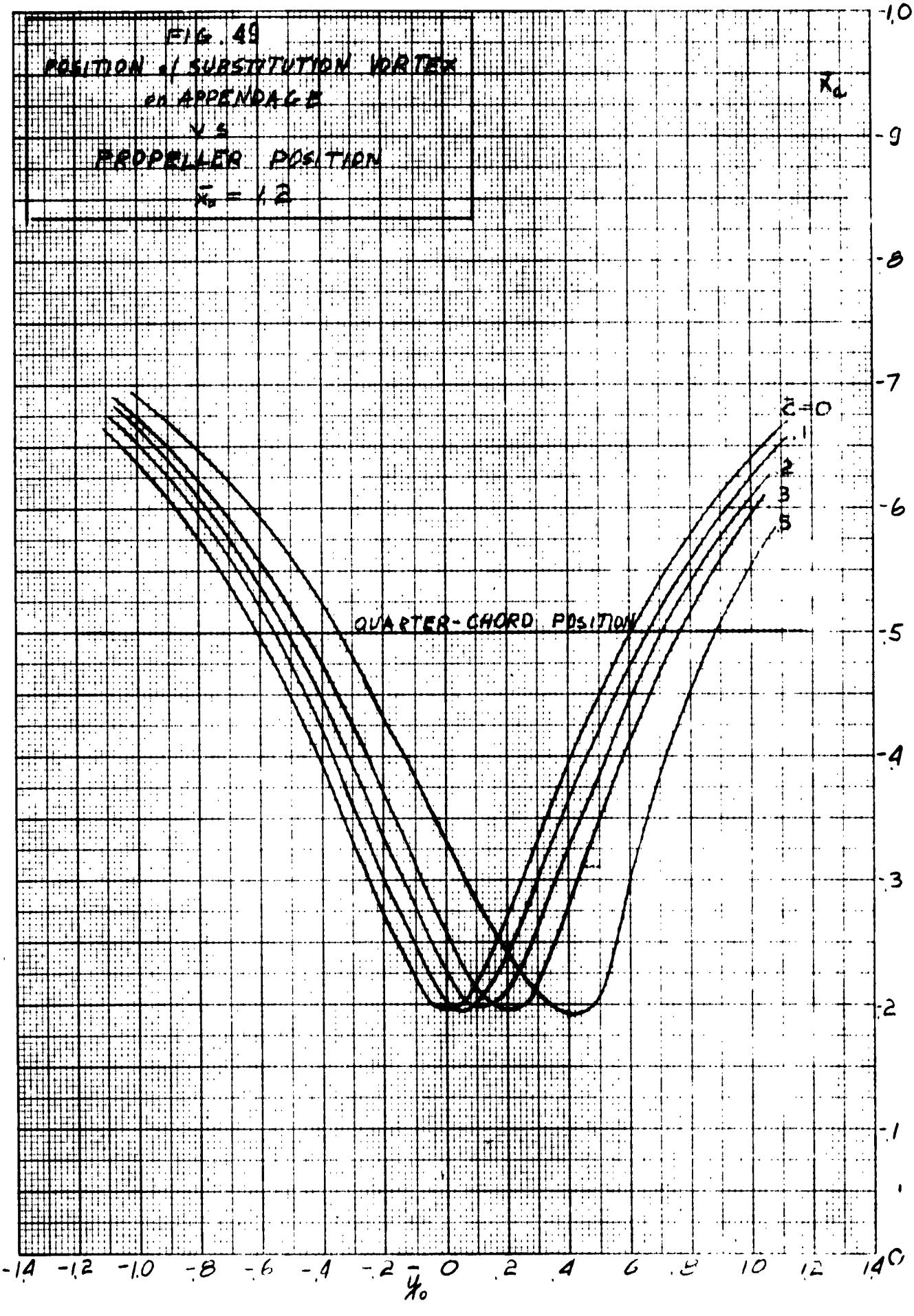

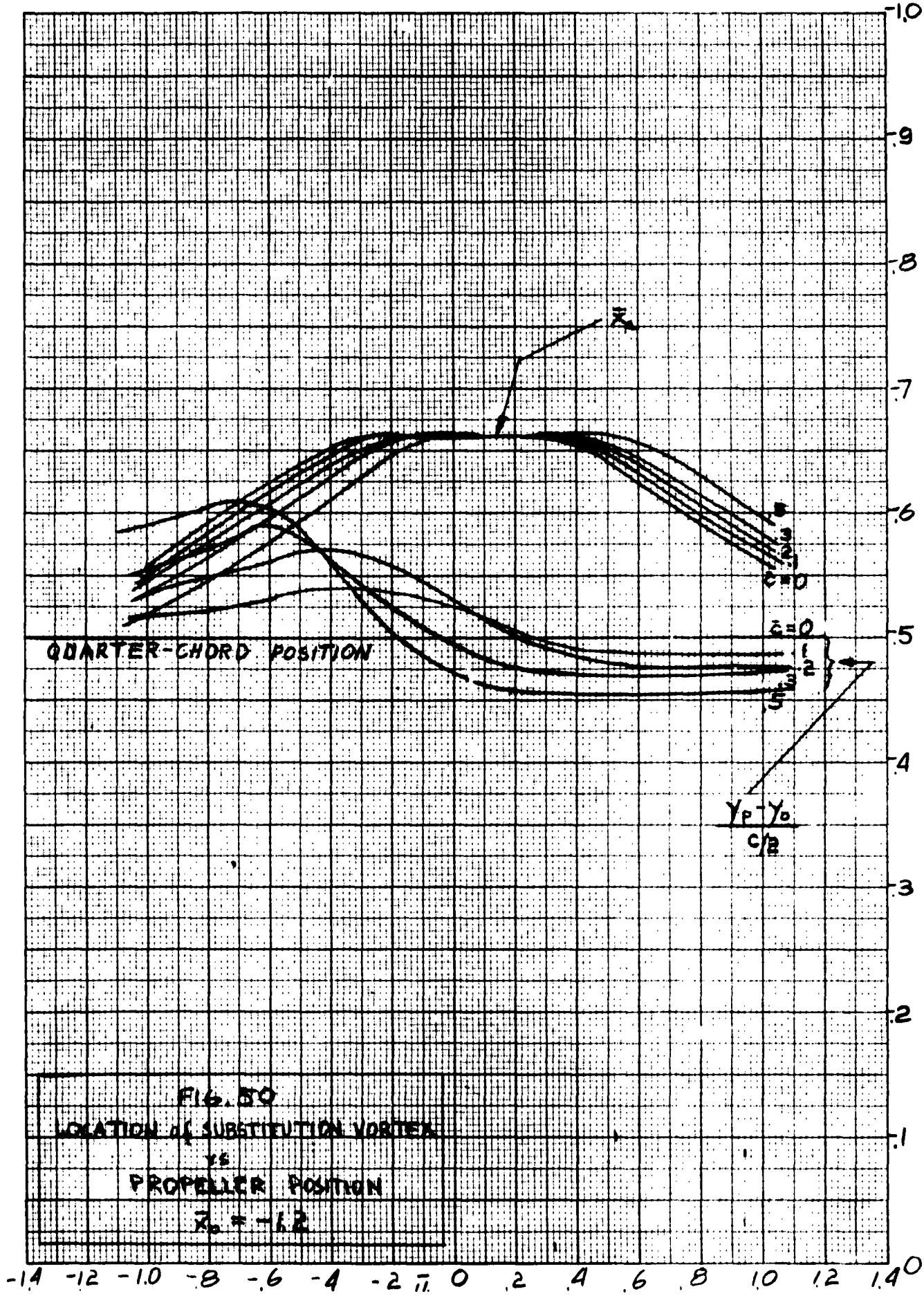

FIG. 50

LOCATION of SUBSTITUTION VORTEX

vs

PROPELLER POSITION

$\bar{x}_0 = -1.2$

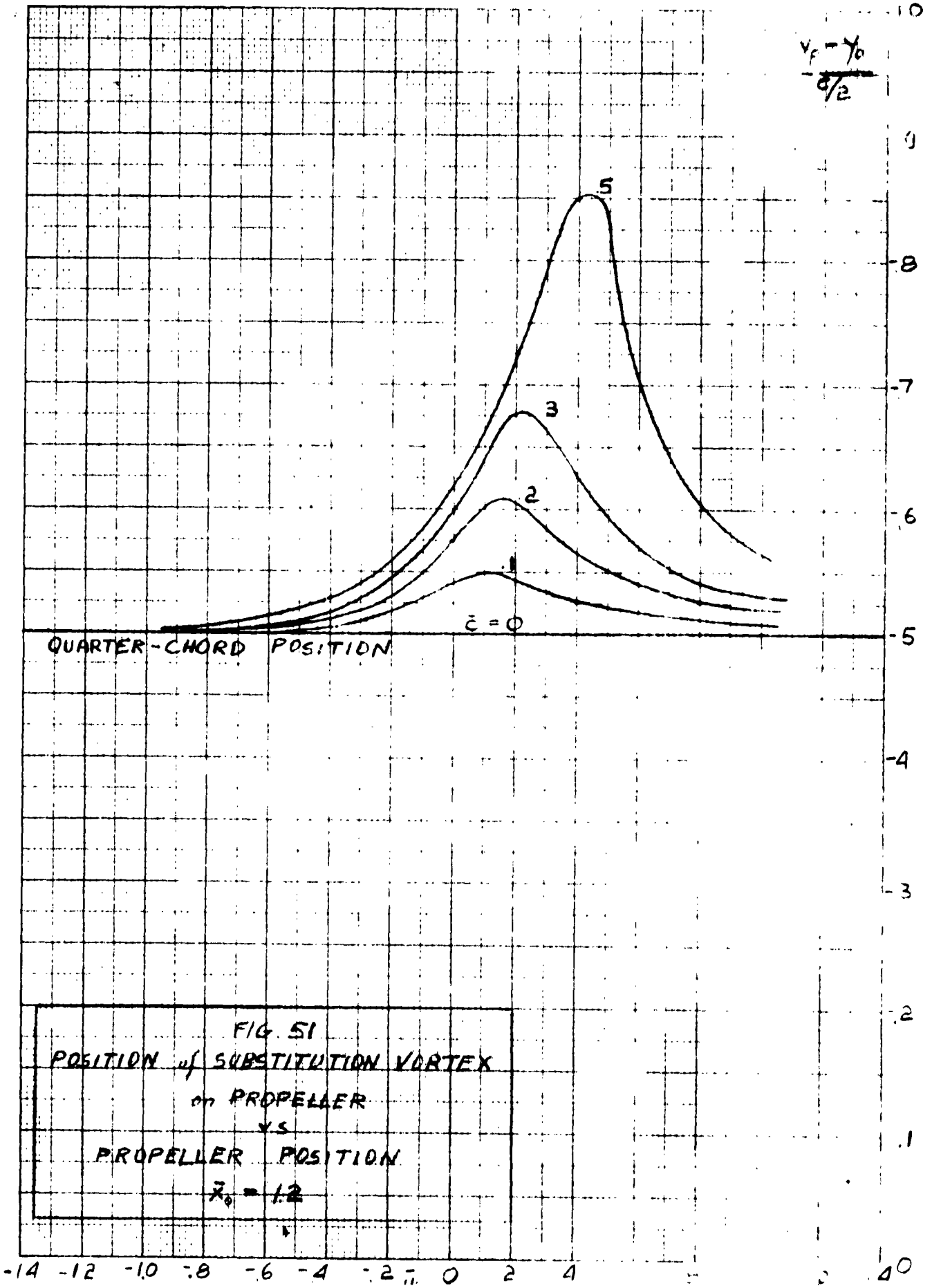

FIG. 51
POSITION of SUBSTITUTION VORTEX
on PROPELLER
vs
PROPELLER POSITION
$\bar{x}_0 = 1.2$

APPENDIX A

EVALUATION OF INTEGRALS

1. Solution of

$$I_1 = \int_{-\ell}^{\ell} \sqrt{\frac{\ell+\eta}{\ell-\eta}} \; \frac{\eta+k_1}{\eta-k_2} \; \frac{d\eta}{(\eta-\eta_1)(\eta-\eta_2)} \tag{A-1}$$

having a singularity at $\eta = k_2$. η_1 and η_2 are complex constants. Writing

$$\frac{\eta+k_1}{(\eta-k_2)(\eta-\eta_1)(\eta-\eta_2)} = \frac{A}{\eta-k_2} + \frac{B}{\eta-\eta_1} + \frac{C}{\eta-\eta_2}$$

we have

$$A = \frac{k_1+k_2}{(k_2-\eta_1)(k_2-\eta_2)}$$

$$B = \frac{k_1+k_2}{(\eta_1-\eta_2)(\eta_1-k_2)}$$

$$C = \frac{k_1+\eta_2}{(\eta_2-k_2)(\eta_2-\eta_1)}$$

Thus the first integral of I_1 becomes

$$I_{11} = \int_{-\ell}^{\ell} \sqrt{\frac{\ell+\eta}{\ell-\eta}} \; \frac{d\eta}{\eta-k_2} \tag{A-2}$$

This is a principal value integral whose value is π.

The second and third terms of I_1 are of the form

$$I_{12} = \int_{-\ell}^{\ell} \sqrt{\frac{\ell+\eta}{\ell-\eta}} \; \frac{d\eta}{\eta \mp p} \tag{A-3}$$

with

$$p = a + ib \qquad a > \ell \ .$$

Multiplying top and bottom of (A-3) by $\sqrt{\ell + \eta}$ and writing

$$s = \ell \cos \theta \qquad\qquad \bar{p} = \frac{a + ib}{\ell}$$

$$I_{12} = \int_{o}^{\pi} \frac{(1+\cos\theta)\,d\theta}{\cos\theta \mp \bar{p}} = \int_{o}^{\pi} \left(1 - \frac{1 \mp \bar{p}}{\cos\theta \mp \bar{p}}\right) d\theta$$

or

$$I_{12} = \pi + (1 \mp \bar{p}) \int_{o}^{\pi} \frac{d\theta}{\cos\theta \mp \bar{p}} \ .$$

The problem is now to integrate the last integral rewritten as

$$I_{13} = \frac{1}{2} \int_{-\pi}^{\pi} \frac{d\theta}{\cos\theta \mp \bar{p}} \tag{A-4}$$

This integral can best be integrated in the complex plane by a contour integration on the unit circle $z = e^{i\theta}$. In this

notation we have

$$\cos\theta = \frac{z + z^{-1}}{2} \qquad d\theta = \frac{dz}{iz}$$

and

$$I_{13} = \frac{1}{2i} \oint \frac{dz}{(z-z_1)(z-z_2)} \tag{A-5}$$

where

a) for $+\bar{p}$

$$z_1 = -p + \sqrt{p^2-1}$$

$$z_2 = -p - \sqrt{p^2-1}$$

with z_1 inside the unit circle.

b) for $-\bar{p}$

$$z_1 = p + \sqrt{p^2-1}$$

$$z_2 = p - \sqrt{p^2-1}$$

with z_2 inside the unit circle

Since the values of the residue for I_{13+} is $\frac{2\pi i}{z_1-z_2}$ and for

I_{13-} $\frac{2\pi i}{z_2-z_1}$ we have

$$I_{13} = \int_0^{\pi} \frac{d\theta}{\cos\theta \pm p} = \pm \frac{\pi}{\sqrt{p^2-1}} \tag{A-6}$$

Also

$$I_{12} = \pi \left[1 - \sqrt{\frac{p \mp 1}{p \pm 1}}\right] \tag{A-7}$$

In terms of our parameters

$$I_{12} = \pi \left[1 - \sqrt{\frac{\eta_{1,2} + \ell}{\eta_{1,2} - \ell}} \right] .$$

and I_1 becomes

$$I_1 = \frac{\pi}{\eta_2 - \eta_1} \left\{ \frac{k_1+\eta_1}{\eta_1-k_2} \sqrt{\frac{\eta_1/\ell + 1}{\eta_1/\ell - 1}} - \frac{k_1+\eta_2}{\eta_2-k_2} \sqrt{\frac{\eta_2/\ell + 1}{\eta_2/\ell - 1}} \right\} \tag{A-8}$$

If in addition η_1 and η_2 are complex conjugates, then we have within the brackets an expression of the form $z_1\bar{z}_2 - \bar{z}_1 z_2$ and since

$$z_1\bar{z}_2 - \bar{z}_1 z_2 = 2i \operatorname{Im} z_1\bar{z}_2$$

$$I_1 = \frac{2\pi i}{\eta_2 - \eta_1} \operatorname{Im} \frac{k_1+\eta_1}{\eta_1-k_2} \sqrt{\frac{\eta_1/\ell + 1}{\eta_1/\ell - 1}} \tag{A-9}$$

2. Solution of

$$I_2 = \int_{a_1}^{a_2} \sqrt{\frac{a_2-y}{y-a_1}} \sqrt{\frac{y-b_1}{y-b_2}} \frac{dy}{y-b} \tag{A-10}$$

where

$$a_2 = y_o + c/2$$

$$a_1 = y_o - c/2.$$

Writing

$$\zeta = \frac{y-y_o}{c/2}$$

we obtain for I_2

$$I_2 = \int_{-1}^{1} \sqrt{\frac{1-\zeta}{1+\zeta}} \sqrt{\frac{\zeta+a_{11}}{\zeta+a_{12}}} \frac{d\zeta}{\zeta+a_{13}} \qquad \text{(A-11)}$$

where

$$a_{11} = \frac{2}{c}\,[y_o - i(x_o+\ell)], \qquad a_{12} = \frac{2}{c}\,[y_o - i(x_o-\ell)]$$

$$a_{13} = \frac{2}{c}\,[y_o - i(x_o-x)].$$

Multiplying top and bottom by $\sqrt{(1-\zeta)\ (a_{11}+\zeta)}$ and breaking up the numerator into partial fractions, we obtain for I_2.

$$I_2 = -\int_{-1}^{1} \frac{d\zeta}{p} + (1-a_{11}+a_{13}) \int_{-1}^{1} \frac{d\zeta}{p} + [a_{11}-a_{13}(1-a_{11}+a_{13})]$$

$$\int_{-1}^{1} \frac{d\zeta}{(a_{13}+\zeta)p}$$

$$= -\ I_{21} + (1-a_{11}+a_{13})\ \ I_{22} + [a_{11}-a_{13}(1-a_{11}+a_{13})]\ \ I_{23}$$

where

$$p = \sqrt{(1-\zeta^2)\ (a_{11}+\zeta)\ (a_{12}+\zeta)}.$$

We shall now attempt to transform I_2 into a function of elliptic integrals by use of the following transformation

$$\zeta = \frac{\cos\phi-\nu}{1-\nu\cos\phi}$$

$$d\zeta = (\nu^2-1)\frac{\sin\phi}{(1-\nu\cos\phi)^2}\,d\phi$$

where ν is a constant to be determined in such a manner as to yield for I_{21}, I_{22}, and I_{23} elliptic integrals.

Taking I_{22} first, we have

$$I_{22} = \frac{[(\nu^2-1)\sin\phi/(1-\nu\cos\phi)^2]d\phi}{\left\{1-\left(\frac{\cos\phi-\nu}{1-\nu\cos\phi}\right)^2\left(a_{11}+\frac{\cos\phi-\nu}{1-\nu\cos\phi}\right)\left(a_{12}+\frac{\cos\phi-\nu}{1-\nu\cos\phi}\right)\right\}^{\frac{1}{2}}}$$

$$= \sqrt{\frac{1-\nu^2}{(a_{11}-\nu)(a_{12}-\nu)}}\int_0^{\pi}\frac{d\phi}{\left[\left(1+\frac{1-a_{11}\nu}{a_{11}-\nu}\cos\phi\right)\left(1+\frac{1-a_{12}\nu}{a_{12}-\nu}\cos\phi\right)\right]^{1/2}}$$

The value of ν now has to be chosen so as to make the coefficient of $\cos\phi$ in the denominator vanish; hence

$$\frac{1-a_{11}\nu}{a_{11}-\nu}+\frac{1-a_{12}\nu}{a_{12}-\nu}=0$$

or

$$\nu = \frac{1 + a_{11}a_{12}}{a_{11} + a_{12}} \pm \sqrt{\left(\frac{1 + a_{11}a_{12}}{a_{11} + a_{12}}\right)^2 - 1}$$

With this value of ν , I_{22} becomes

$$I_{22} = \sqrt{\frac{1 - \nu^2}{(a_{11} - \nu)(a_{12} - \nu)}} \int_0^{\pi} \frac{d\phi}{\sqrt{1 + \left(\frac{1 - a_{11}\nu}{a_{11} - \nu}\right)\left(\frac{1 - a_{12}\nu}{a_{12} - \nu}\right)\cos^2\phi}}$$

By writing $\phi = \theta + \pi/2$ and realizing that we are dealing with an even function the above integral is recognized as twice the complete elliptic integral of the 1st kind, or

$$I_{22} = 2\sqrt{\frac{1 - \nu^2}{(a_{11} - \nu)(a_{12} - \nu)}}\, K(k) \qquad \text{(A-12)}$$

with

$$k^2 = \frac{(1 - a_{11}\nu)(a_{12}\nu - 1)}{(a_{11} - \nu)(a_{12} - \nu)}$$

For I_{21} we have

$$I_{21} = \sqrt{\frac{1 - \nu^2}{(a_{11} - \nu)(a_{12} - \nu)}} \int_0^{\pi} \frac{\cos\phi - \nu}{(1 - \nu\cos\phi)\sqrt{1 - k^2\cos^2\phi}}\, d\phi$$

$$= \sqrt{\frac{1 - \nu^2}{(a_{11} - \nu)(a_{12} - \nu)}} \left\{ -\frac{1}{\nu} \int_0^{\pi} \frac{d\phi}{\sqrt{1 - k^2\cos^2\phi}} + \frac{1 - \nu^2}{\nu} \int_0^{\pi} \frac{d\phi}{(1 - \nu\cos\phi)\sqrt{(1 - k^2\cos^2\phi)}} \right\}$$

$$= \frac{1-\nu^2}{(a_{11}-\nu)(a_{12}-\nu)} \left\{ -\frac{2}{\nu} K(k) + \frac{1-\nu^2}{\nu} \quad I_{211} \right\}$$

Multiplying top and bottom of I_{211} by $(1 + \nu \cos\phi)$

$$I_{211} = \int_0^{\pi} \frac{(1+\nu\cos\phi)d\phi}{(1-\nu)^2\cos^2\phi)\sqrt{1+k^2\cos^2\phi}} + \nu \int_0^{\pi} \frac{\cos\phi \; d\phi}{(1-\nu)^2\cos^2\phi)\sqrt{1-k^2\cos^2\phi}}$$

The first of the above integrals is twice the complete elliptic integral of the 3rd kind. The second integral being odd in ϕ is zero. Thus

$$I_{211} = 2\Pi(\nu^2, k)$$

and

$$I_{21} = \frac{2}{\nu} \sqrt{\frac{1-\nu^2}{(a_{11}-\nu)(a_{12}-\nu)}} [-K(k) + (1-\nu^2)\Pi(\nu^2, k)] \qquad \text{(A-13)}$$

Considering next I_{23}

$$I_{23} = \sqrt{\frac{1-\nu^2}{(a_{11}-\nu)(a_{12}-\nu)}} \int_0^{\pi} \frac{d\phi}{[a_{13} + \frac{\cos\phi - \nu}{1-\nu\cos\phi}]\sqrt{1-k^2\cos^2\phi}}$$

$$= \frac{1-\nu^2}{(a_{11}-\nu)(a_{12}-\nu)(a_{13}-\nu)} \left\{ -\frac{\nu(a_{13}-\nu)}{1-\nu a_{13}} \int_0^{\pi} \frac{d\phi}{\sqrt{1-k^2\cos^2\phi}} + \right.$$

$$+ \left[1 + \frac{\nu(a_{13}-\nu)}{1-\nu a_{13}}\right] \int_o^{\pi} \frac{d\phi}{\left[1 + \frac{1-\nu a_{13}}{a_{13}-\nu} \cos\phi\right] \sqrt{1-k^2\cos^2\phi}} \Bigg\}$$

Multiplying the second integral top and bottom by

$$1 - \frac{1-\nu a_{13}}{a_{13}-\nu} \cos\phi$$

$$I_{23} = \sqrt{\frac{1-\nu^2}{(a_{11}-\nu)(a_{12}-\nu)}} \frac{1}{a_{13}-\nu} \left\{ - \frac{2\nu(a_{13}-\nu)}{1-a_{13}\nu} K(k) \right.$$

$$\left. + \frac{1-\nu^2}{1-\nu a_{13}} \int_o^{\pi} \frac{\left(1 - \frac{1-\nu a_{13}}{a_{13}-\nu} \cos\phi\right) d\phi}{\left[1 - \left(\frac{1-\nu a_{13}}{a_{13}-\nu}\right)^2 \cos^2\phi\right] \sqrt{1-k^2\cos^2\phi}} \right\}$$

or since the second part of the second integral is zero

$$I_{23} = \frac{2}{1-a_{13}} \sqrt{\frac{1-\nu^2}{(a_{11}-\nu)(a_{12}-\nu)}} \left[-\nu K(k) + \frac{1-\nu^2}{a_{13}-\nu} \Pi(\beta^2, k)\right] \qquad \text{(A-14)}$$

$$\text{with } \beta^2 = \left(\frac{1-\nu a_{13}}{a_{13}-\nu}\right)^2$$

The total expression for I_2 is then

$$I_2 = \frac{2(1+\nu)}{(1-\nu a_{13})} \sqrt{\frac{1-\nu^2}{(a_{11}-\nu)(a_{12}-\nu)}}$$

$$\left\{ (1-a_{11}\nu) K(k) + (1-\nu)(1-\nu a_{13}) \Pi(\nu^2, k) \right.$$

$$\left. + \frac{\nu(1-\nu)(a_{11}-a_{13})(1-a_{13})}{a_{13}-\nu} \Pi(\beta^2, k) \right\} \qquad \text{(A-15)}$$

This being a solution of integral (A-10) in terms of complete elliptic integrals of the 1st and 3rd kind.

APPENDIX B

SUBSTITUTION VORTEX FOR AEROFOIL IN FIELD OF ANOTHER VORTEX

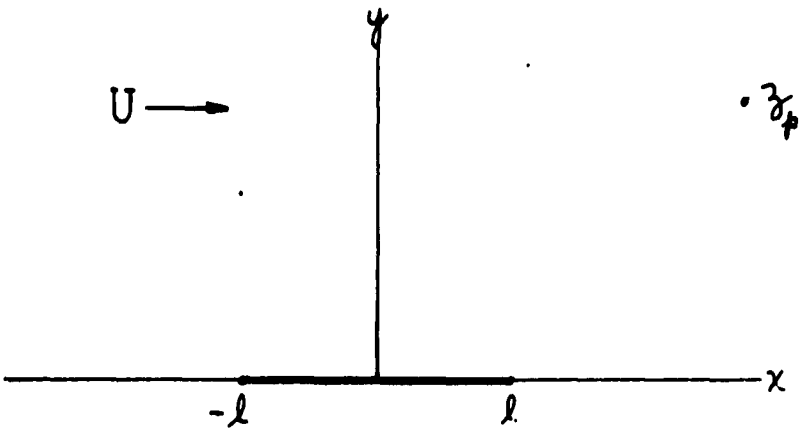

Figure B.1

Let there be a vortex of strength (circulation) Γ_p at z_p. Suppose the flow associated with the vortex in the presence of the aerofoil (a flat plate) has circulation Γ_a around the latter. We seek the location, z_a, of that vortex by which the aerofoil may be replaced, such that the flow at sufficiently large z due to the two vortices approximates the original flow. More precisely, z_a is to be so determined that the flow due to the two vortices agrees with the original flow to terms of order $\frac{1}{z}$.

The configuration in question is shown in Figure B.1, where it will be seen that we have chosen the appendage as the aerofoil which is to be replaced by a vortex. By a treatment entirely analogous to the one we shall describe, the propeller may be similarly replaced, but it will suffice to explain the

method with reference to the appendage and merely quote the results for the propeller.

Let w_1 be the complex potential of the flow associated with the two vortices. Then

B.1) $$w_1 = \frac{i}{2\pi}\Gamma_{op}\log(z-z_p) + \frac{i}{2\pi}\Gamma_{oa}\log(z-z_a)$$

Expanding the second term in inverse powers of z, we have

B.2) $$w_1 = \frac{i}{2\pi}\Gamma_{op}\log(z-z_p) + \frac{i}{2\pi}\Gamma_{a}\log z - \frac{i}{2\pi}\Gamma_{oa}\frac{z_a}{z} + o(\frac{1}{z})$$

where the remainder is a power series in $\frac{1}{z}$ convergent for $|z|>|z_a|$.

Now denote by w_2 the potential of the actual flow induced by the vortex located at z_p in the presence of the aerofoil. We first express w_2 as a function of ζ, where ζ is defined by the transformation

B.3) $$z = \zeta + \frac{\ell^2}{4\zeta}$$

In the ζ plane the aerofoil is mapped into a circle of radius $\frac{\ell}{2}$ with center at $\zeta = 0$. The vortex at z_p maps into a vortex at ζ_p with circulation Γ_{op} Likewise the circulation Γ_{oa} around the aerofoil is preserved.

Using Milne-Thompson's circle theorem[7] in the ζ plane, we get

B.4) $$w_2 = \frac{i\Gamma_{op}}{2\pi}\log(\zeta-\zeta_p) - \frac{i\Gamma_{op}}{2\pi}\log(\frac{\ell^2}{4\zeta} - \overline{\zeta}_p) + \frac{i\Gamma_{oa}}{2\pi}\log\zeta$$

where ζ_p is the image of z_p and the bar over a letter stands for the complex conjugate.

We now express w_2 as a function of z in the following form:

$$(B.5) \quad w_2 = \frac{i\Gamma_{op}}{2\pi} \log(z-z_p) + f(z)$$

where f(z) is a function analytic outside the circle $z = \ell$. We then expand f(z) in inverse powers of z as far as the $\frac{1}{z}$ term.

To this end, we invert the relationship (B.3) to obtain

$$(B.6) \quad \zeta = \frac{z}{2} + \frac{1}{2} \sqrt{z^2-\ell^2}$$

$$(B.7) \quad \zeta_p = \frac{z_p}{2} + \frac{1}{2} \sqrt{z_p^2-\ell^2}$$

where the sign of the square root is such that $\zeta \simeq z$ as $|z| \to \infty$.

We then have

$$(B.8) \quad \zeta = z - \frac{\ell^2}{4z} + o\left(\frac{1}{z}\right)$$

$$(B.9) \quad \frac{1}{\zeta} = \frac{1}{z} + o\left(\frac{1}{z}\right)$$

The remainder terms in (B.8) and (B.9) are power series in $\frac{1}{z}$ which converge for $|z|>\ell$.

We also have

$$(B.10) \quad \zeta-\zeta_p = \frac{z-z_p}{2} + \frac{1}{2} \left[\sqrt{z^2-\ell^2} - \sqrt{z_p^2-\ell^2} \right]$$

It is readily shown that the right side of (B.10) can be expanded to give the following result:

$$(B.11)\quad \zeta-\zeta_p = (z-z_p)\left(1 + \frac{\ell^2}{4\zeta_p}\frac{1}{z} + o(\tfrac{1}{z})\right)$$

Substituting from Equations (B.8) through (B.11) into (B.4), we get

$$(B.12)\quad w_2 = \frac{i\Gamma_{op}}{2\pi}\,\ell og\,\left[(z-z_p)\left(1 + \frac{\ell^2}{4\zeta_p}\frac{1}{z} + o(\tfrac{1}{z})\right)\right]$$

$$- \frac{i\Gamma_{op}}{2\pi}\,\ell og\,\left[-\bar{\zeta}_p\left(1 - \frac{\ell^2}{4\bar{\zeta}_p}\frac{1}{z} + o(\tfrac{1}{z})\right)\right]$$

$$+ \frac{i\Gamma_{oa}}{2\pi}\,\ell og\,\left[z\left(1 - \frac{\ell^2}{4z^2} + o(\tfrac{1}{z^2})\right)\right]$$

We expand the right side of (B.12) as far as terms in $\frac{1}{z}$ and obtain, after neglecting an irrelevant constant

$$(B.13)\quad w_2 = \frac{i\Gamma_{op}}{2\pi}\,\ell og(z-z_p) + \frac{i\Gamma_{oa}}{2\pi}\,\ell og\, z$$

$$+ \frac{i\Gamma_{op}}{2\pi}\frac{\ell^2}{4}\left(\frac{1}{\zeta_p} + \frac{1}{\bar{\zeta}_p}\right)\frac{1}{z} + o(\tfrac{1}{z})$$

where the remainder is a power series convergent for $|z| > \ell$.

Comparison of (B.13) with (B.2) to terms of order $\frac{1}{z}$ now gives

$$(B.14)\qquad \frac{i\Gamma_{op}}{2\pi}\frac{\ell^2}{4}\left(\frac{1}{\zeta_p} + \frac{1}{\bar{\zeta}_p}\right) = -\frac{i}{2\pi}\Gamma_{oa}z_a$$

from which follows

$$z_a = -\frac{\Gamma_{op}}{\Gamma_{oa}}\frac{\ell^2}{4}\left(\frac{1}{\zeta_p} + \frac{1}{\bar{\zeta}_p}\right) \tag{B.15}$$

Equation (B.15) expresses the location of the vortex replacing the appendage in terms of z_p (since ζ_p is related to z_p by (B.7)), and $\frac{\Gamma_{op}}{\Gamma_{oa}}$, the ratio of the propeller circulation to the circulation around the appendage. It is important to note that since Γ_p and Γ_a are real, (B.15) shows that z_a is real and that therefore the substitution vortex for the appendage lies on the appendage regardless of the location z_p of the other vortex. It is likewise true that the substitution vortex for the propeller lies on the propeller.

To determine $\frac{\Gamma_{op}}{\Gamma_{oa}}$ in (B.15), we apply the Kutta condition at the trailing edge of the appendage, i.e., at $z = \ell$. The trailing edge maps into the point $\zeta = \frac{\ell}{2}$ in the ζ plane so that the Kutta condition can be written as

$$\frac{dw_2}{d\zeta} = 0, \quad \zeta = \frac{\ell}{2} \tag{B.16}$$

where w_2 is given by (B.4)

Carrying out the differentiation we obtain

$$\frac{dw_2}{d\zeta} = \frac{i\Gamma_{op}}{2\pi}\left[\frac{1}{\zeta - \zeta_p} + \frac{\frac{\ell^2}{4\zeta^2}}{\frac{\ell^2}{4\zeta} - \bar{\zeta}_p}\right] + \frac{i\Gamma_{oa}}{2\pi}\frac{1}{z} \tag{B.17}$$

Application of (B.16) yields

$$\frac{\Gamma_{op}}{\Gamma_{oa}} = -\frac{2}{\ell}\,\frac{1}{\frac{1}{\frac{\ell}{2} - \zeta_p} + \frac{1}{\frac{\ell}{2} - \bar{\zeta}_p}} \tag{B.18}$$

which when combined with (B.15) gives

$$(B.19) \qquad z_a = \frac{\ell}{2} \frac{\frac{1}{\zeta_p} + \frac{1}{\bar{\zeta}_p}}{\frac{1}{\frac{\ell}{2} - \zeta_p} + \frac{1}{\frac{\ell}{2} - \bar{\zeta}_p}}$$

Equation (B.19) is the desired explicit relationship between z_a, the location of the appendage vortex, and z_p, the location of an arbitrary "exciting" vortex. By way of checking this result, we observe that as z_p (and therefore ζ_p) $\to \infty$, $z_a \to -\frac{\ell}{2}$, the point on the appendage distant $\frac{1}{4}$ chord from the leading edge. This is to be expected since the incident flow approaches a uniform stream as $z_p \to \infty$, and for a uniform incident stream at any angle of attack other than zero, the substitution vortex replacing a thin aerofoil is known[7] to be located at the $\frac{1}{4}$ chord point. An exception arises if $z_p \to \infty$ in a direction parallel to the y axis, in which case the substitution vortex position depends on x_p, the distance from the y axis to the straight line along which $z_p \to \infty$. The reason for this is that two limiting operations are not interchangeable, viz., allowing z_p to $\to \infty$ in an arbitrary direction on the one hand, and allowing that direction to approach perpendicularity to the appendage on the other. If the latter operation is performed first, the result might be expected to be anomalous since in this case the limiting uniform stream impinges on the appendage with a zero angle of attack and therefore induces no circulation.

To determine the position of the substitution vortex for the propeller, we proceed in a manner exactly analogous to the above, except that we must remember that the incident flow on the propeller comes not only from a vortex at z_a but also from a uniform stream traveling with velocity U in the positive x direction. With this minor modification we get the following expression for z_p, the location of the substitution vortex that replaces the propeller:

$$(B.20) \qquad z_p = z_o - i\frac{\pi}{4}\frac{U}{\Gamma_{op}}c^2 - i\frac{1}{16}\frac{\Gamma_{oa}}{\Gamma_{op}}c^2\left(\frac{1}{\zeta'_a}+\frac{1}{\bar{\zeta}'_a}\right)$$

where $z_o = x_o + iy_o$, the position of the center of the propeller, c is the propeller chord, and ζ'_a is defined by

$$(B.21) \qquad \zeta'_a = \frac{1}{2}i\left[z_a - z_o + \sqrt{(z_a-z_o)^2 + \frac{c^2}{4}}\right]$$

Thus Equation (B.20) is the analogue of Equation (B.15) in that it expresses z_p in terms of z_a, Γ, Γ_{oa}, and Γ_{op}. Note that since the last two terms on the right of (B.20) are imaginary, z_p lies on the propeller.

By application of the Kutta condition at the trailing edge of the propeller, we could derive an equation analogous to (B.18). Such an equation, combined with Equations (B.15), (B.18) (or B.19), and (B.20) would give four equations for the determination of the four unknowns, Γ_{op}, Γ_{oa}, z_p, and z_a. However, we already

have a fourth equation, viz., Equation (6-8) for Γ_{ap} in the main text of the report, this having been derived in an independent way which also invokes the Kutta condition at the trailing edge of the propeller. Thus, no further relationships are required.

One final remark should be made concerning a limitation on the use of the substitution vortex method. To terms of order $\frac{1}{z}$, the potential due to the presence of the appendage is equal to that due to the appendage vortex, but this equality holds only for observation points z for which $|z|>\ell$, i.e., observation points exterior to a circle centered on the appendage and having a radius equal to the half chord. Similarly, the potential due to the propeller is approximated by that of the propeller vortex for points outside a corresponding circle centered on the propeller. It follows that in treating the flow with both aerofoils present by the substitution vortex method, neither aerofoil should penetrate the circle associated with the other. This requirement imposes a restriction on the variables ℓ, c, and x_o, viz.,

$$(B.22) \qquad x_o > \ell + \frac{c}{2} \qquad \text{or} \qquad \bar{c}^2 \leq \sqrt{\bar{y}_o^2 + (\bar{x}_o - 1)^2}$$

Thus the method breaks down if the propeller passes too close to the end of the appendage. On the other hand, it seems likely that a slight penetration of the circles by the aerofoils will not seriously spoil the accuracy of the method so that practically speaking, the inequality (B.22) is a little too restrictive.

DISTRIBUTION LIST FOR UNCLASSIFIED TECHNICAL REPORTS ON CONTRACT Nonr-3281(00)

Commanding Officer & Director
David Taylor Model Basin
Washington 7, D.C.
Attn: Contract Research Administrator, Code 513 (50)

Chief of Naval Research
Department of the Navy
Washington 25, D.C.
Attn: Code 438 (2)
Code 411 (1)

Commanding Officer
Office of Naval Research
Branch Office
The John Crerar Library Building
86 East Randolph Street
Chicago 1, Illinois (1)

Commanding Officer
Office of Naval Research
Branch Office
346 Broadway
New York 13, New York (1)

Commanding Officer
Office of Naval Research
Branch Office
1030 East Green Street
Pasadena 1, California (1)

Commanding Officer
Office of Naval Research
Branch Office
1000 Geary Street
San Francisco 9, California (1)

Commanding Officer
Office of Naval Research
Branch Office
Navy No. 100, Fleet Post Office
New York, New York (25)

Chief, Bureau of Naval Weapons
Department of the Navy
Washington 25, D.C.
Attn: Codes RAAD-3 (Aero & Hydro Sec) (1)
RRRE (Research) (1)
RR (Research & Engineering) (1)
SP26 (Ship Installation & Design) (1)

Chief, Bureau of Ships
Department of the Navy
Washington 25, D.C.
Attn: Code 335(Technical Info) (3)
420 (Preliminary Design Branch) (1)
421(Preliminary Design Section) (1)
422 (1)
420(Hull Design Branch) (1)
345(Ship Silencing Branch) (1)

Chief, Bureau of Yards & Docks
Department of the Navy
Washington 25, D.C.
Attn: Code D-400 (Research Division) (1)

Commander
Military Sea Transportation Service
Department of the Navy
Washington 25, D.C. (1)

Director
U.S. Naval Research Laboratory
Washington 25, D.C.
Attn: Code 2021 (Library) (6)

Commander
Long Beach Naval Shipyard
Long Beach, California (1)

Commander
Computation & Exterior Ballistics Lab.
U.S. Naval Proving Ground
Dahlgren, Virginia
Attn: Dr. A. V. Hershey (1)

Commandant
U.S. Coast Guard
1300 E. Street, N.W.,
Washington, D.C. (1)

Secretary Ship Structure Committee
U.S. Coast Guard Headquarters
1300 E. Street, N.W.
Washington 25, D.C. (1)

Superintendent
U.S. Naval Academy
Annapolis, Maryland
Attn: Library (1)

Administrator
U.S. Maritime Administration
Dept. of Commerce
Washington 25, D.C.
Attn: Mr. Vito L. Russo,
Deputy Chief
Office of Ship Construction (1)

Superintendent
U.S. Merchant Marine Academy
Kings Point, L.I., N.Y.
Attn: Capt. L.S. McCready,
Head
Dept. of Engineering (1)

Commanding Officer
Headquarters
U.S. Army Transportation
Research Command
Fort Eustis, Virginia
Attn: Research Reference Center (1)

Commander
U.S. Naval Ordnance Test Station
China Lake, California
Attn: Code 753 (Library Div.) (1)

Superintendent
U.S. Naval Postgraduate School
Monterey, California (1)

Commander
Portsmouth Naval Shipyard
Portsmouth, New Hampshire (1)

Commander
Norfolk Naval Shipyard
Portsmouth, Virginia (1)

Commander
Boston Naval Shipyard
Boston, Massachusetts (1)

Commander
U.S. Naval Proving Ground
Dahlgren, Virginia (1)

Commander
Pearl Harbor Naval Shipyard
Navy No. 128,
Fleet Post Office
San Francisco, California (1)

Commander
San Francisco Naval Shipyard
San Francisco, California (1)

Commander
Mare Island Naval Shipyard
Vallejo, California
Attn: Ship Yard Technical
Library
Building 746, Code 370a (1)

Commander
New York Naval Shipyard
Brooklyn, New York (1)

Commander
Puget Sound Naval Shipyard
Bremerton, Washington (1)

Director
National Aeronautics & Space
Administration
1512 H Street, N.W.
Washington 25, D.C. (1)

Director,
Langley Research Center, NASA
Langley Field, Virginia
Attn: Mr. J.B. Parkinson (1)

Director
National Bureau of Standards
Washington 25, D.C.
Attn: Fluid Mechanics Div.
Dr. G.B. Schubauer (1)
Dr. G.H. Keulegan (1)

Office of Technical Services
Department of Commerce
Washington 25, D.C. (1)

University of California
Berkeley 4, California
Attn: Prof. H.A. Schade, Head (1)
Dept. of Naval Architecture
Dept. Of Eng.
Prof. J. Johnson (1)
Prof. J.V. Wehausen (1)

Prof. M. Albertson
Department of Civil Engineering
Colorado A & M College
Fort Collings, Colorado (1)

Harvard University
Cambridge 38, Massachusetts
Attn: Prof. G. Birkhoff, (1)
Dept. of Math.
Prof. G.F. Carrier, (1)
Div. of Applied Sciences

Professor R.B. Couch, Chairman
Department of Naval Architecture
and Marine Engineering
University of Michigan
Ann Arbor, Michigan (1)

Director
St. Anthony Falls Hydraulic Lab.
University of Minnesota
Minneapolis 14, Minnesota (1)

Commander
Philadelphia Naval Shipyard
Philadelphia, Pennsylvania (1)

Commander
Charleston Naval Shipyard
Charles, South Carolina (1)

Director
Engineering Sciences Division
National Science Foundation
1931 Constitution Ave. N.W.
Washington 25, D.C. (1)

Commander
Armed Services Technical
Information Agency
Arlington Hall Station
Arlington 12, Virginia
Attn: TIPDR (10)

California Institute of
Technology
Pasadena 4, California
Attn: Prof. C.B. Millikan (1)
Dr. T.Y. Wu (1)

Director
Scripps Institute of Oceanography
University of California
La Jolla, California (1)

Iowa Institute of Hydraulic Research
State University of Iowa
Iowa City, Iowa
Attn: Dr. Hunter Rouse, Director (1)
Dr. Louis Landweber (2)

Department of Naval Architecture
and Marine Engineering
Massachusetts Institute of Technology
Cambridge 29, Massachusetts
Attn: Prof. P. Mandel (1)

Professor J.J. Foody,
Head of Engineering Department
State University of New York
Maritime College
Fort Schuyler,
New York 65, New York (1)

Institute of Mathematical Sciences
Library
25 Waverly Place
New York 3, New York
Attn: Prof. J.J. Stoker (1)
Prof. A. Peters (1)
Prof. J. Keller (1)

Professor W.R. Sears, Director
Graduate School of Aeronautical
Engineering
Cornell University
Ithaca, New York (1)

Director
Woods Hole Oceanographic Institute
Woods Hole, Massachusetts (1)

National Research Council
Montreal Road
Ottawa 2, Canada
Attn: Mr. E.S. Turner (1)

Therm Advanced Research
Therm, Incorporated
Ithaca, New York (1)

Hydronautics Incorporated
200 Monroe Street
Rockville, Maryland
Attn: Mr. P. Eisenberg, (1)
President
Mr. M.P. Tulin (1)

Dr. K. Eggers
Institut fur Schiffbau
University of Hamburg
Berliner Tor 21
Hamburg, Germany (1)

Prof. J.E. Cermak
Dept. of Civil Engineering
Colorado State University
Fort Collins, Colorado (1)

Dr. O. Grim
Hamburgische Schiffbau
Versuchsanstalt
Hamburg, Germany (1)

Prof. Laurens Troost, Jr.,
Chairman
National Council for Industrial
Research, TNO
12 Koningskade
P.O. Box 294
The Hague, Netherlands (1)

Dr. Willard J. Pierson Jr.
Department of Oceanography &
Meteorology
New York University
University Heights
New York 53, New York (1)

Director
Ordnance Research Laboratory
Pennsylvania State University
University Park, Pennsylvania (1)

Society of Naval Architects
and Marine Engineers
74 Trinity Place
New York 6, New York (1)

Director,
Davidson Laboratory
Stevens Institute of Technology
711 Hudson Street
Hoboken, New Jersey (2)

Prof. F. Ursell
Department of Mathematics
The University
Manchester 13, England (1)

Dr. R. Timman
DPT of Applied Maths.
Technological University
Julianalaan 132
Delft, Holland (1)

Prof. R.C. MacCamy
Dept. of Mathematics
Carnegie Institute of Tech.
Pittsburgh 13, Pennsylvania (1)

Commanding Officer & Director
U.S. Naval Civil Eng. Lab.
Port Hueneme, California
Attn: Code L54 (1)

Editor
Applied Mechanics Reviews
Southwest Research Institute
8500 Culebra Road
San Antonio 6, Texas (1)